Phase separation behavior due to solution environment asymmetry and salt addition for charged lipid bilayer membranes

by

Guo Jingyu

submitted to
Japan Advanced Institute of Science and Technology
in partial fulfillment of the requirements
for the degree of
Doctor of Philosophy

Supervisor: Professor Takagi Masahiro

School of Materials Science
Japan Advanced Institute of Science and Technology

March,2022

Abstract

[**Background**]

Lipid rafts on biomembranes are thought to have essential functions in signal transduction in living organisms. The structure and function of lipid rafts are expected to contribute to the understanding of cellular functions. Phospholipids, the main components of biomembranes, spontaneously form lipid bilayer structures in water. The liposome, which is closed to the lipid bilayer, has attracted much attention as a model system because its structure is similar to that of biomembranes. Further, the phase separation formed in liposomes consisting of multicomponent phospholipids is helpful as a model system for raft formation studies. From this point of view, studies on phase separation at the liposome membrane surface have been conducted, and many studies have been researched to control the phase separation behavior by using electrically neutral phospholipid membranes.

However, considering the biological environment, the presence of charged lipids, the induction of phase separation under isothermal conditions, and the roles of metal ions and polyamines inside and outside the cell are all critical. Previous studies have reported phase separation of phospholipid membranes containing charged lipids by the addition of metal ions and phase separation induced by osmotic application of the hypotonic solution to neutral lipid membrane vesicles. In conjunction with these studies, we use a system that more closely resembles the biological environment, considering the effects of the presence of charged lipids, isothermal environments, variable temperature environments, the addition of metal ions and polyamines, and the valence of charged lipids.

[**Objective**]

In this thesis, we clarify the changes of phase separation on the DOPS/DPPC binary GUVs in a hypotonic solution under isothermal conditions. We investigated the formation of the phase separation of DOPS/DPPC/Chol trinary GUVs adding monovalent to pentavalent metal salts and amines at room temperature, 30°C, 40°C. Also, we discussed the effect of multivalent charges lipids on the membrane behavior based on line tension calculations.

[**Results**]

First, phase separation was induced by osmotic pressure on the GUVs, and a three-phase coexistence structure was observed: a DPPC-rich phase, a negatively charged DOPS [DOPS(-)] phase, and a neutral DOPS [DOPS(N)] phase. The ionic dissociation of the DOPS head group was found to be essential for phase separation. Next, as the concentrations of metal ions and amines increased, phase separation formation was promoted. It was found that phase separation was more likely to occur at room temperature than at 30°C, 40°C. On the other hand, the concentration at which phase separation was induced significantly varied depending on the type of metal ions or amines. The concentration required for phase separation was temperature-sensitive for amines, which are linear chains. Last, confirmed that charged lipids decreased the domain line tension and that the addition of $CaCl_2$ suppressed the decrease in line tension. It was clarified that electrostatic interaction is involved in the decrease of line tension.

These experimental results suggest that the degree of ionization of charged lipids, osmotic pressure, temperature change, structure and concentration of added salts (especially metal ions and amines), and lipid valence significantly affect raft formation. Our findings may be helpful for the contribution of understanding the formation of ordered structures in living organisms and can be a model for charged lipid membrane.

Keyword:*lipid; charged lipid; phase separation; osmotic pressure; salts; polyamines; line tension*

Contents

Chapter 1

General Introduction

1.1 Cell membranes and raft hypothesis

All biological cells are very complex systems whose function strongly depends on their ability to interact with neighboring cells and the extracellular environment, generally associated with the membrane system of the cell. The peripheral membrane (plasma membrane) and the intracellular membrane system (such as mitochondrial membrane, chloroplast membrane, endoplasmic reticulum membrane, Golgi apparatus membrane, nuclear membrane, etc.) can be referred to as biomembranes. In contrast, biomembranes are an important membrane structure separating the internal and external environments of cells and organelles, and they have semi-permeable properties that mediate important interactions such as the exchange of metabolic substances and biochemical signals. The major components of biomembranes are composed of lipids and proteins. Among them, lipids are mainly phospholipids, but steroids (cholesterol in animal cells) are also present in a significant proportion. [1]

The earliest observations of biomembranes can be traced back to Hooke's experiments in 1665, which successfully observed fly eyes and cork tissues using optical microscopy [2]. Next, in 1972, Singer and Nicolson proposed the landmark model of biomembranes, the fluid mosaic model, in which the biomembranes is a fluidic system and the molecules that constitute biomembranes (including phospholipids and membrane proteins) diffuse freely through the membrane, where proteins cover, embed or penetrate biomembranes in a mosaic shape [3]. (Figure 1.1)

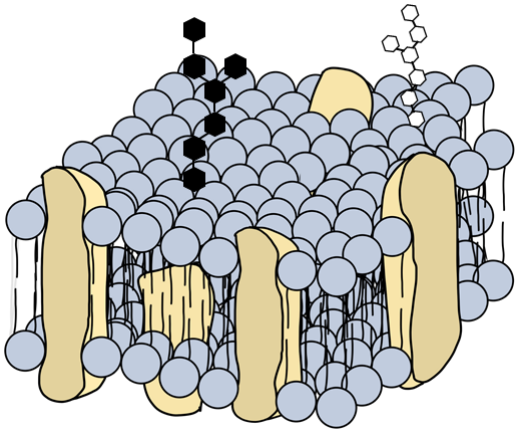

Figure 1.1: Schematic image of the fluid mosaic model

However, the mosaic fluid model was considered incomplete in analyzing the dynamics of biomembranes because it ignored the asymmetry of biomembranes, the role of protein molecules in regulating the mobility of membrane lipid molecules, and the heterogeneity of mobility in various parts of the membrane [4] [5] .

In 1977, Jain and White found that the structure and composition of biomembranes were not completely homogeneous, and proposed the microdomain (or lipid domain) model, called the block mosaic model, which pointed out that biomembranes were composed of dynamic microdomains [6] [7]. After that, in 1997, Simons and Ikonen proposed a kind of raft model, which provided a new understanding of membrane dynamics [8]. Since then, the debate on the structure and function of biomembranes has been active.

According to the raft model, the various components of the biomembranes form a heterogeneous structure rather than being uniformly distributed throughout the membrane and are thought to exist in microdomains (raft domains) [9]. As shown in Figure 1.2, the raft model is thought to form a relatively ordered cholesterol- and saturated lipid-rich phase, which floating on the biomembrane, carrying various membrane proteins [10] [11].

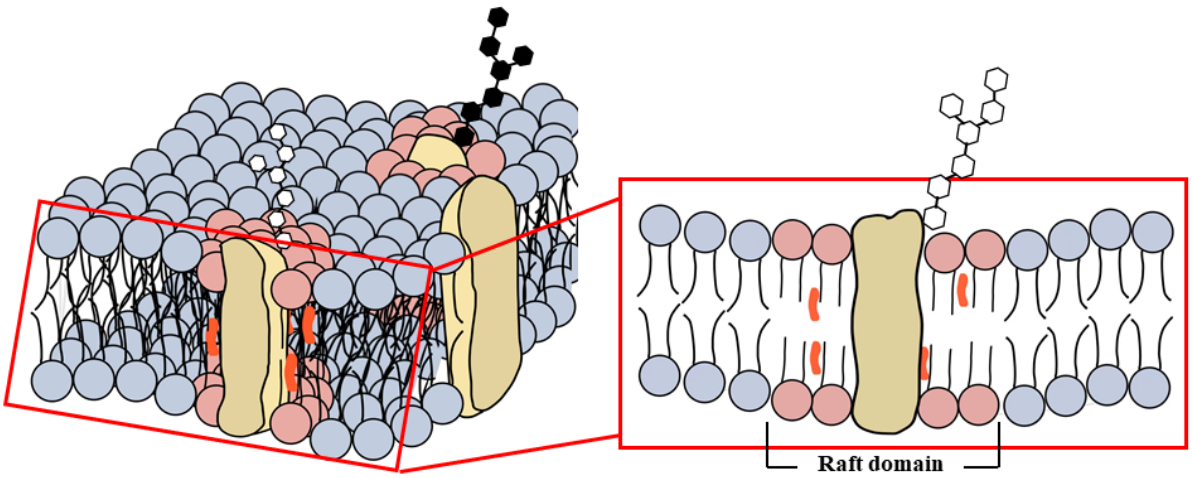

Figure 1.2: Schematic image of the raft model

Various important signal transduction molecules such as G proteins, adenylate cyclase, and some receptors were reported to be located in lipid rafts and it is also speculated involved in intra- and extracellular vesicular transport, thus lipid rafts are thought to have an important role in signal transduction [12] [13].

Recent studies have shown that lipid rafts may be closely associated with lipid dysfunction, including several infections, cardiovascular diseases, tumors, muscular dystrophy, Alzheimer's disease, HIV, and prion diseases [14] . Therefore, elucidating the structure and function of lipid rafts is expected to lead to breakthroughs in cell signaling studies and further advance the understanding of cellular functions.

1.2 Lipids

Lipids are the main components of biomembranes. In 1895, E. Overton conducted experiments on the permeability of plant cells with more than 500 chemicals and found that biomembranes differ in their permeability to different substances, and that substances dissolved in lipids enter the cell more easily through the biomembranes. Thus E. Overton proposed the theory that "Membranes are composed of lipids" [15].

Among the lipids that constitute the biomembranes, phospholipids are the main components, and can play a significant role in activating cells, maintaining metabolism and balanced secretion of hormones, and enhancing the immunity of body and regenerative power. In addition, phospholipids also have the function of promoting fat metabolism, preventing fatty liver, lowering serum cholesterol, improving blood circulation and preventing cardiovascular diseases. [16]

Phospholipid molecules are a kind of amphiphilic molecules that have a hydrophobic part (long hydrocarbon chains) and a hydrophilic part (phosphate group) in their structure. The hydrophilic part consists of glycerin and phosphoric acid, which have high affinity for polar water molecules. The hydrophobic part, consisting of fatty acids, has a high affinity for non-polar substances and a low affinity for polar molecules such as water. [1] (Figure 1.3(a))

Phospholipids are usually named according to the head and the structure of the lipid hydrocarbon chain. For example, Phosphatidyl choline(PC), Phosphatidyl serine(PS), Phosphatidyl ethanolamine(PE), Phosphatidyl inositol(PI), phosphatidic acid(PA) and Phosphatidyl glycerol(PG). These are all common phospholipid head groups. Among them, PC has positive and negative charges and is known as zwitterionic lipid. In contrast, PG, PS and PI exhibit negative charges of different valencies (will be elaborated in the following subsections). The length of the hydrocarbon chains lead to different glycerophospholipids, such as distearoyl, dipalmitoyl. Depending on the structure of the lipid hydrocarbon chain at the tail of phospholipids, it can be classified into two types, saturated and unsaturated lipids. Typical phospholipid chemical structures are shown in Figure 1.3(b). The length and the structure of hydrocarbon chain of phospholipid tail also affects the phase transition temperature (main transition temperature, T_m) of phos-

pholipids. Due to the unsaturated bonds, Unsaturated lipids usually have lower phase transition temperatures (T_m). On the other hand, Phospholipids with shorter hydrocarbon chains have exhibt lower phase transition temperatures (T_m). For the phospholipids possessing the same headgroup and the same length of hydrocarbon chains, the one which have unsaturated bond have lower phase transition temperature (T_m). For example, for saturated lipid DPPC and unsaturated lipid DOPC, their phase transition temperatures T_m are -20°C and 40°C, respectively. [17] [18]

Among the studies on phospholipids, it was first discovered from the human brain by Uauquelin in 1812, and isolated from egg yolk by Gobley in 1844, then named Lecithin after the Greek lekithos (egg yolk) in 1850 [19] [18]. However, to date, how lipids affect biological functions is still not being fully explained. Different lipid compositions exhibit different biomembrane properties and can even affect the activity of membrane proteins and non-membrane proteins, thus regulating biological processes by modulating membrane properties [20]. Therefore, further studies on lipids are necessary and urgent to explain more about biomembrane activities and biological processes.

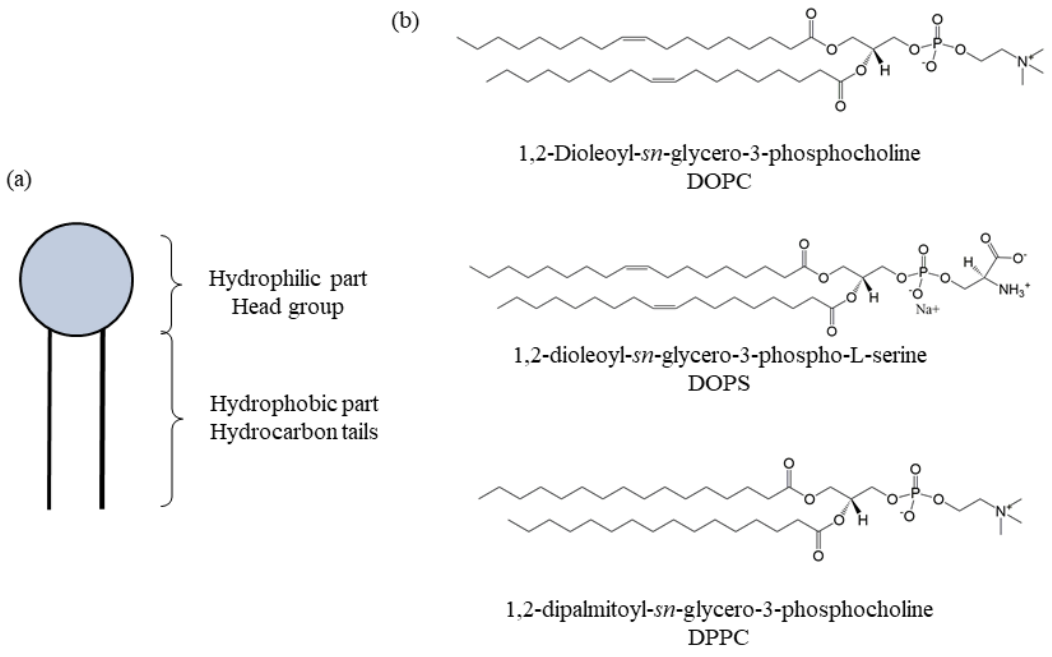

Figure 1.3: (a) Schematic structure of a phospholipid molecule. (b) Chemical structures of typical phospholipids.

1.3 Lipid membranes and liposome

As mentioned above, phospholipids are amphiphilic molecules with hydrophobic tails and a hydrophilic haedgroup. Depends on the difference of molecule size, temperature and concentration , amphiphilic molecules can spontaneously form many kinds of assemblies of very different morphology and size in water, such as micellar, bilayer, and hexagonal. These kinds of assembly structures are formed with hydrophilic groups on the outside and hydrophobic groups on the inside. In such structures, phospholipids have the property of forming bilayers. Furthermore, the ends of the bilayer become energetically unstable when they come into contact with water, so they spontaneously form a closed space and become spherical. [21] This spherical double-membrane structure is called a liposome, and were first reported in 1965 by Bangham et al [22]. (Figure 1.4)

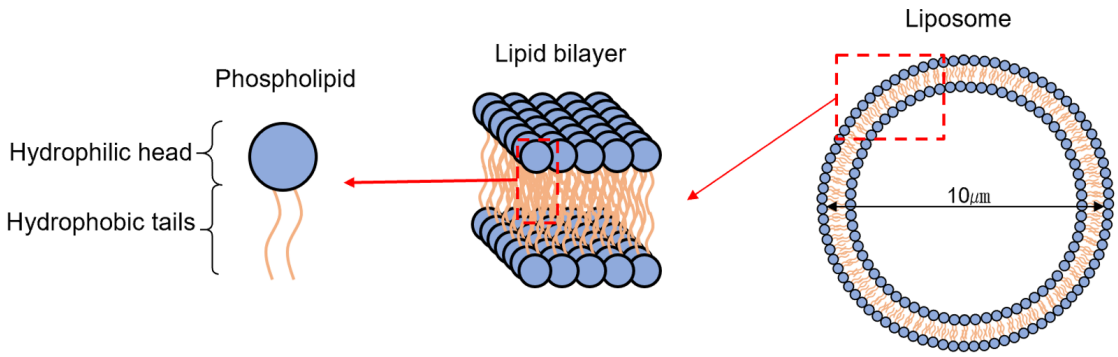

Figure 1.4: Schematic image of lipid, lipid bilayer and liposome.

Biomembranes, which are composed mainly of phospholipids, also have a structure consisting of bilayers. Therefore, with the similar composition and structure with biomembranes, liposomes are often used as a model to explain the physicochemical properties of biomembranes. In addition, liposomes can be prepared in the same size as living cells (known as giant unilamellar vesicles, GUVs) [23] and are more convenient for experimental procedures than living cells, such as preparation, observation, and analysis. [24] [25]

At the same time, liposomes exhibit certain biocompatibility, biodegradability, low toxicity, and ability to capture hydrophilic and lipophilic drugs [17] [26] [27]. Therefore

liposomes are widely used as carriers for numerous molecules in the cosmetic and pharmaceutical industries and are now beginning to unfold heroically in the food and agricultural industries. This also explains why liposomes entered the market quickly in the early 21st century, only 30 years after the first report [28] [29].

There are many methods to prepare liposomes, and several conventional ones include hydration [30], Electro-formation [31] and Coalescence [32], etc. In this thesis, the gentle hydration method (also called the "natural swelling" method), which is considered the optimal method for preparing GUVs [33], was chosen to prepare the liposomes.

1.4 Phase separation

The liposome has also been used in the studies of models for lipid raft. Because of the difficulty of observing raft regions in living cells membrane and the limitations of the complex composition of living cells membranes to control variables, phospholipid bilayers as model biomembrane are generally used [34] [35].

Liposome also has the advantages such as being simple to prepare, easy to control the composition, and easy to observe by optical microscopy. Also, the lipid raft model can be reproduced on liposome membranes. Several studies have reported that phase-separated structures occur in multicomponent liposome membranes, which is very similar to the raft configuration [36]. Such as, Dietrich el at. reported that a phase separation configuration was observed in liposome membranes using three components: saturated lipids, unsaturated lipids, and cholesterol [37].

Phase separation is a phenomenon that is generally explained by the competition between the internal energy and entropy. According to Helmholtz's definition of free energy, the free energy F is defined by $F = U - TS$, where U is the internal energy, T is the absolute temperature, and T is the entropy. When the temperature T is high and the entropy S is large, the entropy term can be made much smaller, resulting in a larger stabilization. Therefore, a mixed state is achieved at high temperatures. On the other hand, when the temperature T is low, the entropy contribution becomes small, and the free energy can be lowered by the internal energy U to achieve larger stabilization. Therefore, a phase separation state is created in which the attraction between lipids of the same species is large.

It is the same for phase separation in liposomes, where a decrease in temperature leads to phase separation between the ordered and disordered phases. It has been reported that at low temperatures multicomponent phospholipid membranes containing unsaturated and saturated lipids being phase separation into an unsaturated-rich phase and a saturated-rich phase, due to differences in the order of hydrocarbon chains in the hydrophobic portion of each lipid. In contrast, at higher temperatures, the components in the membrane tend to be uniformly dispersed and no phase separation occurs. [38] [39]

Figure 1.5 shows the phase diagrams and phase separation structures of the liposomes

using three components: unsaturated lipid DOPC, saturated lipid DPPC, and cholesterol (Chol) [39] [40]. It can be found that the phase separation structure changes with the ratio of the three components and has various forms. The region where riched of unsaturated lipid DOPC, is softer and more fluidity, is called the Liquid-disordered phase, L_d, in Figure 1.5(a1). The region where riched of saturated lipid DPPC, is harder and less fluidity, called as Solid-ordered phase, S_o. S_o/L_d phase separation showen in Figure 1.5(a3). When cholesterol is added, because saturated lipid has a higher affinity for cholesterol, cholesterol is more present in the saturated lipid region, and this makes the region more fluidity and becomes softer (black circular region in Figure 1.5(a2), (b4), (b5) and (b6)), called the liquid-ordered phase, L_o. Also, when the composition ratio is changed, the area of L_d is smaller than the area of L_o, L_d phase tend appear as circular domains, called reverse domain (white circular regions in Figure 1.5(b7) and (b8)).

Based on the observation of such domains, the approach to understanding the universality and fundamental principle of raft domain formation has been taken by studying phase separation in a simple system consisting of several kinds of phospholipids.

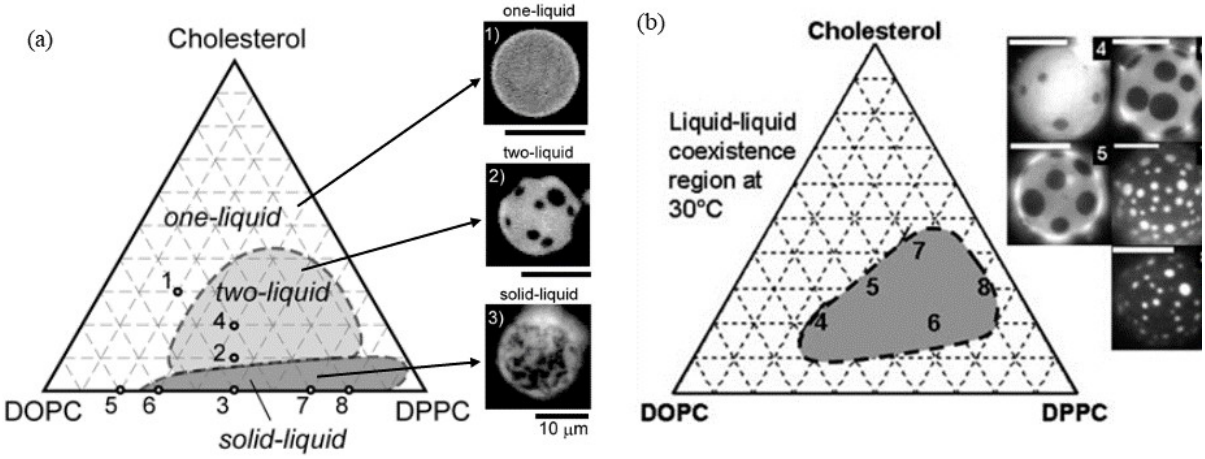

Figure 1.5: Phase diagrams and microscopic images of ternary membranes (DOPC/DPPC/Chol). (a)at 20°C. (a1)one-liquid disorder phase (a2)two-liquid L_o/L_d phase separation (a3)solid-liquid S_o/ L_d phase separation. [40] (b)two-liquid phase separation at 30°C. (b4,b5,b6) L_o/L_d phase separation; (b7, b8) reverse L_o/L_d phase separation. [39]

1.5 Line tension at the phase-separated domain boundary

The raft region is thought to be rich in saturated lipids and cholesterol and can be modeled by the L_o phase of phase separation structure on the ternary lipid membrane [8]. In general, the L_o phase appears circular and can recover after being disturbed externally in shape. Prior studies have reported that this phenomenon is related to the competition between line tension present at L_d/L_o phase boundary and entropy [41]. The line tension is the free energy per unit length of the boundary, can be obtained by the product of the domain boundary length and the interfacial tension called line tension. Since the large domain boundary length costs the excess energy, the L_o phase tends to form the shape with the shortest boundary length under the same area. When many small L_o domains tend to merge into one large L_o phase, the total length of the boundary decreases, and the energy at the boundary then becomes smaller. In contrast, a larger L_o phase leads to an unfavorable state of entropy. Thus line tension competes with entropy and forms an energy suitable shape.

The membrane thickness differ between the coexisting phases. L_o phase is rich in saturated lipids, while L_d phase is rich in unsaturated lipids. Due to the presence of unsaturated bonds, the unsaturated lipid acyl chains are shorter in length, and therefore the L_o phase is considered thicker than the L_d phase. This difference has been confirmed by experiments such as atomic force microscopy and X-ray diffraction [42] [43] [44]. The difference in thickness leads to a hydrophobic portion exposed to water at the boundary between the L_o and L_d phases, resulting in a loss of energy [41]. This energetic disadvantage leads to the generation of most of the boundary line tension [45]. It was found that lipids at L_d/L_o boundary tend to tilt or produce elastic deformations [46]. This lipid deformation or even membrane bending may all compensate for the energetic disadvantage [47].

In addition to this, the line tension varies depending on many other factors [41] [48] [49]. It has been reported that hybrid lipids (lipid with one saturated acyl tail and one unsaturated acyl tail) can be present in the L_o phase, disturbing chain ordering, decreasing

the line tension at the domain boundaries, and leading to the appearance of modulated phases [50]. Previous studies have reported that the addition of some fatty acids also leads to a decrease in line tension [51]. Fatty acids, such as unsaturated and branched fatty acids, can also be present in the L_o phase in small amounts, which disturbs the L_o phase ordering and reduces the physical properties differences between the L_o and L_d phases. Temperature also affects the line tension, and some studies have reported a decrease in line tension due to temperature increase [52].

In addition to being an important indicator to evaluate the physical properties differences between two phases and to change the size and shape of the raft region [53], the line tension may also be related to the distribution of proteins on the biomembrane. Some proteins are reported to appear at the boundary of the raft region, and the presence of proteins reduces the boundary line tension [54] [55] [56]. It is possible that line tension has a role in sorting or directing membrane proteins and thus regulating the distribution of membrane proteins. It has been reported that the boundary of the L_o phase is the site of HIV pseudoviruses fusion with the model membrane [57] [58]. It can be speculated that not only the raft region but also the boundary of the raft region has a crucial role in biological functions. It becomes crucial to study changes in line tension in model membranes that more resemble a real cell, especially for the complex case of adding charged lipids and salts.

1.6 Osmotic pressure for liposome

In addition to modulating the composition of the liposome and the ambient temperature to control the phase separation structure, some studies have also induced phase separation through changes in osmotic pressure [40]. Since the liposome is selectively permeable like the biomembrane, usually non-polar molecules or small molecules, such as water, can pass through the membrane, while polar molecules or large molecules such as glucose and ions cannot pass through the membrane. [1]

1.6.1 liposome in hypertonic solution

In a hypertonic solution, the osmotic pressure inside the liposome will be less than the osmolarity outside the liposome. The solute concentration inside the liposomes will be lower than the solute concentration outside, and water will permeate from inside to the outside of the liposome. [59] [60]

Hamada et al. [61] reported the membrane behavior by setting liposomes in hypertonic solutions. They used liposomes with DPPC/DOPC/Chol=40:40:20 with externally adding glucose solution to make the external concentration higher than the internal concentration. When the concentration in the liposome is lower than outside, the solvent moves out of the liposome, and the volume inside the liposome decreases. However, the surface area of the liposome does not change. For the reduced volume, the original surface area becomes excessive, and the liposome can be transformed into a lower energy shape using the excess area, as shown in Figure 1.6. Furthermore, it has been reported that when osmotic pressure is applied to phase-separated liposomes, the phase-separated domains bud towards the inside of the liposomes and form vesicles, as shown in Figure 1.7.

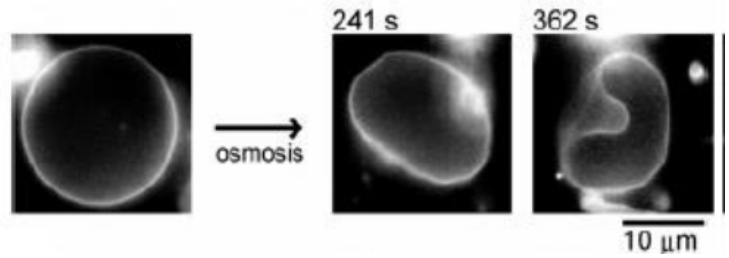

Figure 1.6: Fluorescent images of liposomes. (left)Normal liposome without any osmotic pressure. (middle and right)Deformation of liposomes in hypertonic solutions. [61]

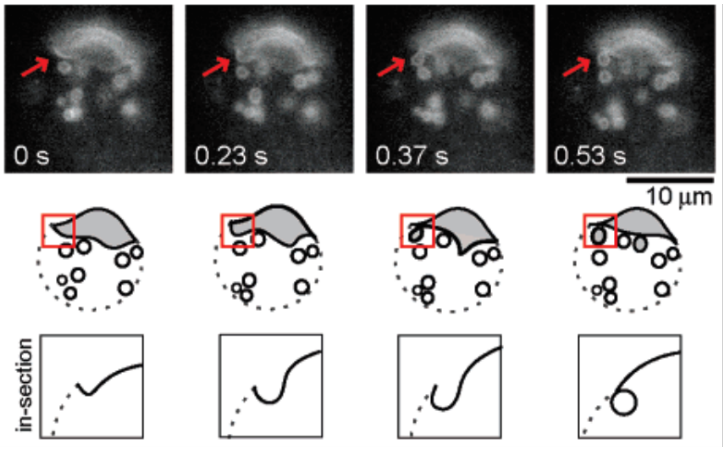

Figure 1.7: Fluorescent images of liposomes. Osmotic pressure is applied to the phase-separated liposomes to form vesicles. [61]

1.6.2 Liposome in hypotonic solution

When the solution concentration inside the liposome is higher than that outside of the liposome, the osmotic pressure inside the liposome is high. Thus water molecules outside the liposome flow into the liposome. [59] This causes the liposome to swell, but the surface area does not change significantly, it can result in the higher internal pressure of the liposome, and apply lateral tension to the liposome membrane, causing it to be stretched. Even though temperature regulation is commonly used to induce phase separation in general studies, some studies have been conducted in recent years to induce phase

separation under isothermal conditions by exposing the liposome to a low osmotic pressure environment. Hamada et al, reported that the membrane tension caused by osmotic pressure induces phase separation even in an isothermal system [40] [62]. (Figure 1.8) In biomembranes, it has been reported that the application of lateral tension induces changes in proteins that regulate signal transduction [63]. The osmotic study of the phase separation structure of liposomes may advance the biophysical understanding of the formation of phase separation in lipid bilayers under tension and isothermal conditions.

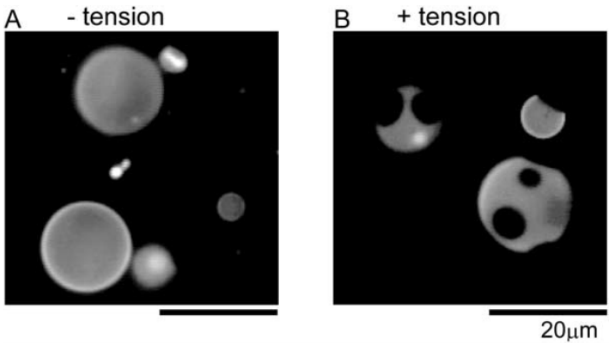

Figure 1.8: Fluorescent images of ternary vesicles DOPC/DPPC/Chol=50/20/30. From (A)one-liquid phase organization, tension-induced transition to (B)two-liquid phase organization. [40]

1.7 Ionic environment in the living body

1.7.1 Charged Lipid

In the studies related to phase separation with liposomes described in 1.4, mostly electroneutral lipids (such as DPPC and DOPC) were used, but a certain amount of charged lipids are also present in biomembranes. (Table 1.1)

Several studies have indicated that these charged lipids play an important role in physiological activities such as membrane potential generation, protein adsorption, and ion channel activity. [64] [65] [66]

For example, phosphatidyl-serine (PS), which was first extracted from the cow brain in 1942, is the major phospholipid component of the brain and is associated with important biomolecular functions such as apoptosis [67]. It is present on the inner side of the cell membrane and varies in the amount in different cells. [68] Like these, there are still many important charged lipids. Therefore, even though liposomes containing charged lipids are more difficult to study due to the electrostatic interactions, many studies have started to focus on liposomes containing charged lipids in the last decade.

Some of the more representative charged liposomes are phosphatidyl-inositol (PI), phosphatidyl-serine (PS), phosphatidyl-glycerol (PG), phosphatidic-acid (PA), and cardiolipin (CL), and so on. Most of them are negatively charged lipids. [69]

Table 1.1: Fractions of lipids in cell membrane

Source	**Cholesterol**	**PC**	**SM**	**PI(-)**	**PS(-)**	**PG(-)**	**PA(-)**	**CL(-)**
Mitochondria								
Internal membrane	3.0	45	2.5	6.0	1.0	2.0	0.7	18.0
External membrane	5.0	50	5.0	13.0	2.0	2.5	1.3	3.5
Cell nucleic membrane	10.0	55	3.0	7.0	3.0	-	1.0	-
E.coli	0	0	-	-	-	15.0	-	5.0

Phosphatidylinositol and phosphoinositide

Phosphatidylinositol is a kind of negatively charged phosphatidylglycerides, commonly called PI or PtdIns (hereafter referred to as PI). PI can be phosphorylated to phosphatidylinositol phosphate (PIP), which has negative divalent charges on the head group with -1 from the Inositol ring and -1 from the phosphate group; phosphatidylinositol bisphosphate (PIP_2), which has negative trivalent charges with -2 from the Inositol ring and -1 from the phosphate group; phosphatidylinositol trisphosphate (PIP_3), which have negative tetravalent charges with -3 from the Inositol ring and -1 from the phosphate group. These derivatives are all called phosphoinositide [70] [71] Typical PI lipid (PtdIns(4,5)P_2) structural showen in Figure 1.9.

In the past, it was thought that phospholipid molecules play a supporting role in biomembranes as Cytoskeleton. However, more and more studies show that they also have an important role in signal transduction processes, such as the PI derivatives PIP_2, PIP_3, etc. are thought to be involved in key signaling pathways in cells [10] [72].

As early as 1964, Hokin et al. [73] demonstrated that PI may be hydrolyzed by cellular stimulation, thus providing the basis for the "PI cycle". (Figure 1.10) Phosphoinositides have been suggested to be concentrated and heterogeneously distributed on biomembranes [8]. As a representative Phosphoinositides, PIP_2 has been extensively studied and reported to have the ability to stabilize the active state of G-protein-coupled receptors (GPCRs, are exist in the raft region) and increase the selectivity of G protein binding [74]. PIP_2 has an unsaturated hydrophobic chain, which has been shown to occur in the liquid disordered phase region of the biomembranes [75]. On the other hand, PIP_2 is decomposed by Phospholipase C (PLC) and is known to be involved in Ca^{2+} signaling [76].(Figure 1.11) Since PIP_2 is trivalent, the interaction of Ca^{2+} with PIP_2 causes it to aggregate near lipid membranes. In addition, PIP_2 concentrated in the membrane may aggregate to form other phases. Figure 1.12 shows a schematic distribution image for some Phosphoinositides on biomembrane. [77]

In recent years, several studies have indicated the presence of small amounts of PI and large amounts of PIP_2 in the raft regions. And it is likely that these regions play important functions, including signal transduction regulation [78] [79].

Generally, the raft region is rich in saturated lipids and cholesterol. Therefore, the presence of unsaturated lipid PI in the raft region may be a bit strange. It does not act as a major component but still plays an important role in interacting with specific substances and producing signaling molecules. So that it becomes crucial to explain why these small amounts of PI and phosphoinositide are present in this region. It is possible that some PIs are present in the cell membrane acting together with metabolic enzymes to function as membrane transport regulators [80].

Previous studies have indicated that the degree of binding of PS lipids to GPCRs is weaker than that of PIP_2 and suggested that the trivalent headgroup of PIP_2 facilitates the binding of GPCRs [74]. On the other hand, McLaughlin et al. reported the different pools of PIP_2 (PIP_2 enriched regions) on biomembrane. They suggest that this PIP_2 enrichment is associated with electrostatic sequestration and point to the possibility of a corresponding local increase in their Ca^{2+} ion concentration. [81] These studies suggested that the PIP_2 headgroup charge has an essential role in PIP_2 function, and studying the headgroup is very important.

As described above, there are many studies on these vital lipids PI and its phosphorylation product phosphoinositide. However, the relationship of these charged lipids to the raft structures and their effect on raft formation remain unresolved. Therefore, it is necessary to study how negatively charged lipids, which have multivalent headgroups, affect the formation of raft regions.

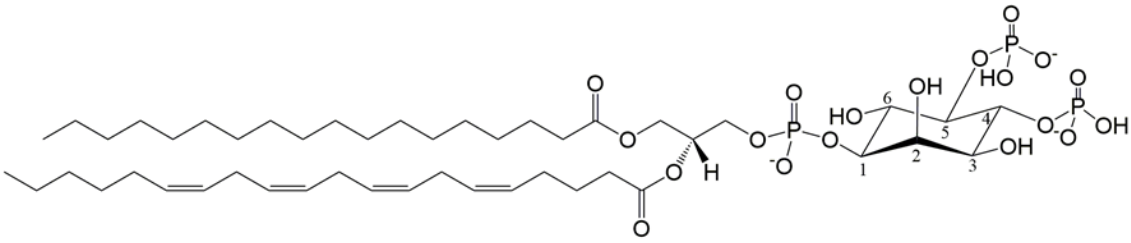

Figure 1.9: Structures of phosphoinositide, PIP_2 [70]

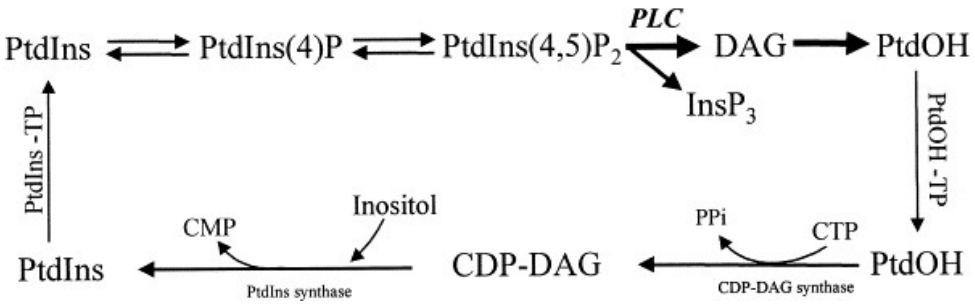

Figure 1.10: A simplified diagram of a PI cycle [70]

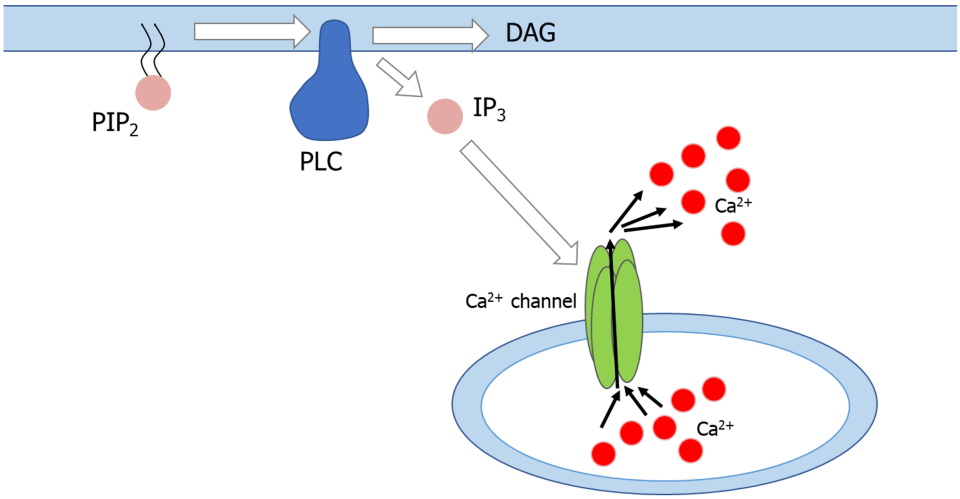

Figure 1.11: PIP_2 decomposed by PLC to produce PIP_3 and act on the Ca^{2+} ion channel.

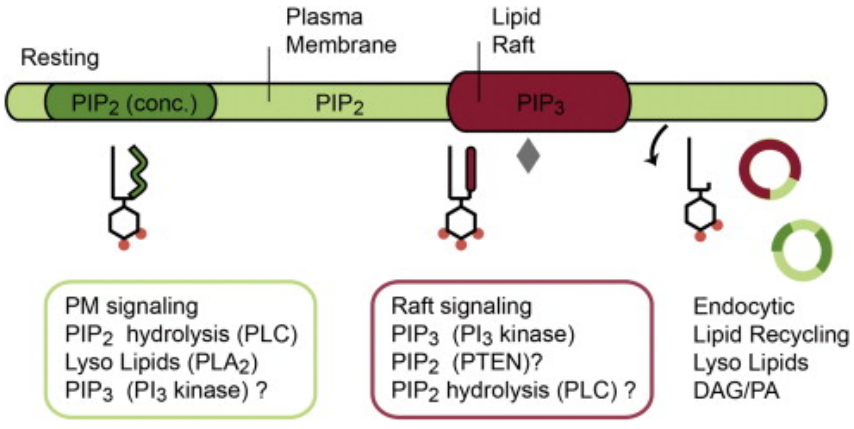

Figure 1.12: Schematic distribution image for some Phosphoinositides on biomembrane. [77]

1.7.2 Intrabiotic ionic environment

In addition to the charged lipids mentioned before, metal ions are also present in living organisms. Compared to the amount of carbon, nitrogen, oxygen, and other elements present in living organisms, the presence of metal ions can be said to be extremely small. However, metal ions still play an important role in living organisms. The absence and homeostasis disruption of certain metals can even lead to disease, such as cancer, diabetes, and Alzheimer's disease. [82] [83] [84] [85]

Several studies have shown that metal ions are needed in living organisms because the organism's functions cannot be performed solely by organic molecules. There are generally two states of metal ions in an organism, one bound to a specific enzyme and one in a free state. The role of these metal ions is reflected in the fact that the variable oxidation state of metal ions gives them a regulated valence, while the higher valence metal ions provide a solution environment of a certain ionic strength, which directly or indirectly allows the protein structure to be more stable [86]. In addition, free metal ions generally act as balancing molecules for the osmotic pressure of the intra- and extracellular environment.

The specific interactions of metal ions with biomembranes not only have crucial effects on membrane structure and function, but are also essential for processes such as cytokinesis, cytokinesis and small molecule transport across the biomembranes. In particular, metal ions such as K^+, Na^+, Ca^{2+}, and Mg^{2+}, which are present as free metal ions, are closely associated with ion channels. Even, it has been shown that membrane fusion is triggered by calcium ions [87]. Furthermore, since the biomembrane raft region contains various proteins related to signal transduction [12], it is not difficult to guess that these free metal ions may have some influence on the formation and its function of the raft region. And the presence of a certain percentage of negatively charged lipids on the biomembrane and how these lipids would interact with these metal cations is also of great interest.

Some studies using negatively charged lipids and metal cations have been published, and I will describe them in detail in the next section. In conclusion, although the role of metal ions is crucial, their relationship with the biomembrane is still unclear.

1.8 Previous studies about phase separation on charged lipid membranes

Several studies in liposomes containing charged lipids have been conducted. In a study with three-component liposomes using negatively charged unsaturated lipids DOPS, electrically neutral saturated lipids DPPC and Chol, phase separation formation was inhibited compared to neutral membranes consisting of DOPC, DPPC, and Chol. On the other hand, the addition of calcium chloride ($CaCl_2$) was reported to enhance the formation of phase-separated structures, and it was suggested that the DOPS-riched regions were attached to calcium ions and budded into the liposome interior then becoming vesicles. (Figure 1.13) [88]

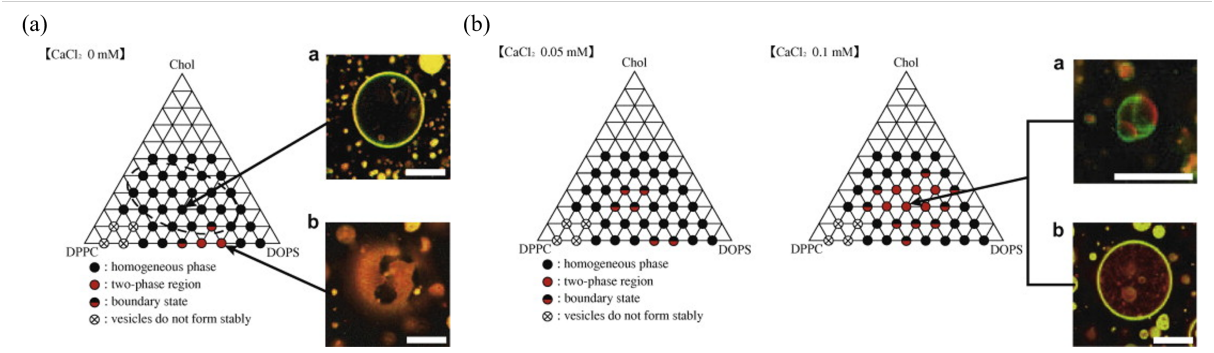

Figure 1.13: Phase diagrams and fluorescent images of DPPC/DOPS/Chol. (a) without calcium chloride solution. (b) addition of calcium chloride solution. [88]

In the simpler system which only used two-component liposomes composed of charged lipids and electrically neutral lipids. Compared to the two-component liposomes consisting of only electrically neutral lipids, the negatively charged unsaturated lipid (DOPG)-containing membranes inhibited phase separation formation, thermal stability of phase separation was reduced, on the other hands, the negatively charged saturated lipid (DPPG)-containing membranes promoted phase separation formation. This suggested that the electrostatic interactions of DOPG and DPPG act differently. Furthermore, it was also reported that when using negatively charged unsaturated lipid DOPG, if NaCl was added

to a system, thermal stability of the phase separation was increased and the phase separation becomes easier. (Figure 1.14) [89]

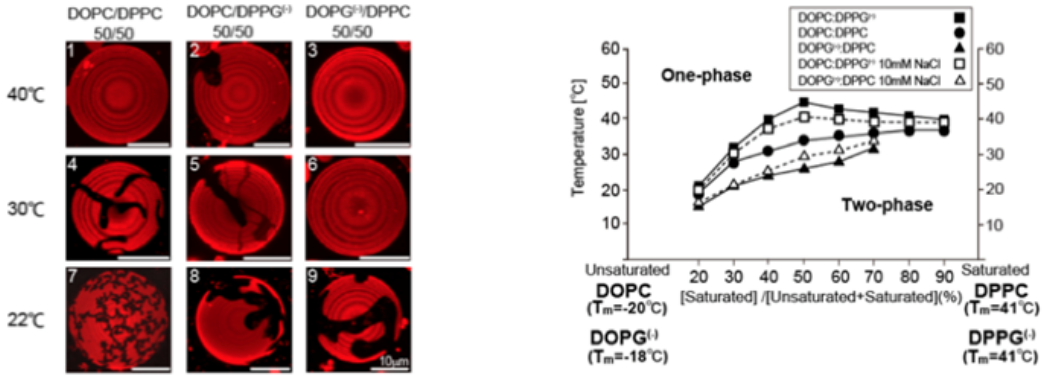

Figure 1.14: Phase separation of charged lipid membranes. (left) Fluorescent images with different lipid composition and different temperature. (right) Phase boundaries between One-phase (homogeneous phase) and Two-phase (phase separation) in binary charged lipid membranes without and with NaCl. [89]

There are also several other researches that have actively used the charged lipids. For example, the addition of Na^+ and Ca^{2+} decreases the lipid diffusion coefficient of negatively charged membranes [90], the binding of calcium ions to liposomes containing negatively charged lipids leads to area contraction of the membrane [91], and so on.

Although all these studies have investigated the liposome containing charged lipids, the effect of charge environment (both adding ions and the charge of the membrane itself) on the phase separation has still not been fully explained. In addition to the charge of the membrane itself, the valence state of the added ions seems to be important, which will be elaborated in this thesis after.

1.9 Polyamine

In addition to metal ions in the living body, there is a class of non-metal ions, amines. Amines refer to cations containing amine nitrogen, which is a non-proteinogenic nitrogen compound. Of these, those with multiple amine nitrogens are called polyamines. Typical polyamine structurals showen in Figure 1.15. Polyamines are water-soluble compounds with small molecular weight and most of them have a linear structure. Due to the rich construction, a variety of different polyamines can be found even for the same valence. Polyamines have similar structures to each other and have similar origins in the biosynthesis process. Therefore, they are produced in association with each other and are widely present in the body at concentrations ranging from 10μM to several mM. [92]

Polyamines are considered to be essential for living organisms and have various important roles, but the details of mechanisms have not yet been clarified [93] [94]. For example, it is currently reported that there is a close interrelationship between the amount of RNA and the concentration of polyamines, but it is only suggested that they act as a regulator of RNA synthesis [95]. Plus, polyamines also can stabilize DNA secondary structure and protein three-dimensional structure and are related to the formation of DNA and protein order [96] [97].

Takagi et al. reported that polyamines could prevent thermal aggregation and deactivation of proteins. Thermally unstable proteins that form insoluble aggregates at high temperatures were used in their study. With the addition of spermine or spermidine, thermal aggregation of thermally unstable proteins was prevented, and the proteins retained some activity. They suggested that this is because polyamines inhibit the interaction between protein molecules. [97].

In addition, it is also known that the thermal stability to the target varies depending on the structure of polyamines [98].

T. Nishino, et al. [99] reported that when a pentavalent branched-chain polyamine called N^4-bis(aminopropyl)spermidine (3(3)(3)4) was added, a structure generated along the DNA called a nano-loop was observed. This kind of polyamine is present in hyperthermophilic archaeon that live at an environment temperatures between 60 and 100°C [100]. It has been suggested that this ordered structure, nano-loop, is one of the factors that sta-

bilize DNA, which takes on a one-dimensional structure under high temperatures. (Figure 1.16)

Whatmore, dysfunction of polyamine metabolism is closely related to cancer therapy development. Many researchers hope to use the specificity of polyamines transmembrane transport system to cure cancer, however, the transmembrane transport mechanism of polyamines is not clear, and the relationship between polyamines and biomembranes is also not clear [101].

Overall, polyamines have an essential role for both proteins and DNA to stabilize their order and structure. The previous section also mentioned the presence of ordered structures (raft structures) in cell membranes. It would be interesting to investigate whether polyamines may also have a stabilizing effect on biomembranes and whether they affect the orderly regions of biomembranes. If polyamine molecules also affect the interactions between lipid molecules, then their presence could impact the formation of raft structures. Also, some studies have indicated that polyamines bind to DNA, RNA, and other biomolecules through electrostatic interactions [102] [103], suggesting the possibility of interactions between polyamines and charged lipid membranes. For these reasons, it becomes crucial to study lipid membrane phase separation in the presence of added polyamines.

Spermidine trihydrochloride
(triamine)

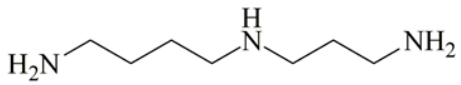

Spermine tetrahydrochloride
(tetraamine)

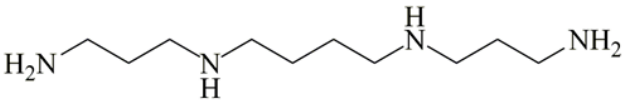

Homocaldopentamine
3(3)(3)4
(pentaamine)

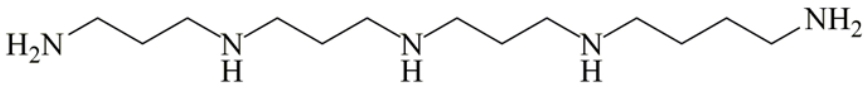

N^4-bis(aminopropyl)spermidine
3(3)(3)4
(pentaamine)

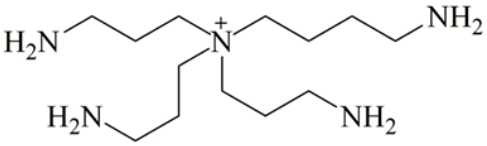

Figure 1.15: Chemical formulas of polyamines.

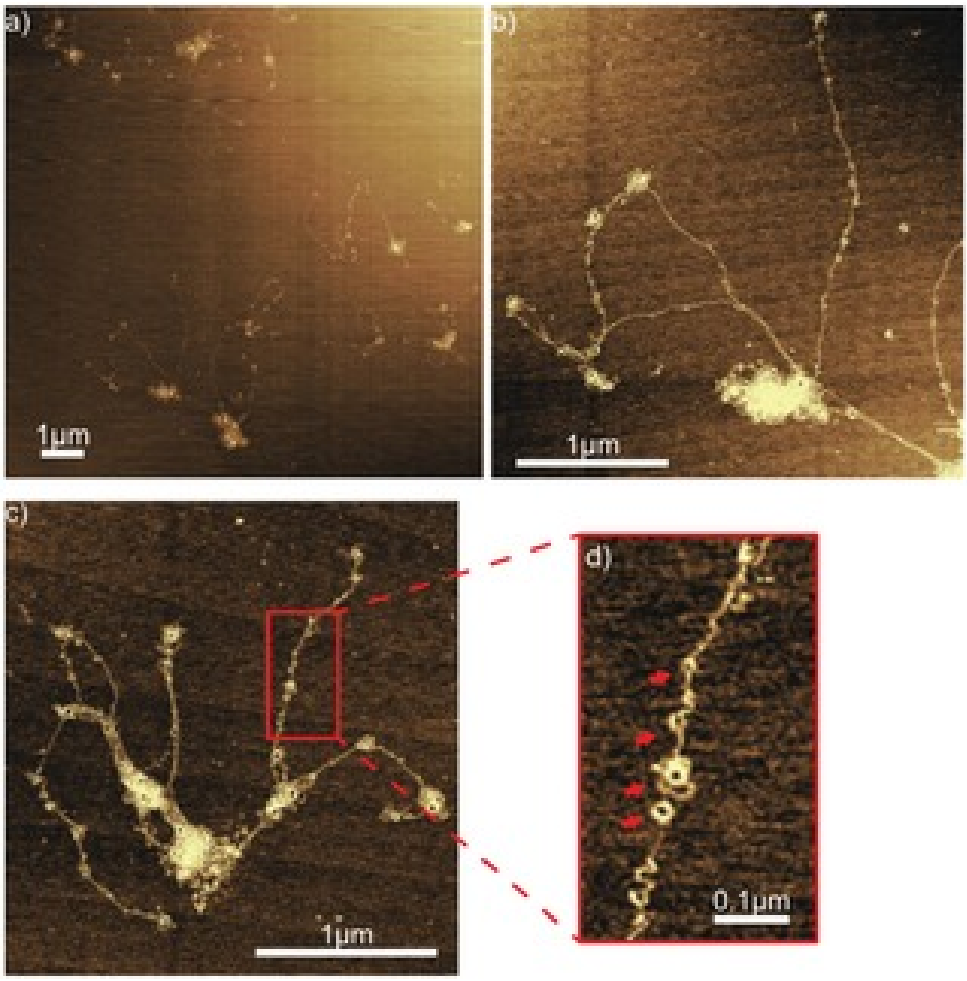

Figure 1.16: AFM images of T4 DNA in the presence of N^4-bis(aminopropyl)spermidine (3(3)(3)4) at 80°C. (a) wide sacn image (b,c) zoom in images and (d) enlarged image of red square in (c), red arrows indicate nano-loops. [99]

1.10 Objectives and outline of this thesis

As mentioned before, GUVs are widely used as a cellular model in various studies. Among them, the phase separation on multicomponent GUVs is considered similar to the lipid raft and is used to study its formation and mechanism of action. The research approach can start with a system consisting of a simple phospholipids component and gradually add complexity to the system, thereby bringing it closer to the environment of biomembranes. This approach can be expected to advance the understanding of cellular functions further.

However, there are still limitations and unstudied blank areas in these lipid membranes studies. In this context, many studies have been conducted to control the phase separation structure in electrically neutral phospholipid membranes by changing the temperature. However, considering the biological environment, the presence of charged lipids, the induction of phase separation under isothermal conditions, and the role of metal ions and polyamines inside and outside the cell are critical. Previous studies have reported phase separation induced by the addition of metal ions in phospholipid membranes containing charged lipids [88] [89] and phase separation caused by applied osmotic pressure to neutral lipid membrane vesicles in hypotonic solutions [40].

Thus, in this thesis, we focused on the behavior of membranes containing charged lipids while approaching the actual raft model. The details are shown as follows:

In chapter 2, we investigated the effect of membrane tension due to osmotic pressure and pH on lipid membranes containing negatively charged lipids. The experiments were performed in an isothermal environment. Binary liposomes consisting of negatively charged unsaturated lipid DOPS and neutral saturated lipid DPPC were prepared, and phase separation structures were observed by osmotic pressure application using fluorescence microscopy and confocal laser microscopy.

In chapter 3, we investigated the effects of adding salts, including metal ions and polyamines, on the phase separation of negatively charged lipid membranes. Also, we reveal the change of thermal stability of phase separation by changing the temperature. First, we studied the phase separation in charged lipid membranes by adding various salts with different valence, sizes, and structures. Monovalent to pentavalent salts (metal ions

and amines) were added to DOPS/DPPC/Chol three-component liposomes at arbitrary concentrations and observed by fluorescence microscopy. Second, we changed the ambient temperature during observation and performed microscopic observation at three temperatures: room temperature, 30°C, and 40°C to investigate the effect of various salts on the thermal stability of the phase separation region.

In chapter 4, we explored the effect of multivalent anionic lipids on the phase separation. We added monovalent negatively charged unsaturated lipids DOPI, DOPS, or trivalent negatively charged unsaturated lipids (DOPI(4,5)P_2, PIP_2) to DOPC/DPPC/Chol three-component liposomes and measured the interfacial tension of the phase-separated domains. The change of the interfacial tension of the phase-separated domain by the multivalent negatively charged phospholipids was discussed.

Overall, this thesis takes a stepwise approach of increasing complexity. Firstly, a study was conducted using monovalent negatively charged lipids to investigate whether the charge situation of the headgroup of the lipid would affect the lipid membranes phase separation. Next, various ions were added based on the last step to observe the phase separation under ions influence, analyze the interaction between the negatively charged lipids headgroups and the ions, and explore the effect of external environmental to charged lipid membranes. Finally, the complexity of negatively charged lipids was increased, and multivalent negatively charged lipids were selected to observe their phase separation behavior on the membrane.

In general, this thesis aims to clarify the physical role of charged lipids in the formation of phase separation in lipid membranes by studying the effects of osmotic tension, solution pH, salt structure, salt concentration, temperature, and lipid valence, and tried to discuss the importance of the electrostatic interaction of charged lipids in raft formation. It is hoped that this thesis will explain the importance of charge to biomembrane and contribute to understanding biomembrane mechanisms through electrostatic interactions.

Reference

[1] B. Alberts, D. Bray, K. Hopkin, A. D. Johnson, J. Lewis, M. Raff, K. Roberts, and P. Walter. *Essential cell biology*. Garland Science, 2015.

[2] R. Hooke. *Micrographia: or some physiological descriptions of minute bodies made by magnifying glasses, with observations and inquiries thereupon*. Courier Corporation, 2003.

[3] S. J. Singer and G. L. Nicolson. The fluid mosaic model of the structure of cell membranes. *Science*, 175(4023):720–731, 1972.

[4] J. E. Rothman and J. Lenard. Membrane asymmetry. *Science*, 195(4280):743–753, 1977.

[5] J. D. Nickels, J. C. Smith, and X. Cheng. Lateral organization, bilayer asymmetry, and inter-leaflet coupling of biological membranes. *Chemistry and Physics of Lipids*, 192:87–99, 2015.

[6] M. K. Jain and H. B. White III. Long-range order in biomembranes. *Advances in Lipid Research*, 15:1–60, 1977.

[7] D. E. Wolf, W. Kinsey, W. Lennarz, and M. Edidin. Changes in the organization of the sea urchin egg plasma membrane upon fertilization: indications from the lateral diffusion rates of lipid-soluble fluorescent dyes. *Developmental Biology*, 81(1):133–138, 1981.

[8] K. Simons and E. Ikonen. Functional rafts in cell membranes. *Nature*, 387(6633):569–572, 1997.

[9] K. Simons and G. Van Meer. Lipid sorting in epithelial cells. *Biochemistry*, 27(17):6197–6202, 1988.

[10] D. A. Brown and E. London. Structure and function of sphingolipid-and cholesterol-rich membrane rafts. *Journal of Biological Chemistry*, 275(23):17221–17224, 2000.

[11] M. Vestergaard, T. Hamada, and M. Takagi. Using model membranes for the study of amyloid beta: lipid interactions and neurotoxicity. *Biotechnology and Bioengineering*, 99(4):753–763, 2008.

[12] L. D. Zajchowski and S. M. Robbins. Lipid rafts and little caves: compartmentalized signalling in membrane microdomains. *European Journal of Biochemistry*, 269(3):737–752, 2002.

[13] K. Simons and J. L. Sampaio. Membrane organization and lipid rafts. *Cold Spring Harbor perspectives in biology*, 3(10):a004697, 2011.

[14] J. Fantini, N. Garmy, R. Mahfoud, and N. Yahi. Lipid rafts: structure, function and role in hiv, alzheimer's and prion diseases. *Expert Reviews in Molecular Medicine*, 4(27):1–22, 2002.

[15] C. E. Overton. *Über die osmotischen Eigenschaften der lebenden Pflanzen-und Tierzelle*. Fäsi & Beer, 1895.

[16] D. Cao, A. Qiu, and X. Wang. The structure, nature, function and researching situation of phospholipids. *Liangshi yu Youzhi*, 5:3–7, 2004.

[17] J. Li, X. Wang, T. Zhang, C. Wang, Z. Huang, X. Luo, and Y. Deng. A review on phospholipids and their main applications in drug delivery systems. *Asian Journal of Pharmaceutical Sciences*, 10(2):81–98, 2015.

[18] J. L. Robertson. The lipid bilayer membrane and its protein constituents. *Journal of General Physiology*, 150(11):1472–1483, 2018.

[19] E. Baer. From the trioses to the synthesis of natural phospholipids: A research trail of forty years. *Journal of the American Oil Chemists' Society*, 42(4):257–266, 1965.

[20] T. Harayama and H. Riezman. Understanding the diversity of membrane lipid composition. *Nature Reviews Molecular Cell Biology*, 19(5):281–296, 2018.

[21] V. Guida. Thermodynamics and kinetics of vesicles formation processes. *Advances in Colloid and Interface Science*, 161(1-2):77–88, 2010.

[22] A. D. Bangham, M. M. Standish, and J. C. Watkins. Diffusion of univalent ions across the lamellae of swollen phospholipids. *Journal of Molecular Biology*, 13(1):238–IN27, 1965.

[23] B. E. Cohen and A. D. Bangham. Diffusion of small non-electrolytes across liposome membranes. *Nature*, 236(5343):173–174, 1972.

[24] Y. P. Patil and S. Jadhav. Novel methods for liposome preparation. *Chemistry and Physics of Lipids*, 177:8–18, 2014.

[25] A. Akbarzadeh, R. Rezaei-Sadabady, S. Davaran, S. W. Joo, N. Zarghami, Y. Hanifehpour, M. Samiei, M. Kouhi, and K. Nejati-Koshki. Liposome: classification, preparation, and applications. *Nanoscale Research Letters*, 8(1):1–9, 2013.

[26] G. Gregoriadis, P. D. Leathwood, and B. E. Ryman. Enzyme entrapment in liposomes. *FEBS Letters*, 14(2):95–99, 1971.

[27] Y. Fan and Q. Zhang. Development of liposomal formulations: From concept to clinical investigations. *Asian Journal of Pharmaceutical Sciences*, 8(2):81–87, 2013.

[28] T. M. Allen and P. R. Cullis. Liposomal drug delivery systems: from concept to clinical applications. *Advanced Drug Delivery Reviews*, 65(1):36–48, 2013.

[29] P. Fernandez, N. Willenbacher, T. Frechen, and A. Kühnle. Vesicles as rheology modifier. *Colloids and Surfaces A: Physicochemical and Engineering Aspects*, 262(1-3):204–210, 2005.

[30] J. P. Reeves and R. M. Dowben. Formation and properties of thin-walled phospholipid vesicles. *Journal of Cellular Physiology*, 73(1):49–60, 1969.

[31] M. I. Angelova and D. S. Dimitrov. Liposome electroformation. *Faraday Discussions of the Chemical Society*, 81:303–311, 1986.

[32] N. Oku and R. C. MacDonald. Differential effects of alkali metal chlorides on formation of giant liposomes by freezing and thawing and by dialysis. *Biochemistry*, 22(4):855–863, 1983.

[33] K. Akashi, H. Miyata, H. Itoh, and K. Kinosita Jr. Preparation of giant liposomes in physiological conditions and their characterization under an optical microscope. *Biophysical Journal*, 71(6):3242–3250, 1996.

[34] J. L. Thomas, D. Holowka, B. Baird, and W. W. Webb. Large-scale co-aggregation of fluorescent lipid probes with cell surface proteins. *The Journal of Cell Biology*, 125(4):795–802, 1994.

[35] K. Jacobson and C. Dietrich. Looking at lipid rafts? *Trends in Cell Biology*, 9(3):87–91, 1999.

[36] F. A. Heberle and G. W. Feigenson. Phase separation in lipid membranes. *Cold Spring Harbor Perspectives in Biology*, 3(4):a004630, 2011.

[37] C. Dietrich, L. A. Bagatolli, Z. N. Volovyk, N. L. Thompson, M. Levi, K. Jacobson, and E. Gratton. Lipid rafts reconstituted in model membranes. *Biophysical Journal*, 80(3):1417–1428, 2001.

[38] S. L. Veatch and S. L. Keller. Organization in lipid membranes containing cholesterol. *Physical Review Letters*, 89(26):268101, 2002.

[39] S. L. Veatch and S. L. Keller. Separation of liquid phases in giant vesicles of ternary mixtures of phospholipids and cholesterol. *Biophysical Journal*, 85(5):3074–3083, 2003.

[40] T. Hamada, Y. Kishimoto, T. Nagasaki, and M. Takagi. Lateral phase separation in tense membranes. *Soft Matter*, 7(19):9061–9068, 2011.

[41] P. I. Kuzmin, S. A. Akimov, Y. A. Chizmadzhev, J. Zimmerberg, and F. S. Cohen. Line tension and interaction energies of membrane rafts calculated from lipid splay and tilt. *Biophysical Journal*, 88(2):1120–1133, 2005.

[42] C. Yuan, J. Furlong, P. Burgos, and L. J. Johnston. The size of lipid rafts: an atomic force microscopy study of ganglioside gm1 domains in sphingomyelin/dopc/cholesterol membranes. *Biophysical Journal*, 82(5):2526–2535, 2002.

[43] J. C. Lawrence, D. E. Saslowsky, J. M. Edwardson, and R. M. Henderson. Real-time analysis of the effects of cholesterol on lipid raft behavior using atomic force microscopy. *Biophysical Journal*, 84(3):1827–1832, 2003.

[44] M. Gandhavadi, D. Allende, A. Vidal, S. A. Simon, and T. J. McIntosh. Structure, composition, and peptide binding properties of detergent soluble bilayers and detergent resistant rafts. *Biophysical Journal*, 82(3):1469–1482, 2002.

[45] T. Baumgart, S. T. Hess, and W. W. Webb. Imaging coexisting fluid domains in biomembrane models coupling curvature and line tension. *Nature*, 425(6960):821–824, 2003.

[46] T. A. Harroun, W. T. Heller, T. M. Weiss, L. Yang, and H. W. Huang. Theoretical analysis of hydrophobic matching and membrane-mediated interactions in lipid bilayers containing gramicidin. *Biophysical Journal*, 76(6):3176–3185, 1999.

[47] E. London. A new role for lipid domains? *Nature Chemical Biology*, 11(6):383–384, 2015.

[48] D. Lee, Y. Min, P. Dhar, A. Ramachandran, J. N. Israelachvili, and J. A. Zasadzinski. Relating domain size distribution to line tension and molecular dipole density in model cytoplasmic myelin lipid monolayers. *Proceedings of the National Academy of Sciences*, 108(23):9425–9430, 2011.

[49] W. Tsai and G. W. Feigenson. Lowering line tension with high cholesterol content induces a transition from macroscopic to nanoscopic phase domains in model biomembranes. *Biochimica et Biophysica Acta (BBA)-Biomembranes*, 1861(2):478–485, 2019.

[50] T. M. Konyakhina, S. L. Goh, J. Amazon, F. A. Heberle, J. Wu, and G. W. Feigenson. Control of a nanoscopic-to-macroscopic transition: modulated phases in four-component dspc/dopc/popc/chol giant unilamellar vesicles. *Biophysical Journal*, 101(2):L8–L10, 2011.

[51] N. Shimokawa, R. Mukai, M. Nagata, and M. Takagi. Formation of modulated phases and domain rigidification in fatty acid-containing lipid membranes. *Physical Chemistry Chemical Physics*, 19(20):13252–13263, 2017.

[52] A. J. García-Sáez, S. Chiantia, and P. Schwille. Effect of line tension on the lateral organization of lipid membranes. *Journal of Biological Chemistry*, 282(46):33537–33544, 2007.

[53] R. D. Usery, T. A. Enoki, S. P. Wickramasinghe, M. D. Weiner, W. Tsai, M. B. Kim, S. Wang, T. L. Torng, D. G. Ackerman, F. A. Heberle, J Katsaras, and G. w. Feigenson. Line tension controls liquid-disordered+ liquid-ordered domain size transition in lipid bilayers. *Biophysical Journal*, 112(7):1431–1443, 2017.

[54] F. Dumas, M. M. Sperotto, M. Lebrun, J. Tocanne, and O. G. Mouritsen. Molecular sorting of lipids by bacteriorhodopsin in dilauroylphosphatidylcholine / distearoylphosphatidylcholine lipid bilayers. *Biophysical Journal*, 73(4):1940–1953, 1997.

[55] A. Alessandrini and P. Facci. Unraveling lipid/protein interaction in model lipid bilayers by atomic force microscopy. *Journal of Molecular Recognition*, 24(3):387–396, 2011.

[56] J. B. Hutchison, R. M. Weis, and A. D. Dinsmore. Change of line tension in phase-separated vesicles upon protein binding. *Langmuir*, 28(11):5176–5181, 2012.

[57] S. Yang, V. Kiessling, J. A. Simmons, J. M. White, and L. K. Tamm. Hiv gp41–mediated membrane fusion occurs at edges of cholesterol-rich lipid domains. *Nature Chemical Biology*, 11(6):424, 2015.

[58] S. Yang, V. Kiessling, and L. K. Tamm. Line tension at lipid phase boundaries as driving force for hiv fusion peptide-mediated fusion. *Nature Communications*, 7(1):1–9, 2016.

[59] N. Sperelakis. *Cell physiology source book: essentials of membrane biophysics*. Elsevier, 2012.

[60] S. Nebel, P. Ganz, and J. Seelig. Heat changes in lipid membranes under sudden osmotic stress. *Biochemistry*, 36(10):2853–2859, 1997.

[61] T. Hamada, Y. Miura, K. Ishii, S. Araki, K. Yoshikawa, M. Vestergaard, and M. Takagi. Dynamic processes in endocytic transformation of a raft-exhibiting giant liposome. *The Journal of Physical Chemistry B*, 111(37):10853–10857, 2007.

[62] N. Wongsirojkul, N. Shimokawa, P. Opaprakasit, M. Takagi, and T. Hamada. Osmotic-tension-induced membrane lateral organization. *Langmuir*, 36(11):2937–2945, 2020.

[63] J. A. Lundbæk, S. A. Collingwood, H. I. Ingólfsson, R. Kapoor, and O. S. Andersen. Lipid bilayer regulation of membrane protein function: gramicidin channels as molecular force probes. *Journal of The Royal Society Interface*, 7(44):373–395, 2010.

[64] M. A. Lemmon. Phosphoinositide recognition domains. *Traffic*, 4(4):201–213, 2003.

[65] I. Lassing and U. Lindberg. Specific interaction between phosphatidylinositol 4, 5-bisphosphate and profilactin. *Nature*, 314(6010):472–474, 1985.

[66] M. J. Berridge and R. F. Irvine. Inositol phosphates and cell signalling. *Nature*, 341(6239):197–205, 1989.

[67] J. Folch. Brain cephalin, a mixture of phosphatides. separation from it of phosphatidyl serine, phosphatidyl ethanolamine, and a fraction containing an inositol phosphatide. *Journal of Biological Chemistry*, 146(1):35–44, 1942.

[68] M. B. Naeini, V. Bianconi, M. Pirro, and A. Sahebkar. The role of phosphatidylserine recognition receptors in multiple biological functions. *Cellular & Molecular Biology Letters*, 25(1):1–17, 2020.

[69] G. Di Paolo and P. De Camilli. Phosphoinositides in cell regulation and membrane dynamics. *Nature*, 443(7112):651–657, 2006.

[70] B. Payrastre, K. Missy, S. Giuriato, S. Bodin, M. Plantavid, and M. Gratacap. Phosphoinositides: key players in cell signalling, in time and space. *Cellular Signalling*, 13(6):377–387, 2001.

[71] L. Stephens, F. T. Cooke, R. Walters, T. Jackson, S. Volinia, I. Gout, M. D. Waterfield, and P. T. Hawkins. Characterization of a phosphatidylinositol-specific phosphoinositide 3-kinase from mammalian cells. *Current Biology*, 4(3):203–214, 1994.

[72] C. Huang, S. Feng, and D. W. Hilgemann. Direct activation of inward rectifier potassium channels by pip_2 and its stabilization by $g\beta\ \gamma$. *Nature*, 391(6669):803–806, 1998.

[73] M. R. Hokin and L. E. Hokin. Metabolism and physiological significance of lipids. *by RMC Dawson and DN Rhodes, John Wiley and Sons Ltd., London*, page 423, 1964.

[74] H. Yen, K. K. Hoi, I. Liko, G. Hedger, M. R. Horrell, W. Song, D. Wu, P. Heine, T. Warne, Y. Lee, et al. Pip_2 stabilises active states of gpcrs and enhances the selectivity. *Nature*, 559, 2018.

[75] G. Van Den Bogaart, K. Meyenberg, H. J. Risselada, H. Amin, K. I. Willig, B. E. Hubrich, M. Dier, S. W. Hell, H. Grubmüller, U. Diederichsen, et al. Membrane protein sequestering by ionic protein–lipid interactions. *Nature*, 479(7374):552–555, 2011.

[76] A. Rice, J. Parrington, K. T. Jones, and K. Swann. Mammalian sperm contain a ca2+-sensitive phospholipase c activity that can generate $insp_3$ from pip_2 associated with intracellular organelles. *Developmental biology*, 228(1):125–135, 2000.

[77] S. B. Hansen. Lipid agonism: The pip_2 paradigm of ligand-gated ion channels. *Biochimica Et Biophysica Acta (BBA)-Molecular and Cell Biology of Lipids*, 1851(5):620–628, 2015.

[78] Y. Liu, L. Casey, and L. J. Pike. Compartmentalization of phosphatidylinositol 4, 5-bisphosphate in low-density membrane domains in the absence of caveolin. *Biochemical and Biophysical Research Communications*, 245(3):684–690, 1998.

[79] M. G. Waugh, D. Lawson, S. K. Tan, and J. J. Hsuan. Phosphatidylinositol 4-phosphate synthesis in immunoisolated caveolae-like vesicles and low buoyant density non-caveolar membranes. *Journal of Biological Chemistry*, 273(27):17115–17121, 1998.

[80] P. De Camilli, S. D. Emr, P. S. McPherson, and P. Novick. Phosphoinositides as regulators in membrane traffic. *Science*, 271(5255):1533–1539, 1996.

[81] S. McLaughlin, J. Wang, A. Gambhir, and D. Murray. Pip_2 and proteins: interactions, organization, and information flow. *Annual review of biophysics and biomolecular structure*, 31(1):151–175, 2002.

[82] L. A. Finney and T. V. O'Halloran. Transition metal speciation in the cell: insights from the chemistry of metal ion receptors. *Science*, 300(5621):931–936, 2003.

[83] J. Szpunar. Metallomics: a new frontier in analytical chemistry. *Analytical and Bioanalytical Chemistry*, 378(1):54–56, 2004.

[84] C. Giorgi, A. Danese, S. Missiroli, S. Patergnani, and P. Pinton. Calcium dynamics as a machine for decoding signals. *Trends in Cell Biology*, 28(4):258–273, 2018.

[85] B. Zhao and L. Wan. Metal metabolic homeostasis disruption and early initiation of mechanism for alzheimer's disease. *Progress in Biochemistry and Biophysics*, 39(8):756–763, 2012.

[86] C. E. Outten and T. V. O'Halloran. Femtomolar sensitivity of metalloregulatory proteins controlling zinc homeostasis. *Science*, 292(5526):2488–2492, 2001.

[87] D. Papahadjopoulos, S. Nir, and N. Düzgünes. Molecular mechanisms of calcium-induced membrane fusion. *Journal of Bioenergetics and Biomembranes*, 22(2):157–179, 1990.

[88] N. Shimokawa, M. Hishida, H. Seto, and K. Yoshikawa. Phase separation of a mixture of charged and neutral lipids on a giant vesicle induced by small cations. *Chemical Physics Letters*, 496(1-3):59–63, 2010.

[89] H. Himeno, N. Shimokawa, S. Komura, D. Andelman, T. Hamada, and M. Takagi. Charge-induced phase separation in lipid membranes. *Soft Matter*, 10(40):7959–7967, 2014.

[90] A. Filippov, G. Orädd, and G. Lindblom. Effect of nacl and $cacl_2$ on the lateral diffusion of zwitterionic and anionic lipids in bilayers. *Chemistry and Physics of Lipids*, 159(2):81–87, 2009.

[91] C. G. Sinn, M. Antonietti, and R. Dimova. Binding of calcium to phosphatidylcholine–phosphatidylserine membranes. *Colloids and Surfaces A: Physicochemical and Engineering Aspects*, 282:410–419, 2006.

[92] R. Hidese, K. M. Tse, S. Kimura, E. Mizohata, J. Fujita, Y. Horai, N. Umezawa, T. Higuchi, M. Niitsu, T. Oshima, T Imanaka, and T. Inoue. Active site geometry of a novel aminopropyltransferase for biosynthesis of hyperthermophile-specific branched-chain polyamine. *The FEBS Journal*, 284(21):3684–3701, 2017.

[93] M. D. Groppa and M. P. Benavides. Polyamines and abiotic stress: recent advances. *Amino Acids*, 34(1):35, 2008.

[94] R. A. Casero Jr and A. E. Pegg. Polyamine catabolism and disease. *Biochemical Journal*, 421(3):323–338, 2009.

[95] L. Miller-Fleming, V. Olin-Sandoval, K. Campbell, and M. Ralser. Remaining mysteries of molecular biology: the role of polyamines in the cell. *Journal of Molecular Biology*, 427(21):3389–3406, 2015.

[96] J. Pelta, F. Livolant, and J. L. Sikorav. Dna aggregation induced by polyamines and cobalthexamine. *Journal of Biological Chemistry*, 271(10):5656–5662, 1996.

[97] M. Kudou, K. Shiraki, S. Fujiwara, T. Imanaka, and M. Takagi. Prevention of thermal inactivation and aggregation of lysozyme by polyamines. *European Journal of Biochemistry*, 270(22):4547–4554, 2003.

[98] Y. Terui, M. Ohnuma, K. Hiraga, E. Kawashima, and T. Oshima. Stabilization of nucleic acids by unusual polyamines produced by an extreme thermophile, thermus thermophilus. *Biochemical Journal*, 388(2):427–433, 2005.

[99] T. Nishio, Y. Yoshikawa, Wakao F., N. Umezawa, T. Higuchi, S. Fujiwara, T. Imanaka, and K. Yoshikawa. Branched-chain polyamine found in hyperthermophiles induces unique temperature-dependent structural changes in genome-size dna. *ChemPhysChem*, 19(18):2299, 2018.

[100] K. Okada, R. Hidese, W. Fukuda, M. Niitsu, K. Takao, Y. Horai, N. Umezawa, T. Higuchi, T. Oshima, Y. Yoshikawa, T. Imanaka, and S. Fujiwara. Identifica-

tion of a novel aminopropyltransferase involved in the synthesis of branched-chain polyamines in hyperthermophiles. *Journal of Bacteriology*, 196(10):1866–1876, 2014.

[101] M. Rong, Z. Chen, D. Jiang, and B. Kang. The role and mechanism of polyamine in cancer therapy. *Biotechnology Bulletin*, 32(2):46–50, 2016.

[102] E. Raspaud, I. Chaperon, A. Leforestier, and F. Livolant. Spermine-induced aggregation of dna, nucleosome, and chromatin. *Biophysical journal*, 77(3):1547–1555, 1999.

[103] N. C. de la Peña, J. A. Sosa-Melgarejo, R. R. Ramos, and J. D. Méndez. Inhibition of platelet aggregation by putrescine, spermidine, and spermine in hypercholesterolemic rabbits. *Archives of medical research*, 31(6):546–550, 2000.

Chapter 2

Three-phase coexistence in binary charged lipid membranes in hypotonic solution

This chapter is based on the integration, update, and abridgment of the following publications:

- J. Guo, H. Ito, Y. Higuchi, K. Bohinc, N. Shimokawa, M. Takagi. (2021). Three-Phase Coexistence in Binary Charged Lipid Membranes in a Hypotonic Solution. *Langmuir*, 37(32), 9683-9693. [1]

2.1 Chapter Introduction

Biomembranes are membrane structures that distinguish the internal and external environments of cells, and the main component is phospholipid. Phospholipids are amphiphilic molecules that spontaneously form a closed bilayer membrane structure in water called liposome. Liposomes are widely usedas simple model biomembrane systems because of its composition and structure are similar to biomembranes. Among them, in multicomponent liposomes, different ratios of lipid molecules that constitute the membranes, or changes in ambient temperature, can make phase separation structures appear [2] [3] [4]. This phase separation structure is thought to be highly similar to the raft region on biomembranes so that the phase separation structure can be used as a model for lipid raft. It is now known that raft structure is related to some critical cellular functions, such as membrane trafficking and cellular signal transduction [5] [6]. The studies of phase separation structures on model membranes can contribute to understanding cellular processes.

Several studies have shown that the phase separation structure disappears with increasing temperature due to mixing entropy. The effect of temperature on phase separation determines, to some extent, the thermodynamic properties of lipid membranes. However, since the environment in organisms is generally at a constant temperature, it is essential to understand how the phase separation structure will change at a constant temperature [7].

From considering this aspect of the natural environment in organisms, the negatively charged lipids such as phosphatidylserine(PS); phosphatidylglycerol(PG); phosphatidylinositol(PI) in biological membranes should not be ignored. These negatively charged lipids play a crucial role in biological membranes, such as membrane potential generation, protein adsorption, and ion channel activity. [8] [9] [10]. In recent years researchers have started to focus on the behavior of membrane structures containing charged lipids. Unlike liposomes composed of neutral lipids, the phase separation of liposomes containing charged lipids is inhibited by electrostatic repulsion between charged lipids. However, at the same time, it has been shown the addition of salts can induce the phase separation because of screening of the electrostatic repulsion. The addition of salts is a method that does not

change the temperature but can control the phase separation behavior. [11] [12] [13]

In addition, it has been indicated that in solutions with hypotonic solution, osmotic pressure can induce phase separation in neutral lipid membranes [14] [15]. The osmotic pressure in the organism is also crucial, as it is closely related to blood pressure, fluid metabolism, etc. The lateral tension on the membrane induced by the osmotic pressure can even affect the ion channel activity [16].

Due to the semipermeable, GUVs can be affected by osmotic pressure and thus shrink or swell, thus allowing osmotic pressure studies to be performed using GUVs. The swelling due to osmotic pressure suppresses membrane fluctuations and makes the fluctuation entropy lower. Due to the presence of the solid-ordered phase, the membrane fluctuation in the phase separation state membrane is more minor than those of the homogeneous membrane. Therefore, under the applied osmotic pressure, the homogeneous membrane with large membrane fluctuation strongly suppressed the fluctuation and relatively becomes unstable than the phase separated membrane. Also, in the experiment with vesicles adsorbed to a solid substrate, a similar phase separation behavior was observed [17]. The application of osmotic pressure is also a method that does not change the temperature but can control the phase separation behavior. Although the experiments of osmotic swelling on the phase separation in electrically neutral membranes have been performed, the effect of applied osmotic pressure on charged lipid membranes is not clear yet.

In this chapter, we used fluorescence microscopy and confocal laser scanning microscopy to investigate the phase separation of lipid membranes containing charged lipids in hypotonic solutions. The model membranes containing charged lipids used consisted of the negatively charged unsaturated lipid dioleoylphosphatidylserine (DOPS) and the zwitterionic saturated lipid dipalmitoylphosphatidylcholine (DPPC).

First, we investigated the phase separation behavior in hypotonic solutions of different pH values, which was used to examine the effect of ionization of the headgroup of DOPS on the phase separation behavior. Considering the ionization of DOPS, even though the model membrane consists of only two components, DOPS and DPPC, we can still treat it as a system similar to the presence of three components. Second, to investigate the position of each constituent on the model membrane, we used positively charged particles adsorbed onto the membrane and identified the specific constituents by the degree

of adsorption. Finally, we performed coarse-grained molecular dynamics simulations to analyze and discuss the stability of the phase separation structure and the mechanism of coexistence of the three phases.

2.2 Materials and Methods

2.2.1 Materials

The zwitterionic saturated lipid, 1,2-dipalmitoyl-sn-glycero-3-phosphocholine (DPPC), and the negatively charged unsaturated lipid, 1,2-dioleoyl-sn-glycero-3-phospho-l-serine (sodium salt) (DOPS), were purchased from Avanti Polar Lipids, Inc(Alabaster, AL).

Rhodamine B 1,2-dihexadecanoyl-sn-glycero-3-phosphoethanolamine, triethylammonium salt (Rho-DHPE) and Texas Red 1,2-dihexadecanoyl-sn-glycero-3-phosphoethanolamine, triethylammonium salt (Texas Red DHPE) was obtained from Thermo Fisher Scientific (Waltham, US). 1,2-Dipalmitoyl-sn-glycero-3-phosphoethanolamine-N-(7-nitro-2-1,3-benzoxadiazol-4-yl) (ammonium salt) (NBD-PE) was obtained from Avanti Polar Lipids (Alabaster, AL). 1,1'-dioctadecyl-3,3,3',3'-tetramethylindocarbocyanine perchlorate (DiI) was obtained from PromoKine (Heidelberg, Germany). Molecular structure of lipids and fluorescent probes are showen in Figure 2.1 and 2.2.

D(+)-Glucose was purchased from Nacalai Tesque (Kyoto, Japan). D_2O was purchased from SCETI (Tokyo, Japan). Deionized water (specific resistance $\geq$ 18 MΩ) used in this study was obtained from a Millipore Milli-Q purification system (Burlington, MA).

- Unsaturated lipids

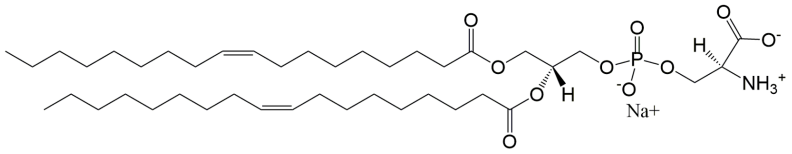

1,2-dioleoyl-*sn*-glycero-3-phospho-L-serine
DOPS (Negatively charged lipid)

- Saturated lipids

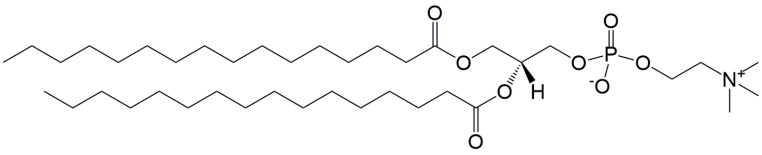

1,2-dipalmitoyl-*sn*-glycero-3-phosphocholine
DPPC (Zwitterionic lipid)

Figure 2.1: Molecular structure of lipids

- Fluorescent probes

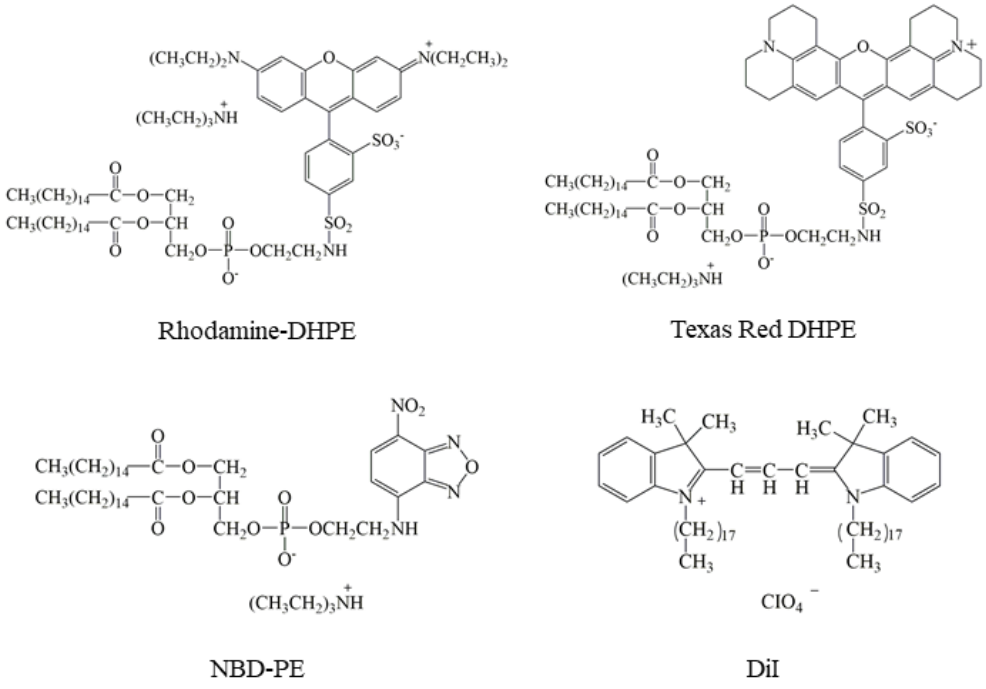

Figure 2.2: Molecular structure of fluorescent probes

2.2.2 Preparation of giant unilamellar vesicles

Giant unilamellar vesicles (GUVs) were prepared by the natural swelling method. All lipids were dissolved in a 2:1 (v/v) chloroform/methanol solution, and afforded concentrations of 2mM. All kind of fluorescent probes were dissolved in chloroform, afford concentrations of 0.1mM. Lipids (DOPS and DPPC) were mixed in three kinds of ratios, DOPS/DPPC=70/30, DOPS/DPPC=50/50, DOPS/DPPC=30/70, and for each ratio the total volumes were kept with 20μL. For fluorescence microscopy observation, Rho-DHPE 2μL was used. The control group used fluorescence microscopy was added Texas Red DHPE or Dil 2μL as the same way. For confocal laser scanning microscopy observation, Rho-DHPE 2μL and NBD-PE 4μL were used at the same time. After well mixed, dried the mixed solution with nitrogen gas, then put the formed lipid films into a vacuum desiccator for at least 3h. To produce the liposomes, films were then pre-hydration for 10min using 5μL Milli-Q water at 55°C. Then, hydrated using 195μL glucose solution or pH-adjusted glucose solution at 37°C for at least 3h and under 24h. The pH-adjusted glucose solution was prepared by adding HCl or NaOH solution, and pH value was measured by pH meter (LAQUA act D-72, HORIBA, Japan). Glucose was dissolved by these HCl and NaOH solutions and can obtain the pH-adjusted glucose solution. Also, the pH value of Milli-Q water for preparing the glucose solution without HCl and NaOH was measured to make sure it was near to 7 (the measured value was 6.96±0.14). And results used glucose solution dissolved by Milli-Q water were used as the results for pH=7. The concentrations of glucose were 100 and 200mM and were used depending on the osmotic pressure required. The preparation process are shown in the Figure 2.3.

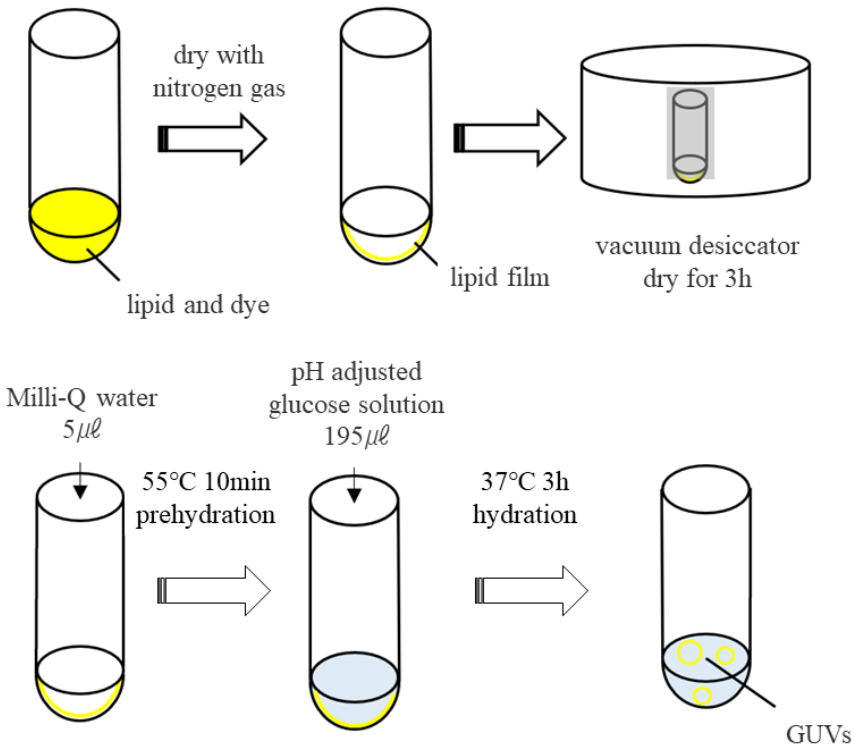

Figure 2.3: Preparation of GUVs

2.2.3 Microscopic observations under osmotic stress

Before microscopic observation, apply osmotic pressure to the prepared GUV solution. Mixed GUV solution with water which has the same pH as the glucose solution used for GUVs, to dilute the glucose concentration outside the GUVs and make the concentration outside lower than inside to apply an osmotic pressure. Because the membranes of GUVs are semipermeable like cell membranes, water can inflow through the membranes. Thus, water entered the inside of GUVs, the volume inside the GUV was increased. Since the membrane area of the GUV remains unchanged, the membrane was stretched by the increased volume, resulting in a lateral tension. (Figure 2.4)

After mixed, wait for 3min before observation. After adding water, make concentration differences Δc = 0, 20, 40, 60, 80, or 100 mM across the lipid membrane. We used a 200 mM glucose solution to make concentration differences Δc=0, 80, and 100 mM. In

addition, 100 mM glucose solution was used to make concentration differences Δc=20, 40, and 60 mM.

We used a small chamber, as shown in the Figure 2.5, for microscopic observation. A silicon sheet with a circular hole in the middle was placed on the slide glass, and the prepared GUVs solution was dripped into the circular hole and added a cover glass on top. Then the observation was performed at room temperature ($\sim$ 22.5 $\pm$ 2.5°C) using a fluorescence microscope (IX71, Olympus) and a confocal laser scanning microscope (FV-1000, Olympus). We kept the observation time of each sample within 90s. This is because too long observation time can lead to photo-induced oxidation. For each lipid composition and concentration difference, we observed 90 GUVs with diameters 5μm $\sim$ 20μm to obtain statistical data.

In addition, we prepared an observation chamber with two small compartments separated by a polycarbonate membrane filter (pore size 0.4 μm, Whatman) to take a real-time video of the phase separation process, the chamber is shown in Figure 2.6. The experiment was performed only at Δc = 100 mM. The GUVs solution was dropped in the lower chamber and covered with cover glass, and then the entire chamber was inverted on the confocal laser scanning microscope (FV-1000, Olympus). After finding the GUVs suitable for observation, we added Milli-Q water to the upper chamber and set the moment to 0 s. The Milli-Q water percolated through the polycarbonate membrane filter into the lower chamber. As the water infiltrates, the GUVs solution is diluted, and, as with direct addition, the osmotic pressure causes the GUVs to swell, resulting in lateral tension.

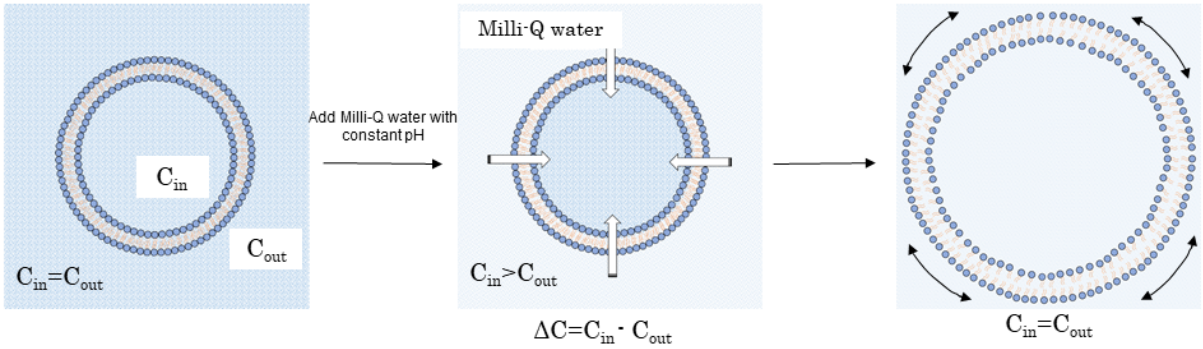

Figure 2.4: Schematic illustration of osmotic pressure addition

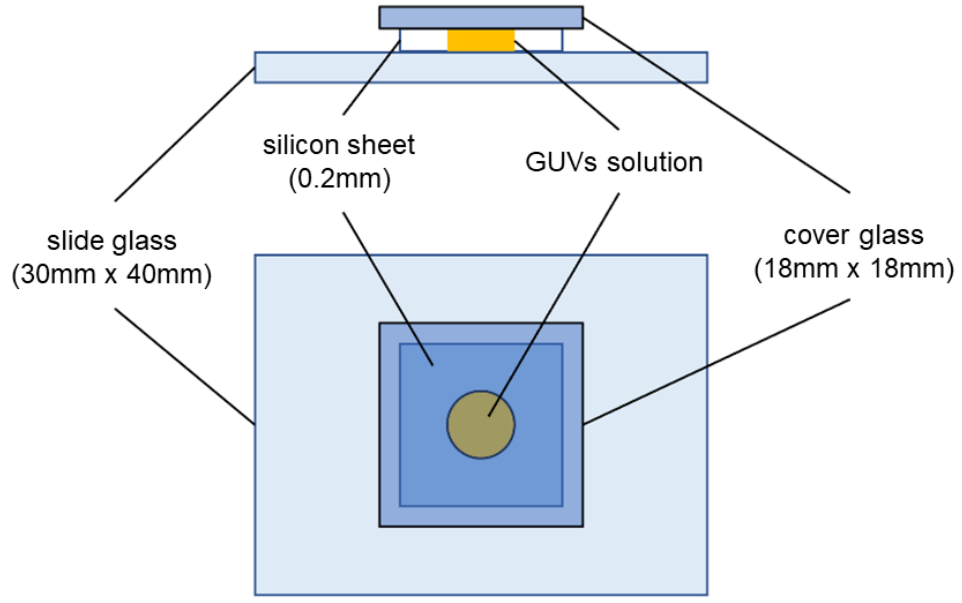

Figure 2.5: Schematic illustration of chamber for microscopic observation

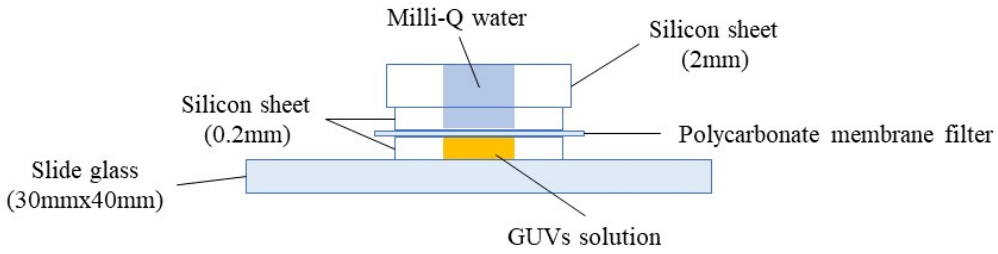

Figure 2.6: Schematic of chamber for real time microscopic observation

2.2.4 Adsorption of Particles onto GUVs

To identify the different regions created during phase separation, we observed the adsorption of positively charged particles on the GUVs. We used amine-modified polystyrene latex beads (fluorescent orange aqueous suspension, 2.5 wt %, mean particle size 1 μm) purchased from Merck. The colloidal suspension was well diluted to 370 times using Milli-Q water and later mixed with GUVs solution in a ratio of colloidal suspension: GUVs solution = 2:35. The samples were observed using a fluorescence microscope or confocal laser scanning microscope, and the number of particles adsorbed on the different phase separation regions was counted.

2.2.5 Coarse-grained molecular dynamics simulations

The coarse-grained molecular dynamics simulations used in this study took the model proposed by Cooke et al [18]. Also this model was used in previous studies to simulate the interaction between charged lipid membranes and nanoparticles [19] [20] [21]. And in this chapter we develop it to simulate the phase separation of charged lipid mixtures with three components.

The lipid molecules are modeled as a hydrophilic head composed of one bead and a hydrophobic tail consisting of two beads. These beads are connected linearly through springs. The short-range repulsive potential is used to represent the excluded volume interaction between two beads separated by a distance r and can be expressed by the following equation,

$$V_{\mathrm{re}}(r;b_i) = \begin{cases} 4v[(\frac{b_i}{r})^{12} - (\frac{b_i}{r})^{6} + \frac{1}{4}] & r \le r_c \\ 0 & r > r_c \end{cases} \tag{2.1}$$

where r_c is the cutoff length for the excluded volume interactions. r_c is defined as b_i, $r_c = 2^{1/6}b_i$. i represents three possibilities, head-head, head-tail, or tail-tail. $b_{head-head} =$

$b_{head-tail} = 0.95\sigma$ and $b_{tail-tail} = \sigma$ were set for stable bilayer formation. σ represents the unit of length and corresponds to the cross-sectional diameter of a single lipid molecule, here aproximately 7 Å. $v = k_{\mathrm{B}}T$ is the unit of energy, where k_{B} is the Boltzmann constant and T is the absolute temperature.

The stretching potential of the spring between the connecting beads can be expressed as,

$$V_{\mathrm{st}}(r) = \frac{1}{2}k_{\mathrm{st}}(r-\sigma)^2 \tag{2.2}$$

and the bending potentials of the spring between the connecting beads can be expressed as,

$$V_{\mathrm{be}}(\theta) = \frac{1}{2}k_{\mathrm{be}}(1-\cos\theta)^2 \tag{2.3}$$

where $k_{\mathrm{st}} = 500v$ and $k_{\mathrm{be}} = 60v$ are the spring constant and the bending stiffness of a lipid molecule, respectively. θ is the angle between the adjacent bond vectors. Plus, the hydrophobic attractions between hydrophobic beads are represented by,

$$V_{\mathrm{at}}(r) = \begin{cases} -v & r < r_{\mathrm{c}} \\ -v\cos^2[\frac{\pi(r-r_{\mathrm{c}})}{2w_{\mathrm{c}}}] & r_{\mathrm{c}} \le r \le r_{\mathrm{c}} + w_{\mathrm{c}} \\ 0 & r > r_{\mathrm{c}} + w_{\mathrm{c}} \end{cases} \tag{2.4}$$

where w_{c} is the cutoff length for the hydrophobic attraction. In this equation, we can represented qualitatively the ordered or disordered phases in the lipid membranes by varying the value of w_{c}. That is, when w_{c} is larger, the membrane can be considered as ordered phase (saturated lipid-rich phase), while when w_{c} is small it can be considered as disordered phase (unsaturated lipid-rich phase). [18] Since our experiments focus on the phase behavior of charged lipid membranes, we also need to represent the role of charged lipids in our simulations. For this purpose, we considered the electrostatic repulsion between the DOPS headgroups. Expressed by the following Debye–Hückel potential as,

$$V_{\mathrm{el}}(r) = v l_{\mathrm{B}} z_1 z_2 \frac{\exp(-r/l_{\mathrm{D}})}{r} \tag{2.5}$$

where l_{B} is the Bjerrum length, which is σ (approximately 7 Å). And Debye screening

length l_{D} is defined as,

$$l_{\mathrm{D}} = \sigma\sqrt{\frac{\varepsilon k_{\mathrm{B}} T}{n_0 e^2}} \tag{2.6}$$

where ε is the dielectric constant of the solution. e is the elementary charge. n_0 is the salt concentration and was set at 100mM. z_1 and z_2 are the valence of charged headgroup and were set at -1, bcause DOPS has the negative monovalent charge.

With respect to the stochastic dynamics of each bead, they obey the Langevin equation,

$$m\frac{d^2 r_i}{dt^2} = -\eta\frac{dr_i}{dt} + \boldsymbol{f}_i^V + \boldsymbol{\xi}_i \tag{2.7}$$

where i denotes the i-th bead. Mass coefficient m and drag coefficientand η are $m = \eta = 1$. And by the derivatives of eqs(2.1)-(2.5) we can calculated the force $\boldsymbol{f}_i^V$. The constant τ was used as the units for the timescale, where $\tau = \eta\sigma^2/v$, and the time increment was set to $dt = 7.5 \times 10^{-3}\tau$. For the Brownian force $\boldsymbol{\xi}_i$ can calculat with the fluctuation–dissipation theorem as,

$$\langle \boldsymbol{\xi}_i(t)\boldsymbol{\xi}_j(t')\rangle = 6v\eta\delta_{ij}\delta(t-t') \tag{2.8}$$

where δ_{ij} is the Kronecker delta and $\delta(t-t')$ is Dirac delta function.

Using this model, we simulated a ternary mixture of negatively charged unsaturated lipids (A-lipids), neutral unsaturated lipids (B-lipids), and neutral saturated lipids (C-lipids). The calculated composition (the number of lipids) is A/B/C = 1000/1000/3000. A-lipids correspond to charged DOPS referred as DOPS(-). B-lipids correspond to protonated DOPS referred as DOPS(N). C-lipids correspond to DPPC. The initial state of the calculation was a spherical lipid bilayer with a homogeneously mixed lipid distribution. The same calculation was performed six times to ensure data reproducibility and to obtain representative results.

2.2.6 Fluorescence anisotropy measurements

To reveal the order of the lipid tail, we measured the fluorescence anisotropy of 1,6-Diphenyl-1,3,5-hexatriene (DPH) in a single lipid membrane of DOPS. DPH is a kind of fluorescence anisotropy probe commonly used to investigate the kinetic characteristics of

lipid bilayers. The fluorescence anisotropy of DPH can be used as a parameter of the fluidity of the lipid tail in lipid bilayer (lipid order). Fluorescence anisotropy measures the extent to which the fluorescent probe DPH wobbles with lipid tails. If the lipid tails are highly ordered, the DPH molecule tends to be stationary and emits fluorescence in the same direction as the incident light. However, if the lipid tails are disordered, the DPH molecules wobble with the tails, and the fluorescence emitted is polarized in a different direction from the incident light. For this experiment, single component GUVs of DOPS were used.

Giant unilamellar vesicles (GUVs) were prepared by the natural swelling method. DOPS was dissolved in a 2:1 (v/v) chloroform/methanol solution, and afforded concentrations of 20mM. DPH was dissolved in chloroform, afford concentrations of 0.2mM. DOPS 65μL and DPH 30μL were well mixed and dried with nitrogen gas, then put the formed lipid films into a vacuum desiccator for at least 3h. To prepare the GUVs, films were then added with 50μL Milli-Q water and mixed well. Put the mixed solution in sonication set as 55°C which is above the DOPS main transition temperature T_{m} =-11℃ for 1 h to form vesicles. After sonicated, 200 Milli-Q water was mixed with the GUVs solution and then filtered more than 20 times on a heated platform at 55°C with a Mini-Extruder which set a pore size 400nm filter, to obtain vesicles with smaller and uniform sizes. Mini-Extruder was purchased from Avanti Polar Lipids, Inc(Alabaster, AL). Take 100 μL of the prepared vesicles solution and mix it with 1900 μL of Milli-Q water or pH-adjusted Milli-Q water, and place it in a quartz cuvette for fluorescence anisotropy measurement.

Examined for changes in membrane fluidity using a FP-6500 spectrofluorometer (JASCO Co. Tokyo, Japan) set with two polarizers (JASCO Co. Tokyo, Japan). The temperature range for measurement was 20-35°C with an interval of 2°C. After placing the sample, the sample was allowed to stabilize for 10 min at the required temperature. The excited wavelength was λ_{ex}=357 nm, and the fluorescence intensity was monitored at λ_{em}=430 nm. Anisotropy values r was calculated as,

$$r = \frac{I_{\mathrm{VV}} - GI_{\mathrm{VH}}}{I_{\mathrm{VV}} + 2GI_{\mathrm{VH}}} \tag{2.9}$$

where I is fluorescence intensities, V and H are the settings of the excitation and emission

polarizers, V delegate vertical, and H delegate horizontal. G is the correction factor, $G = I_{HV}/I_{HH}$ and need to calculate for each sample. Each pH and temperatures were measured three times to calculate the average value. The orderliness of the measured lipid bilayer was discussed based on the obtained r values. A larger r value represents a relatively more order state of the lipid bilayer.

2.3 Results

2.3.1 Phase separation induced by osmotic stress

In order to observe whether osmotic pressure can induce phase separation in membranes containing charged lipids, real-time observation was performed with a special observation chamber as described in 2.2. In this experiment, lipid composition was DOPS/DPPC=30/70 and the pH of the solution was set as pH=7. Milli-Q water was added to the upper chamber during observation. The difference in glucose concentration was Δc = 100 mM when the solutions in the upper and lower chambers were completely mixed. The observation results are shown in Figure 2.7. After the addition of Milli-Q water, at 3 s, we observed a homogeneous GUV. At 12 s, we observed that this GUV started to form phase separation and the phase separation is progressed over time, with a significant phase separation observed at 34 s. This shows that the addition of Milli-Q water quickly induces the phase separation.

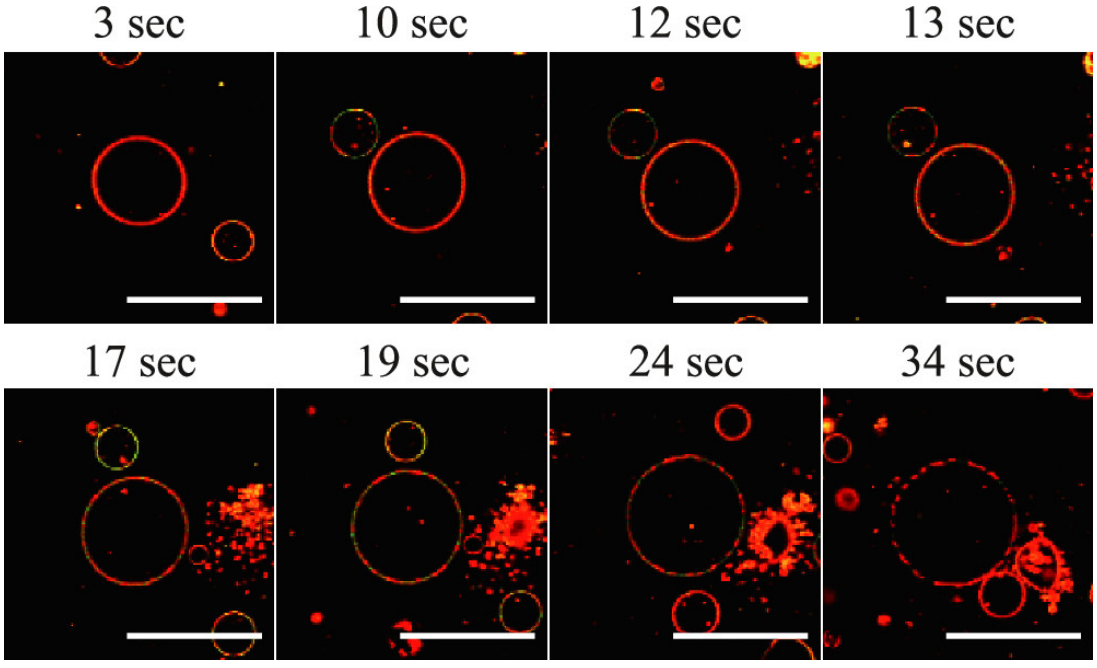

Figure 2.7: Real-time phase separation process images from the homogeneous phase-to-phase-separated state induced by osmotic pressure. Scale bars are 10 μm.

We observed phase separation structure at $\Delta c = 100$ mM in hypotonic solutions. And, two kinds of phase separation structures were observed using confocal laser scanning microscopy, as in Figure 2.8(a) and (b). For the two fluorescent probes used in this observation, Rho-DHPE is generally distributed in the unsaturated lipid-rich L_d phase, while NBD-PE tends to be distributed in the relatively ordered phase. Therefore it can be expected that the red region should correspond to the unsaturated lipid DOPS-rich L_d phase, and the green region should correspond to the S_o composed of saturated lipid DPPC. The fluorescence intensity along the white line in the merged image was measured and is presented in Figure 2.8(c), shows the two fluorescence intensities behave in opposite ways. There are only two regions on the lipid membranes, the red Rho-DHPE riched region, $I_{\mathrm{NBD}} > I_{\mathrm{Rho}}$, and the green NBD-PE riched region, $I_{\mathrm{NBD}} < I_{\mathrm{Rho}}$, where I_{NBD} and I_{Rho} indicate the fluorescent intensities of NBD-PE and Rho-DHPE, respectively.

Interestingly, we observed a three-phase coexistence like shown in Figure 2.8(b). Although we only used two lipids, we still observed this phase separation with the coexistence of three phases. These phases are red with Rho-DHPE, green with NBD-PE, and dark with no fluorescent probes. For this phase separation structure, we also measured the fluorescence intensity at the corresponding white line and shown in Figure 2.8(b). It can be seen that the measurement results present three states. Red Rho-DHPE rich region with $I_{\mathrm{NBD}} < I_{\mathrm{Rho}}$; green NBD-PE rich region with $I_{\mathrm{NBD}} > I_{\mathrm{Rho}}$; and dark region with less Rho-DHPE and NBD-PE. The dark region with less content of both Rho-DHPE and NBD-PE is only found in three-phase coexistence GUVs and is the main feature to distinguish the three-phase coexistence from the two-phase coexistence. Further analysis revealed that at the boundary, the fluorescence intensity of the red region dominated by Rho-DHPE was gradually decreased, while the fluorescence intensity of the green region dominated by NBD-PE was abruptly decreased. This indicates that the line tension at the boundary of the red and green regions is lower, while the line tension at the boundary of green and dark regions is larger. Therefore, it can be assumed that the red and green regions are riched in the same kind of lipid, while the dark region is riched in the different ones. Considering that the dark region hardly includes any fluorescent probes, we believe this part is an more ordered phase which riched in DPPC. However, it is still not possible to distinguish the specific lipid distribution in the red and green regions. Due to the

ionization properties of the DOPS headgroup, we consider that there are two different ionized states of DOPS, the negatively charged DOPS (DOPS(-)) and the undissociated (neutral) DOPS (DOPS(N)). Thus, we consider that the red and green regions may be the more disordered phase which riched in different properties DOPS.

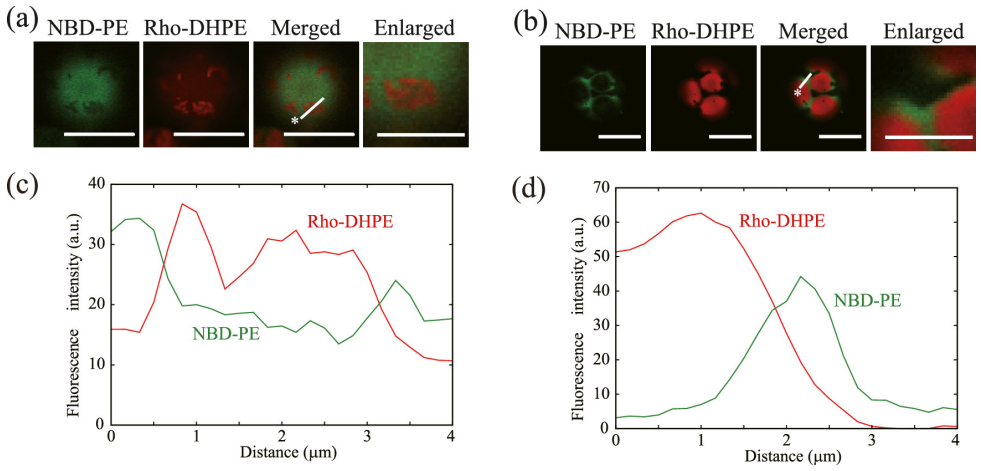

Figure 2.8: Confocal laser scanning microscopy images and fluorescence intensity profiles of GUVs at DOPS/DPPC=30:70 under Δc = 100mM. (a) Two-phase coexistence (b) Three-phase coexistence (c,d) Fluorescence intensity profiles along the white lines in the merged images in (a,b). Scale bars are 10 μm.

To investigate if other factors will affect the phase separation behavior, we also examined the effects of glucose concentration, the type of sugar we used, and the type of fluorescent probes. First, to examine that the glucose concentration does not affect the phase separation, and it is the concentration difference that induced the phase separation, we conducted experiments using various glucose concentrations while fixing that the concentration difference Δc = 0 mM. We observed at different glucose concentrations, ensuring that $\Delta c = 0$ mM. The results showed that the phase separation remained almost unchanged even when the glucose concentration was changed, in Figure 2.9(a). Therefore, we excluded the effect of glucose concentration and can assume that the concentration difference induced the lipid membrane phase separation.

Second, to examine that glucose does not specifically cause phase separation, we tried to experiment with other sugars. We performed the observation of imposed concentration

difference using sucrose, and the same phase separation structure was observed at DOPS/DPPC = 30/70, $\Delta c = 100$ mM, like in Figure 2.9(b). Therefore we concluded that the type of sugar did not affect the phase separation.

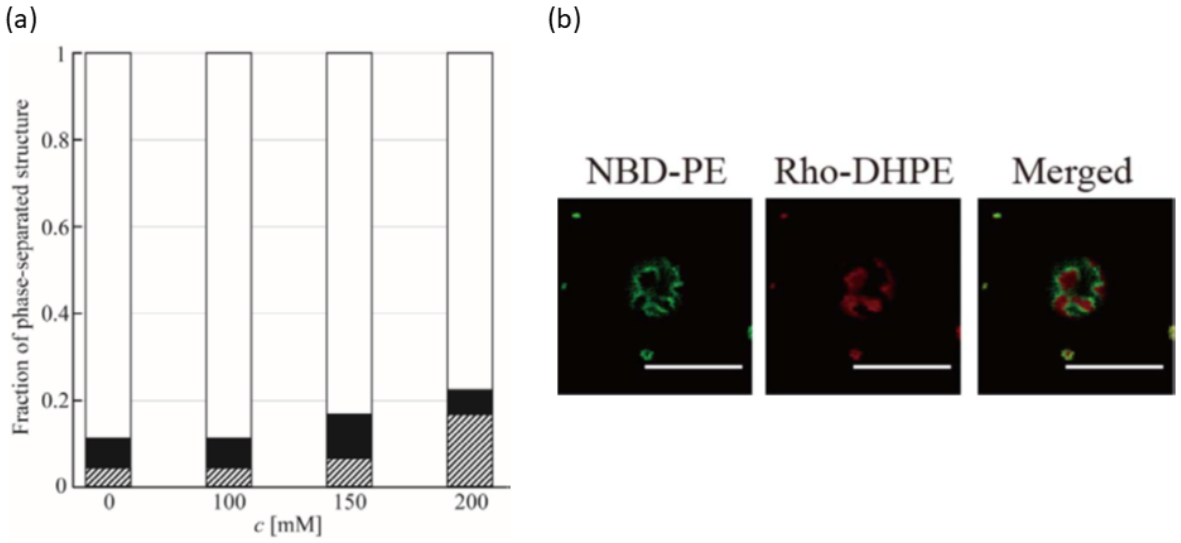

Figure 2.9: The glucose concentration does not affect the phase separation and glucose does not specifically cause phase separation. (a) Fraction of phase separated structure for DOPS/DPPC = 30/70 at pH = 7 with different glucose concentration c. Ensuring that $\Delta c = 0$ mM. The phase behavior was not influenced by the glucose concentration c and strong phase separation was not induced. (b) Fluorescence microscopy images of three-phase coexistence at DOPS/DPPC = 30:70 under $\Delta c = 100$mM using sucrose instead of glucose. Scale bars are 10 μm.

Last, we used two fluorescent probes Texas Red DHPE and DiI, for phase separation observation and measured the fluorescence. The results showed that the three-phase coexistence were observed, in Figure 2.10. This demonstrates that three-phase coexistence are independent of the type of fluorescent probes, and the three-phase coexistence structure is not subject to the choice of fluorescent probes.

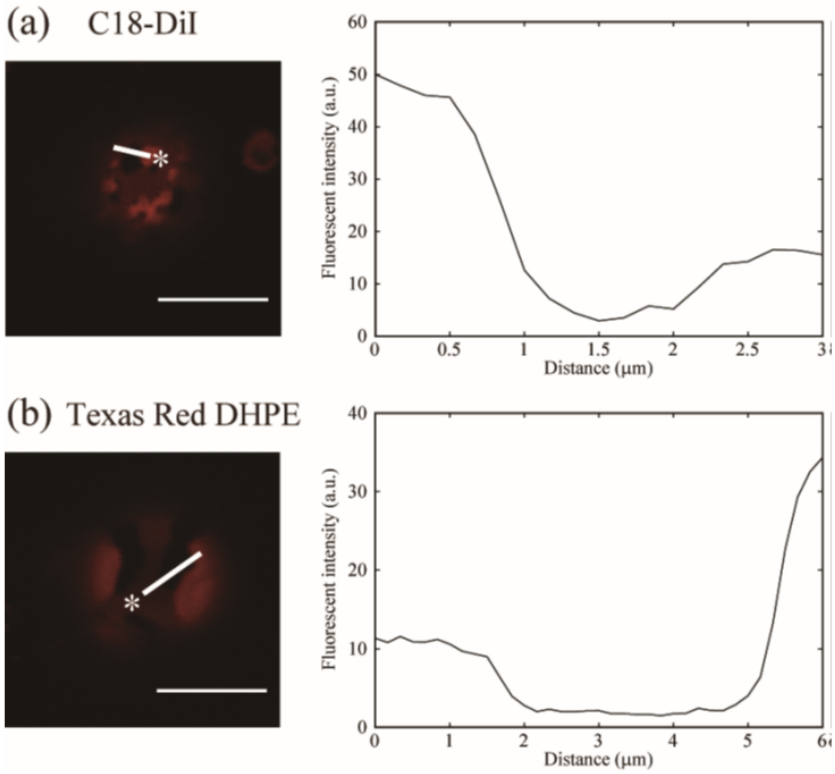

Figure 2.10: Fluorescence microscopy images and fluorescence intensity profiles of three-phase coexistence at DOPS/DPPC = 30:70 under $\Delta c = 100$mM with (a) DiI fluorescent probe and (b) Texas Red DHPE fluorescent probe. Scale bars are 10 μm.

2.3.2 Investigation of phase composition in three-phase coexistence

In the previous subsection, we described the phase separation structure of the three-phase coexisting states. We speculate that the dark region is the ordered phase rich in DPPC and the red and green regions contain two ionized states of DOPS, but we have not yet discerned the specific composition of the red and green regions. To distinguish, we performed adsorption experiments using positively charged particles. Positively charged particles were added from the outside of GUVs. Due to the presence of electrostatic attraction, these positively charged particles were expected to selectively adsorb to the

DOPS(-) riched region, which shows a negative charge. Since the phase separation in negatively charged lipid membranes may be affected by positively charged particles, we performed experiments at low concentrations of positively charged particles. We observed 36 particles and took confocal laser scanning microscopy images.

Results are shown in Figures 2.11. From the resulting image, it can be seen that the positively charged particles are selectively adsorbed on the green areas. Even though the area of the green region is relatively small, it still adsorbed 80% of the particles. Hamada et al. [22] reported that in experiments with neutral particles and neutral lipid membranes, particles larger than 200 nm tend to adsorb to the disordered phase. In comparison, smaller particles tend to adsorb to the ordered phase. In this experiment, we used a particle size of 1 μm, which is larger than 200 nm, so it can be presumed that it will preferentially adsorb to the DOPS riched disordered phase. The red and green regions are different ionization states of DOPS but have the same priority in terms of the degree of order. However, the results showed that the positively charged particles tend to adsorb to the green region, which can be explained by the fact that the green region is negatively charged and consists of DOPS(-). On the other hand, we can conclude that the red region is rich in DOPS(N).

Also, it is worth noting that for the distribution of the fluorescent probes we used, we generally assume that NBD-PE will be distributed to relatively ordered regions, but this cannot prove that the order degrees of those regions are precisely the same. So even the result showed that NBD-PE is distributed in DPPC in two-phase coexistence and DOPS(-) in three-phase coexistence, this does not prove that the degree of order is the same in DPPC and DOPS(-).

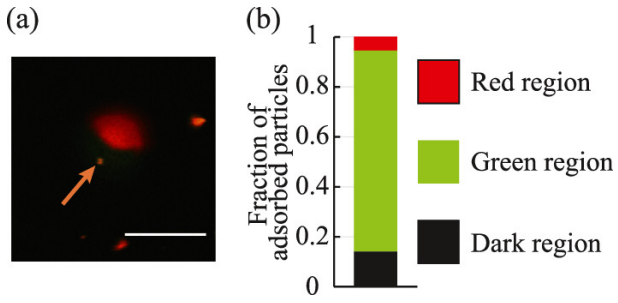

Figure 2.11: (a) Fluorescence microscopy images and (b) fraction of adsorbed particles on each phase-separated region. Scale bars are 10 μm.

2.3.3 Phase separation induced by tension under different pH conditions

After the previous discussion, we revealed that the three-phase coexistence might be composed of DPPC, DOPS(-), and DOPS(N)-rich phases. Since DOPS(-) and DOPS(N) are based on the ionization of the DOPS headgroup, we speculate that if the ionization fraction of DOPS changes, the amounts of DOPS(-) and DOPS(N) will also change. The change in their ratio would affect the phase behavior. Therefore, we tried to change the lipid ratios of GUV formation. Also we tried to change the pH of the GUV solution and applied osmotic pressure at that pH, then observed the tension-induced phase separation structure. Fluorescence microscopy and confocal microscopy were performed using a chamber as described in Figure 2.5. The lipid ratios of GUVs were DOPS/DPPC = 30/70, 50/50, and 30/70, the pH of the glucose solution was 6, 7, 8 and 9. The results are summarized in Figure 2.12 and typical confocal laser scanning microscopy images are showen in Figure 2.14.

The results showed that almost no phase separation structure was observed in all ratios when the GUVs were at $\Delta c = 0$ mM. This is consistent with the results of previous studies [11]. And the results also showed that all lipid ratios and pH values show an increasing trend of phase separation with increasing Δc. This result is consistent with the previous results using neutral lipids [14] [15]. It indicates that the membrane tension due to osmotic swelling can induce phase separation even for charged lipids-included membranes. The results were more evident at the ratio of DOPS/DPPC=30/70, where about 10% of GUVs were in the three-phase separation at pH=8, about 30-50% of GUVs were in the three-phase separation at pH=7, and more GUVs were in the three-phase separation at pH=6. However, at pH=5, the percentage of the three-phase coexistence state decreased to 20-30% instead. In addition, at the ratio of DOPS/DPPC=50/50, we hardly observed GUVs in the three-phase coexistence at pH=8 or pH=7, but they were abundantly present in the solution at pH=6.

Thus, we suggest that the generation of the three-phase coexistence state depends on the pH. This allows that the degree of ionization of the DOPS headgroup varies depending on the pH. And the ratio of DOPS(-) and DOPS(N) depends on the degree of ionization

of the DOPS headgroup then affects the phase behavior of the three-phase coexistence.

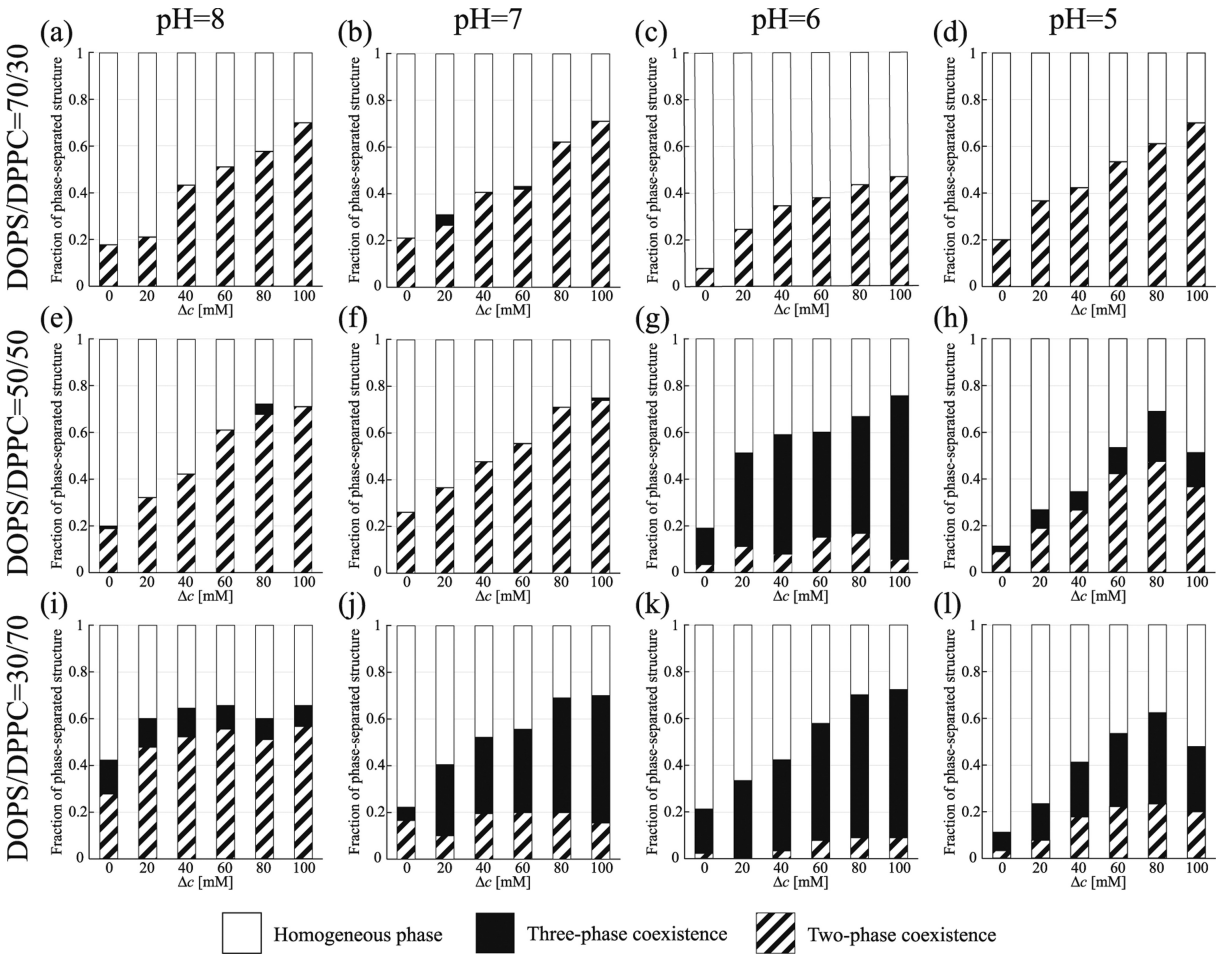

Figure 2.12: Fraction of the phase separation structure of DOPS / DPPC as a function of glucose concentration difference across lipid membrane.

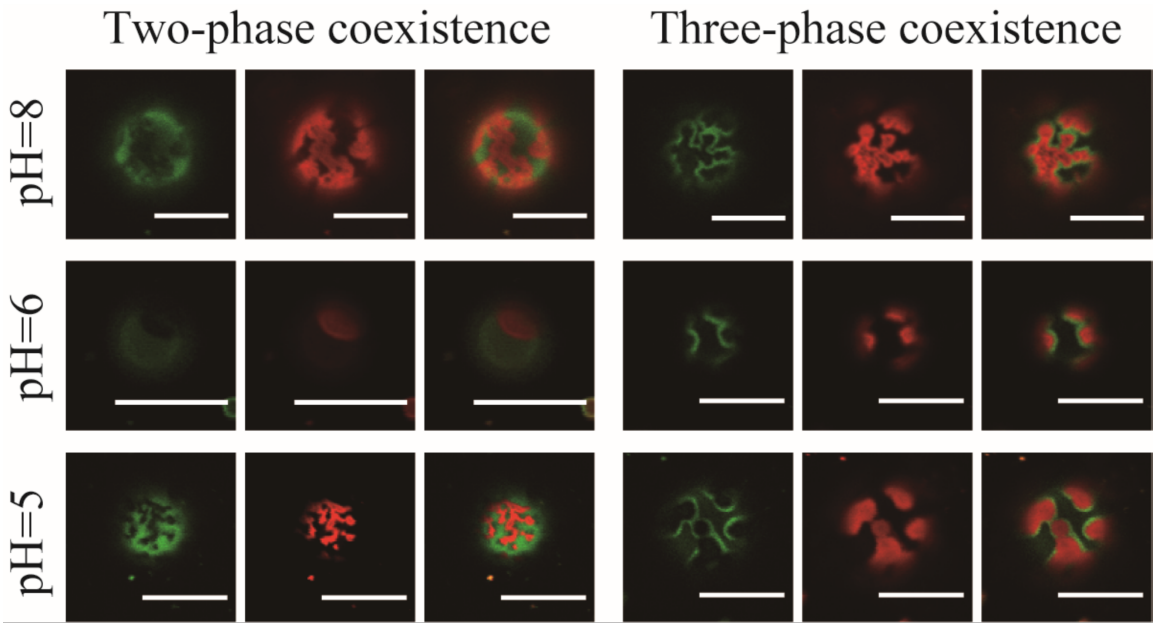

Figure 2.13: Fluorescence microscopy images at $\Delta c = 100$mM for DOPS/DPPC =30/70 at pH = 8, 6, and 5. Scale bars are 10 μm.

2.3.4 Coarse-grained molecular dynamics simulations

Further, to clarify the stability of the three-phase coexistence structure, we carried out a Coarse-grained molecular dynamics simulations. The results above, show that the three phases consist of DPPC, DOPS(-), and DOPS(N). So we tried to simulate this situation.

We prepared a system with three kinds of lipid, including a negatively charged unsaturated lipid representing DOPS(-) (A-lipid), a neutral unsaturated lipid representing DOPS(N) (B-lipid), and a neutral saturated lipid representing DPPC (C-lipid). Set the ratio of these three lipids as A/B/C = 1000/1000/3000. We set the cutoff length for the attractive potential w_c, based on the results of fluorescence intensity like showen in Figure 2.8 (b) and (d).

The fluorescence intensity of the red region dominated by Rho-DHPE was gradually decreased at the red and green regions boundary, indicating that the line tension at the boundary was low and the two regions are rich in the same kind of lipids. Simulat as A and B lipids, represent two different states of DOPS, they have the same

unsaturated hydrocarbon tails. Thus, we assume that $w_c^{AA} = w_c^{BB} < w_c^{CC}$. And the fluorescence intensity of the green region dominated by NBD-PE was abruptly decreased at the boundary of green and black regions, indicating that the green and black regions were strongly separated from each other and enriched with different types of lipids. These two regions are simulat as B-riched and C-riched regions. since A-lipid and B-lipid have the same unsaturated hydrocarbon, the phase separation between them is relatively weak. In contrast, the phase separation between AC and BC is stronger because of the different hydrocarbon tails. Thus, we set $w_c^{AB} > w_c^{BC} = w_c^{AC}$. Finally, to form the stable three-phase coexistence, we assume the relationship $w_c^{AA} = w_c^{BB} > w_c^{AB}$. Combining the above relationships between the physical properties of lipids, we set $w_c^{AA} = 1.7\sigma, w_c^{BB} = 1.7\sigma, w_c^{CC} = 1.8\sigma, w_c^{AB} = 1.55\sigma, w_c^{BC} = 1.5\sigma, w_c^{AC} = 1.5\sigma$.

The results are shown in Figure 2.14. Green beads indicate negatively charged unsaturated lipids [A-lipids, DOPS(-)], red beads indicate neutral unsaturated lipids [B-lipids, DOPS(N)], and gray beads indicate neutral saturated lipids (C-lipids, DPPC). It can be seen that the coarse-grained molecular dynamics simulations successfully reproduced the three-phase separation structure observed by microscopy, in Figure2.14(a). All results showed that the A-lipid rich region surrounds the B-lipid rich circular region.

Figure 2.14(b) shows the lipid density distribution from the center of the red region. The red B-lipid rich region first appears, followed by the green A-lipid rich region, followed by the gray C-lipid rich region. Both the snapshot and the lipid density profile are essentially the same as the results presented in Figure 2.8(b) and (d). Thus, this structure of three-phase coexistence (DOPS(N) rich phase surrounded by the DOPS(-) rich phase and then surrounded by the DPPC rich phase) is proven to be energetically stable.

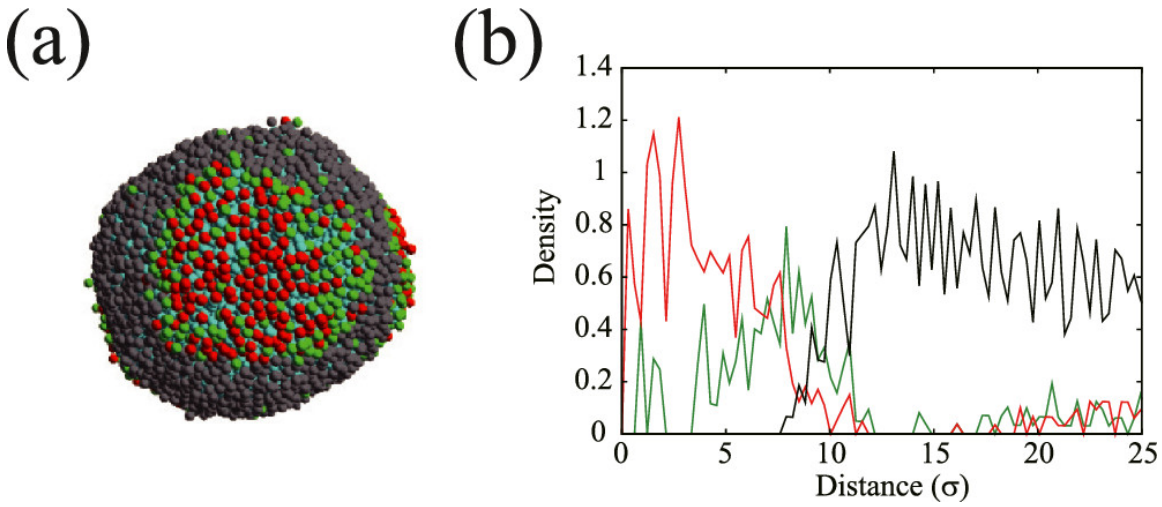

Figure 2.14: Coarse-grained molecular dynamics simulations results. (a)Snapshot of three-phase coexistence, and (b) bead density profile from the center of the domain rich in B-lipids. The green, red, and gray beads and lines represent of A-lipids, B-lipids, and C-lipids, respectively.

2.4 Discussion

2.4.1 Phase separation induced by osmotic pressure

The membrane tension caused by osmotic stress can induce phase separation in charged lipid membranes, which is similar to the mechanism of osmotic stress-induced phase separation in neutral lipid membranes and can be explained as the loss of membrane fluctuation entropy [15] [17]. Homogeneous lipid membranes with liquid disordered phase are soft and fluctuating. In contrast, phase separation membranes with ordered phases are stiffer and have relatively less fluctuation. The osmotic swelling causes the membrane to develop lateral tension, suppressing thermal membrane fluctuation. The fluctuation entropy loss in homogeneous membranes under osmotic stress is more significant than that in the phase separation state. Homogeneous membranes become relatively unstable than phase separation membranes.

Experimentally, we observed that tension due to osmotic stress could induce phase separation of negatively charged lipid membranes, it can be assumed that this tension is competition with electrostatic repulsion in the charged lipid phase region. Phase separation does not occur in lipid membranes if the effect of electrostatic repulsion dominates. If tension due to osmotic stress overwhelms, phase separation will occur. The result shows that increased osmotic pressure promotes phase separation on charged lipid membranes. Thus it can be considered that tension gradually dominates over and overcomes the effect of electrostatic repulsion due to negatively charged lipids.

2.4.2 Ionization state of the DOPS headgroup

As described in before, we believe that the observed three-phase coexistence structure may be due to the ionization of the headgroup of DOPS. The headgroup of DOPS contains three different polar groups: phosphate, carboxy, and amine moieties. Where each

phosphate and carboxy group has a monovalent negative charge, and amine groups have a monovalent positive charge. Therefore, the net charge of DOPS is -1. The dissociation of the ions depends on the pH of the solution. The dissociation fraction α can be expressed by the following equation.

$$\alpha = \begin{cases} \frac{1}{10^{\mathrm{p}K_\mathrm{a}-\mathrm{pH}}} & \text{for the phosphate and carboxy groups} \\ \frac{1}{1+10^{\mathrm{pH}-\mathrm{p}K_\mathrm{a}}} & \text{for the amine groups} \end{cases} \tag{2.10}$$

In Figure 2.15 we show the fraction of ionic dissociation as a function of pH. It can be seen that phosphate and amine groups with pK_a of 2.6 and 11.55, respectively, pH varies around 7 do not affect their ionic dissociation so much. However, the carboxy group has a pK_a of 5.5, which makes it very sensitive to changes in pH around 7. [23]

Then, according to Figure 2.15(a), we calculated the relative charge of PS as a function of pH in Figure 2.15(b). The relative charge is almost close to -1 at pH = 7 and 8, the exact values are -0.969 and -0.997, respectively, which means most carboxyl groups are dissociated. The relative charge increases as the pH decreases, from -0.759 at pH = 6 to -0.236 at pH = 5, which means that the amount of dissociated carboxyl groups decreases. Therefore, it can be concluded that at pH = 7 and 8, the system have almost only two components, DOPS(-) and DPPC. However, at pH = 5 and 6, the system contains three components, DOPS(-), DOPS(N), and DPPC. In the experiment with DOPS/DPPC=30/70, the proportion of three-phase coexistence gradually increased as the pH decreased from 8 to 6, but a decrease in the proportion of three-phase coexistence was observed for the pH decrease from 6 to 5. This is because the pH reduction process actually increases the ratio of DOPS(N), which promotes the formation of the three-phase coexistence. And, at pH=5, the excessive increase in the DOPS(N) ratio exceeds the DOPS(-) ratio, making the whole system near to a two-component system consisting of DOPS(N) and DPPC. So this can be interpreted as the reduction of the DOPS(-) ratio inhibits the formation of the three-phase coexistence. In Figure 2.15(c), we summarize a Gibbs triangle to present the phase behavior of the quasi-ternary lipid at $\Delta c = 100$mM.

In addition, it can be found from the results that at pH=7 and 8, even though the relative charges are both close to -1 and are both almost composed of two components, we still observed three-phase coexistence. This means that it becomes important to explain what exactly pK_a depends on, and it could possibly depend on lipid composition,

molecular assembly structure, or even membrane tension. From our experimental results, pK_a is likely to be over 5.5. Some prior studies have also reported that the apparent pK_a of PS is exceed 5.5 [24] Therefore further measurement of pK_a should be performed by titration analysis to reveal the exact value.

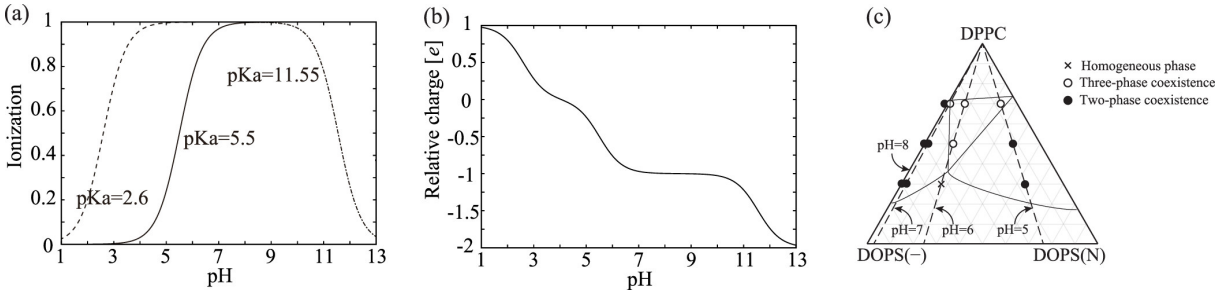

Figure 2.15: (a)Fraction of the ionized polar groups in the DOPS headgroup as a function of pH. (b)Relative charge of DOPS as a function of pH. (c)Gibbs triangle for a quasi-ternary lipid mixture composed of DOPS(-), DOPS(N), and DPPC, difference in glucose concentration across the lipid membranes $\Delta c = 100$mM.

2.4.3 Structure of three-phase coexistence

Combining the results of the adsorption experiments using charged particles in 2.3.2 and the coarse-grained molecular dynamics simulations in 2.3.4, we suggest that on the DOPS/DPPC lipid membrane, the circular region riched in DOPS(N) is surrounded by the DOPS(-) riched region, and then surrounded by the DPPC enriched region. In Figure 2.16, we show a schematic representation of the three-phase coexistence structure.

As introduced in 1.4, the phase separation between saturated and unsaturated lipids is generally due to differences in the hydrophobic chains. As DOPS and DPPC have different hydrophobic chains, it can be considered that the separation of the DPPC-rich phase and the DOPS-rich phase is caused by the different saturation of the DPPC and DOPS hydrophobic chains, and here we do not discuss this in detail about this. In the following sentences, the discussion of the three-phase coexistence structure will in terms of why DOPS(-) and DOPS(N) are separated into two phases, as well as where DOPS(-) is located on lipid membranes and its shape.

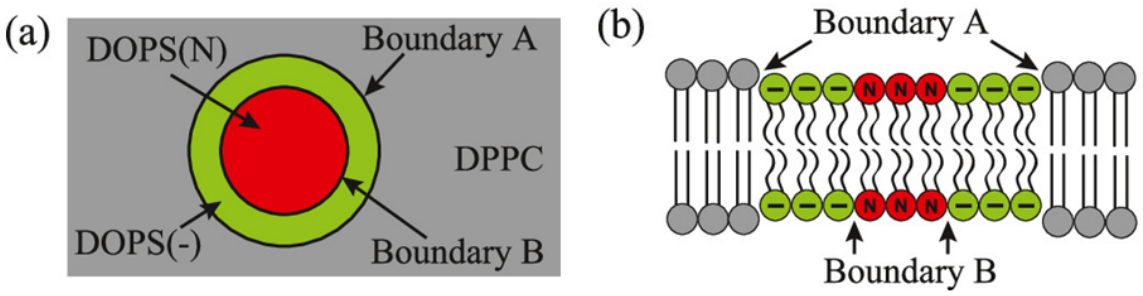

Figure 2.16: Schematic illustration of the domain structure in the case of three-phase coexistence. (a)top view, (b)side view

First, we discuss the phase separation of DOPS(-) and DOPS(N). From the hydrophobic tail, DOPS(-) and DOPS(N) should be mixed due to having the same unsaturated tail. From the headgroup, there are electrostatic repulsion between DOPS(-), and they should be mixed in order to reduce the electrostatic interactions. However, we observed the phase separation behavior between DOPS(-) and DOPS(N). By the measurements in 2.8, we analyze that the line tension at the boundary between DOPS(-) and DOPS(N)(boundary B) is not high. However, we cannot observe a domain shape fluctuation that indicates lower line tension. So it can be guessed that there is a physical property difference between the two states of the DOPS phase. Our opinion is that there is an attractive interaction between DOPS(N). This attractive interaction can overcome the loss of free energy due to the electrostatic repulsion between DOPS(-), which induces the separation of DOPS(-) from DOPS(N).

A prior study reported that intermolecular hydrogen bonding between protonated PS headgroups might lead to attraction between DOPS(N) molecules [25]. To verify this, we replaced H_2O (Milli-Q water) with D_2O for the same experiment. The lipids used were DOPS/DPPC = 30/70, at $\Delta c = 100$mM. The results are shown in Figure 2.17. No phase separation structure was observed in $\Delta c = 0$mM, but with the increase of osmolarity, in $\Delta c = 100$mM, we observed phase separation structures. This result is essentially the same as that obtained using H_2O. However, compared to 50% of the three-phase coexistence in DOPS/DPPC = 30/70, $\Delta c = 100$mM using H_2O, as shown in Figure 2.12(j). The three-phase coexistence in the results using D_2O was only 10%, which was inhibited. This is

because D_2O inhibits the hydrogen bonding between the protonated DOPS molecules, which leads to the difficulty of three-phase formation. It can be assumed that part of the reason for the stable existence of the three-phase coexistence is the hydrogen bonding between the protonated PS.

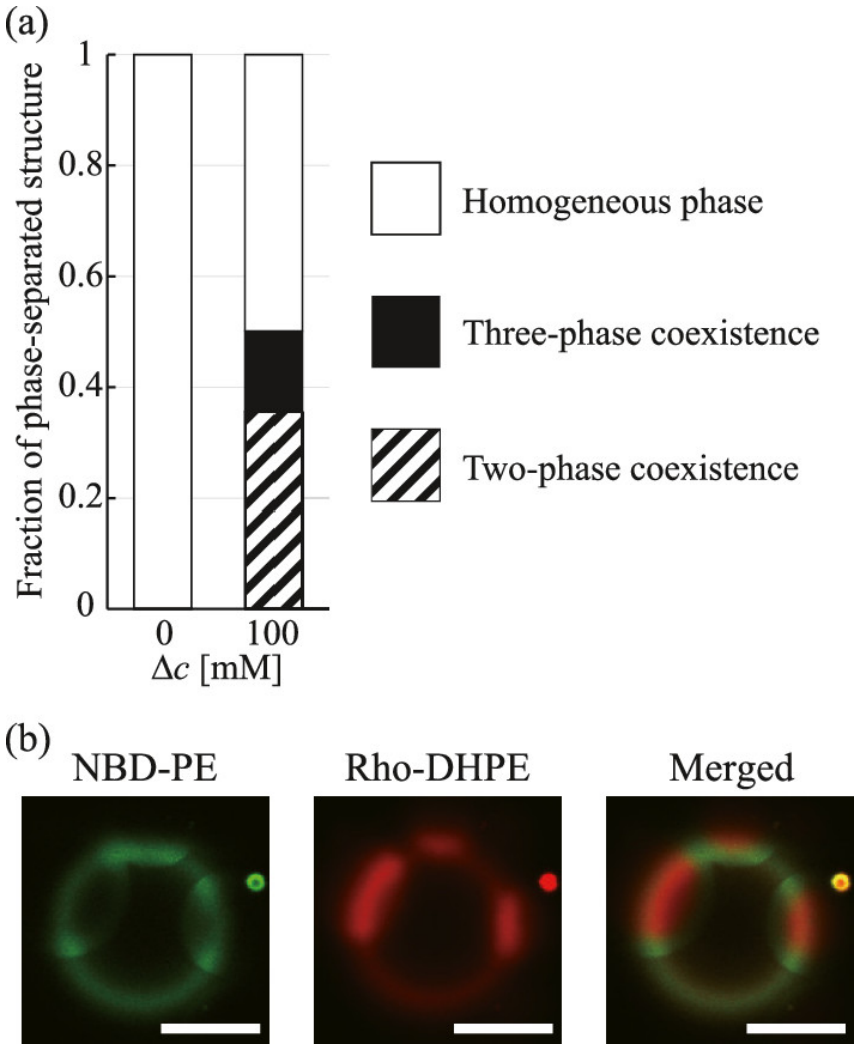

Figure 2.17: Investigation of intermolecular hydrogen bonding between protonated PS headgroups affect at DOPS/DPPC = 30/70 in D_2O. (a)Fraction of the phase-separated structure as a function of the concentration difference across the lipid membranes. The white, black, and hatched bars represent the homogeneous phase, three-phase coexistence, and two-phase coexistence, respectively. (b)Confocal laser scanning microscopy images showing the three-phase coexistence. $\Delta c = 100$mM. Scale bars are 10 μm

In addition, the fluorescence anisotropy of the fluorescent probe, 1,6-diphenyl-1,3,5-hexatriene (DPH), was measured in order to clarify the effect of the hydrophobic tail of DOPS(N) and DOPS(-). Experiments were performed using membranes containing only one lipid, DOPS, at various pH, and we summarize the results in Figure 2.18. At pH=7, the fluorescence anisotropy is low, fluctuating around 0.1, because DOPS is an unsaturated lipid and forms a disordered state. However, the fluorescence anisotropy remains almost unchanged even if the pH is changed, indicating that the DOPS(-) and DOPS(N) contents, which vary due to pH change, have almost no effect on the hydrocarbon chain orderliness. This means the interaction between DOPS(-) and DOPS(N) may be in the same disordered state, and the interaction between the hydrocarbon tails of DOPS(-) and DOPS(N) is virtually identical. Indicates that the reason for the separation between DOPS(-) and DOPS(N) does not come from the hydrophobic tail. It may be because of the hydrophilic head, in agreement with our discussion above.

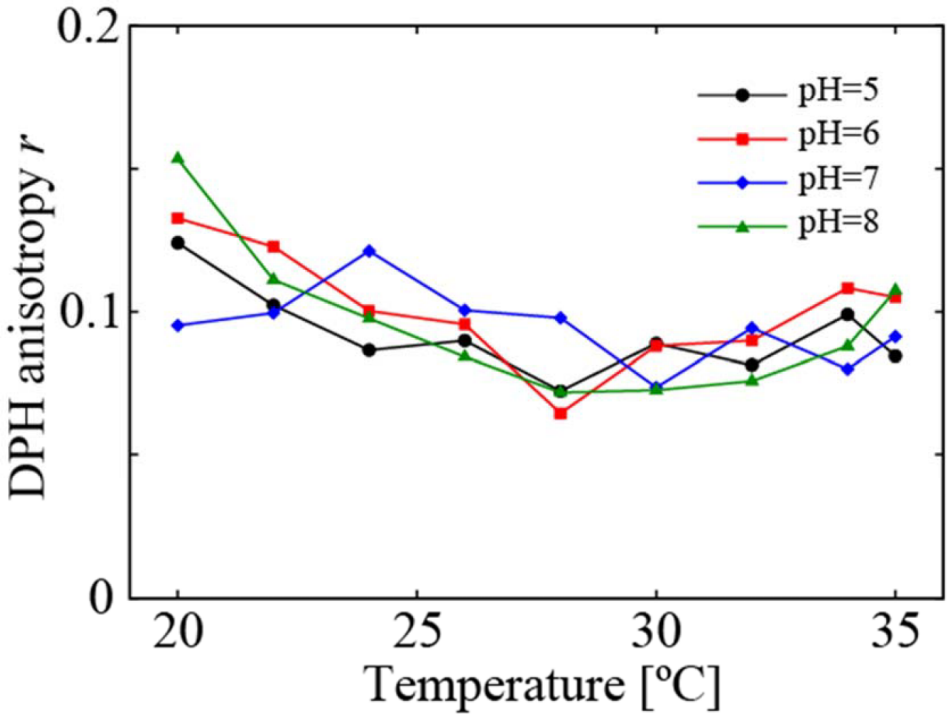

Figure 2.18: DPH fluorescence anisotropy r at pH=5, 6, 7, and 8 as a function of the temperature.

The relationship between the PS ionization profile and the phase separation of model membranes has been reported in other studies. The study by Bandekar et al. [26] used a charged lipid included membrane containing DOPC, distearylphosphatidylserine(DSPS) and cholesterol, while also varied the solution's pH. Their experimental results indicated the dissociation of DSPS into DSPS(N) and DSPS(-). Similar to our results, they observed a phase-separated structure with DSPS(N)-rich regions surrounded by DSPS(-)-rich regions. This is due to the presence of hydrogen bonding-mediated attraction between DSPS(N) molecules. Unlike their experiments, the temperature was not changed in our experiments, and only two lipids were used as well as we used charged lipids that were unsaturated. The DSPS used in the study by Bandekar et al. has a relatively long saturated tail, which leads to a stronger intermolecular van der Waals attraction and easier formation of aggregated phase structures. In contrast, the unsaturated lipid DOPS we used had a minor attraction. However, we observed phase separation structures. This is also siding evidence that the attraction of the protonated PS part is strong, and the ionization of PS lipids affect the phase formation. The phase formation does not depend on the structure of the PS lipids tails.

Then, we discuss the phase formed by DOPS(-) and its shape. It is well known that there is electrostatic repulsion between charged lipids, and the formation of charged lipid-rich regions may increase the free energy. Electrostatic interactions are long-range interactions, and their total electrostatic interaction is equal to the sum of all interacting charge pairs. One-dimensional band domains increase the distance between the interacting pairs and can reduce the total electrostatic interaction. For this reason, the DOPS(-)-rich phase will exhibit a one-dimensional band-shaped domain instead of a two-dimensional circular domain. The formed band region makes the DOPS(-) rich region in contact with the DPPC and DOPS(N) rich regions at boundary A and boundary B, respectively. This can effectively reduce the electrostatic interactions near the boundaries. This possibility has been discussed theoretically in the prior study [27].

In Figure 2.12(h) and (i) a decrease in the amount of phase separation at $\Delta c = 100\text{mM}$ can be found in experiments for DOPS/DPPC = 50/50 and 30/70. It has been reported that membrane tension caused by osmotic pressure leads to an increase in line tension at the boundary of the phase separation domain. That means going from a homogeneous

state to a phase separation state may cause a loss of free energy. [15] The transition from a homogeneous state to the formation of a stable phase separation state requires overcoming the energy barrier. If the energy barrier to be overcome is greater than the thermal energy, the application of osmotic pressure does not change the homogeneous state of the lipid membrane. [28] Therefore, we speculate that the number of GUVs in the phase separation state decreases significantly when Δc is large, and the GUVs are mainly in the homogeneous state. An energy barrier may exist at the larger Δc, where the line tension increases to maximum. If the threshold tension is exceeded, rupture and pore formation become energetically favorable, allowing the GUV to release a small fraction of the intra-vesicular solute [29], after which the line tension decreases instead. To explain this phenomenon, it is necessary to measure the line tension at the phase separation boundary. Furthermore, it is of great interest to clarify whether the line tension is dependent on pH.

In the previous section 2.3.2, in order to reveal the composition of each phase, we performed an adsorption experiment using positively charged particles. This can undoubtedly define the composition to some extent. But in the future, it may be possible to confirm this by more detailed means. For example, direct measurement of the crucial parameter, local surface charge density, on the membrane surface, which strongly affects the localization and regulation of membrane proteins in the cell membrane. It has been reported [30] that it is possible to measure local surface charge using quantitative surface charge microscopy on supported lipid bilayer membranes in a phase-separated state. Although supported lipid bilayer membranes and vesicle membranes are not completely identical in their phase separation behavior, this experiment may still provide us with some explanation. It is expected that this technique can be used in future experiments to directly observe the distribution of DOPS(-) and DOPS(N) in phase-separated membranes.

At the same time, it is possible to confirm the experiments in this chapter theoretically. Earlier, a theoretical model was reported by Mengistu et al. [31], whose theoretical model can describe the phase separation behavior of lipid membranes containing charged and neutral lipids. This model also considers the effect of pH on the phase separation behavior. However, unlike our experiments, the negatively charged lipid described in their theoretical model contains only one negative charge group. In contrast, the DOPS

we used includes both one positive charge and two negative charge groups. Therefore, their theoretical model cannot fully describe the fact that we found that DOPS(-) and DOPS(N) exist simultaneously and have different intermolecular interactions. Thus, it is indispensable that to propose a theoretical model that takes these effects into account.

2.5 Chapter conclusion

In this chapter, we investigated the phase separation behavior of lipid membranes containing unsaturated charged lipids (DOPS) induced by osmotic stress. Phase separation was induced by subjecting GUVs in a hypotonic solution. A three-phase coexistence structure was observed, especially at DOPS/DPPC = 30/70. Due to the ionization of the DOPS headgroup, we consider that the three phases are rich in DPPC, charged DOPS [DOPS(-)], and neutral DOPS [DOPS(N)], respectively. Adsorption experiments using positively charged particles identify the three phases and show that the DPPC-rich phase surrounds the DOPS(-)-rich phase and this DOPS(-)-rich phase surrounds a circular region of DOPS(N) in the center. This arrangement was successfully reproduced by the coarse-grained molecular dynamics simulations, which demonstrated that the three-phase coexistence structure could be energetically stable. At the same time, with the shape and arrangement of such regions, the charged lipid-rich domain [DOPS(-)] has a one-dimensional band shape, which increases the distance between charged lipids and weakens the electrostatic interactions. The hydrogen bonds between DOPS(N) also play a stabilizing role, are favorable for the stability of the three phases. However, some details of interactions at the nanoscale are still not clear, such as those between charged lipids, water, and counter ions. Thus, it is crucial to explain microscopically what interactions in hydrophilic headgroups form ordered structures by using charged lipids.

As introduced at the beginning of this chapter, the study of phase separation under isothermal conditions is essential because the body temperature of most living organisms is constant. We demonstrated that, even in the charged lipid membranes, lateral tension due to the osmotic pressure could induce phase separation at a constant temperature. On the other hand, some studies have shown that adding salt can alter lipid membranes' thermal stability and cause phase separation [12], as we will discuss in the next chapter.

Reference

[1] J. Guo, H. Ito, Y. Higuchi, K. Bohinc, N. Shimokawa, and M. Takagi. Three-phase coexistence in binary charged lipid membranes in a hypotonic solution. *Langmuir*, 37(32):9683–9693, 2021.

[2] S. L. Veatch and S. L. Keller. Organization in lipid membranes containing cholesterol. *Physical Review Letters*, 89(26):268101, 2002.

[3] S. L. Veatch and S. L. Keller. Separation of liquid phases in giant vesicles of ternary mixtures of phospholipids and cholesterol. *Biophysical Journal*, 85(5):3074–3083, 2003.

[4] G. W. Feigenson. Phase diagrams and lipid domains in multicomponent lipid bilayer mixtures. *Biochimica et Biophysica Acta (BBA)-Biomembranes*, 1788(1):47–52, 2009.

[5] K. Simons and E. Ikonen. Functional rafts in cell membranes. *Nature*, 387(6633):569–572, 1997.

[6] K. Simons and J. L. Sampaio. Membrane organization and lipid rafts. *Cold Spring Harbor Perspectives in Biology*, 3(10):a004697, 2011.

[7] A. Samad, Y. Sultana, and M. Aqil. Liposomal drug delivery systems: an update review. *Current Drug Delivery*, 4(4):297–305, 2007.

[8] C. Cabanos, M. Wang, X. Han, and S. B. Hansen. A soluble fluorescent binding assay reveals pip2 antagonism of trek-1 channels. *Cell Reports*, 20(6):1287–1294, 2017.

[9] S. Pöyry and I. Vattulainen. Role of charged lipids in membrane structures—insight given by simulations. *Biochimica et Biophysica Acta (BBA)-Biomembranes*, 1858(10):2322–2333, 2016.

[10] S. McLaughlin and A. Aderem. The myristoyl-electrostatic switch: a modulator of reversible protein-membrane interactions. *Trends in Biochemical Sciences*, 20(7):272–276, 1995.

[11] N. Shimokawa, M. Hishida, H. Seto, and K. Yoshikawa. Phase separation of a mixture of charged and neutral lipids on a giant vesicle induced by small cations. *Chemical Physics Letters*, 496(1-3):59–63, 2010.

[12] H. Himeno, N. Shimokawa, S. Komura, D. Andelman, T. Hamada, and M. Takagi. Charge-induced phase separation in lipid membranes. *Soft Matter*, 10(40):7959–7967, 2014.

[13] B. Kubsch, T. Robinson, R. Lipowsky, and R. Dimova. Solution asymmetry and salt expand fluid-fluid coexistence regions of charged membranes. *Biophysical Journal*, 110(12):2581–2584, 2016.

[14] T. Hamada, Y. Kishimoto, T. Nagasaki, and M. Takagi. Lateral phase separation in tense membranes. *Soft Matter*, 7(19):9061–9068, 2011.

[15] N. Wongsirojkul, N. Shimokawa, P. Opaprakasit, M. Takagi, and T. Hamada. Osmotic-tension-induced membrane lateral organization. *Langmuir*, 36(11):2937–2945, 2020.

[16] F. Sachs. Stretch-activated ion channels: what are they? *Physiology*, 25(1):50–56, 2010.

[17] V. D. Gordon, M. Deserno, C. M. J. Andrew, S. U. Egelhaaf, and W. C. K. Poon. Adhesion promotes phase separation in mixed-lipid membranes. *EPL (Europhysics Letters)*, 84(4):48003, 2008.

[18] I. R. Cooke, K. Kremer, and M. Deserno. Tunable generic model for fluid bilayer membranes. *Physical Review E*, 72(1):011506, 2005.

[19] N. Shimokawa, H. Ito, and Y. Higuchi. Coarse-grained molecular dynamics simulation for uptake of nanoparticles into a charged lipid vesicle dominated by electrostatic interactions. *Physical Review E*, 100(1):012407, 2019.

[20] H. Ito, Y. Higuchi, and N. Shimokawa. Coarse-grained molecular dynamics simulation of binary charged lipid membranes: Phase separation and morphological dynamics. *Physical Review E*, 94(4):042611, 2016.

[21] H. Himeno, H. Ito, Y. Higuchi, T. Hamada, N. Shimokawa, and M. Takagi. Coupling between pore formation and phase separation in charged lipid membranes. *Physical Review E*, 92(6):062713, 2015.

[22] T. Hamada, M. Morita, M. Miyakawa, R. Sugimoto, A. Hatanaka, M. C. Vestergaard, and M. Takagi. Size-dependent partitioning of nano/microparticles mediated by membrane lateral heterogeneity. *Journal of the American Chemical Society*, 134(34):13990–13996, 2012.

[23] G. Cevc, A. Watts, and D. Marsh. Titration of the phase transition of phosphatidylserine bilayer membranes. effects of ph, surface electrostatics, ion binding, and head-group hydration. *Biochemistry*, 20(17):4955–4965, 1981.

[24] G. B. Kempegowda, S. Karve, A. Bandekar, A. Adhikari, T. Khaimchayev, and S. Sofou. ph-dependent formation of lipid heterogeneities controls surface topography and binding reactivity in functionalized bilayers. *Langmuir*, 25(14):8144–8151, 2009.

[25] J. M. Boggs. Lipid intermolecular hydrogen bonding: influence on structural organization and membrane function. *Biochimica et Biophysica Acta (BBA)-Reviews on Biomembranes*, 906(3):353–404, 1987.

[26] A. Bandekar and S. Sofou. Floret-shaped solid domains on giant fluid lipid vesicles induced by ph. *Langmuir*, 28(9):4113–4122, 2012.

[27] G. V. Bossa, M. A. Brown, K. Bohinc, and S. May. Modeling the electrostatic contribution to the line tension between lipid membrane domains using poisson–boltzmann theory. *International Journal of Advances in Engineering Sciences and Applied Mathematics*, 8(2):101–110, 2016.

[28] K. Oglęcka, P. Rangamani, B. Liedberg, R. S. Kraut, and A. N. Parikh. Oscillatory phase separation in giant lipid vesicles induced by transmembrane osmotic differentials. *eLife*, 3:e03695, 2014.

[29] A. Ertel, A. G. Marangoni, J. Marsh, F. R. Hallett, and J. M. Wood. Mechanical properties of vesicles. i. coordinated analysis of osmotic swelling and lysis. *Biophysical Journal*, 64(2):426–434, 1993.

[30] T. Fuhs, L. H. Klausen, S. M. Sønderskov, X. Han, and M. Dong. Direct measurement of surface charge distribution in phase separating supported lipid bilayers. *Nanoscale*, 10(9):4538–4544, 2018.

[31] D. H. Mengistu, K. Bohinc, and S. May. A model for the electrostatic contribution to the ph-dependent nonideal mixing of a binary charged–zwitterionic lipid bilayer. *Biophysical Chemistry*, 150(1-3):112–118, 2010.

Chapter 3

Salt-induced phase separation in charged lipid membranes: Valence, size and structure of salt

3.1 Chapter Introduction

Phospholipids, the main component of biomembranes, can spontaneously form lipid bilayer structures in water [1]. The closed lipid bilayer is called a liposome. The structure of liposomes is identical to that of biomembranes. Lipisomes can prepared as same size as living cells, called giant unilamellar vesicles (GUVs). Because of the similar composition and size with living cells, GUVs are commonly used as a model system. A number of studies have reported that the phase separation structure occurs in multicomponent GUV, which is considered to be highly similar to the raft region on biomembranes [2] [3] [4]. It has been reported that lipid raft regions are associated with important cellular functions such as membrane trafficking and cell signaling [5] [6]. The study of phase-separated structures on model membranes contributes to the understanding of cellular processes. To clarify the lipid raft structure mechanism, GUVs have been used as model biomembranes.

In particular, multicomponent phospholipid membranes containing both unsaturated lipids and saturated lipids undergo phase separation at low temperatures into a disordered unsaturated lipid-rich phase and an ordered saturated lipid-rich phase, due to differences in the order of hydrocarbon chains in each lipid. On the other hand, three-component phospholipid membranes containing unsaturated lipid, saturated lipid, and cholesterol may form a raft-like structure rich in saturated lipids and cholesterol [3] [7]. Therefore, an approach to understanding the universality and fundamental principle of raft formation has been taken by investigating phase separation in a simple system consisting of several types of phospholipids.

Phase separation studies in lipid membranes have focused on neutral lipid membranes, where phase separation is induced by temperature change. However, negatively charged phospholipids are present in biomembranes and are involved in membrane potential and channel activity [8]. Therefore, in the last decade, studies on phase separation and membrane deformation in negatively charged lipid membranes have been conducted.

It was shown that the phase separation of charged lipid membranes was inhibited due to electrostatic repulsion between charged lpids. However, at the same time, it has been reported that the addition of salt, such as NaCl and $CaCl_2$, can induce phase separation of negatively charged lipid membranes due to strong screening effect of the electrostatic

repulsion [9] [10]. What is of interest here is whether adding cations of different valence states affects the phase separation behavior differently.

As cations in the living organism, metal ions play an essential role in biological activities. In addition to balancing molecules for the osmotic pressure of the intracellular and extracellular environment, they also regulate processes such as cell division, cell proliferation, and transport of small molecules across biomembranes [11] [12] [13]. One kind of representative metal ions is calcium ions, which regulate cellular functions in most organisms, and is involved in the control of cell proliferation, differentiation, calcium-permeable channels, transporters, and ATPases [14] [15]. Expect metal ions, which are simple cations, non-metal cations polyamines are also present in the living organism. Polyamines are a kind of compound that have two or more amino groups, the positive charge provided by amino groups, and generally in a linear skeleton. The most common natural polyamines are putrescine, spermidine, spermidine, etc. [16] [17] In addition, there are also branched polyamines with complex structures, such as N^4-aminopropylspermidine (3(3)4) and N^4-bis(aminopropyl)spermidine (3(3)(3)4) from hyperthermophilic archaeon organisms [18]. Polyamines have a lot of functions, such as the stabilization of RNA and DNA, the stabilization of proteins, cell proliferation, and programmed cell death. Some studies have shown that polyamines can enhance or inhibit gene expression and that this effect depends on the concentration of polyamines [19] [20] [21]. Moreover, different structures have different thermal stability to functional regions, such as DNA. For example, the branched polyamine N^4-bis(aminopropyl)spermidine (3(3)(3)4) has been reported can induce DNA to form a nano-loop structure. This ordered structure is thought to be related to the stabilization of primary constructed DNA at high temperatures and was not found when polyamines such as spermine were added. [22] Because of the presence of negatively charged lipids in the biomembrane, polyamines with positively charges may affect the raft region of the membrane. Howere, altough other studies have showen a promote of DNA ordering and protein stabilizationcite [23] [24], but the effectof polyamines on the ordering and stability of the biomembrane has not been explainedclearly. The stability and orderliness of the biomembrane are closely related to the formation of lipid rafts. Thus it becomes interesting to explain the relationship between cationic polyamines and biomembranes containing negatively charged lipids and the effect on thermal stability

and order of the membrane. It is also necessary to investigate the difference of stabilizing influence in the phase separation region between polyamines and metal ions, which are all cations in the living organism.

In this context, we consider that it is necessary to conduct phase separation research with a systems that are close to the biotic environment. To approach the ionic environment within the living organism, we will study phase separation in systems containing charged lipids and the addition of metal ions and amines.

In this chapter, we study the phase separation behavior of lipid membranes containing charged lipids in response to the addition of salts use fluorescence microscopy and confocal laser scanning microscopy. Also, we changed the temperature to reveal the thermal stability of phase separation. Here we used eleven different salts including metal ions and amines. First, we investigated the phase separation behavior induced by eleven different salts at room temperature to clarify how the valence, size, and structure of added salts affect phase separation behavior. Then we increased the observation temperature and investigated the changes in the phase separation structure at 30°C and 40°C with added salts. Finally, we measured the mobility of charged lipids without and with the addition of salt use the supported lipid bilayer (SLB). Then analyzed the effect of salt addition on the mobility of charged lipids in membranes. Comprehensively discussed the relationship between the phase separation behavior and the difference in valence, size, structure of the added salts.

3.2 Materials and Methods

3.2.1 Materials

The zwitterionic saturated lipid, 1,2-dipalmitoyl-sn-glycero-3-phosphocholine (DPPC), the negatively charged unsaturated lipid, 1,2-dioleoyl-sn-glycero-3-phospho-l-serine (sodium salt) (DOPS), and cholesterol (Chol) were purchased from Avanti Polar Lipids, Inc (Alabaster, AL). Rhodamine B 1,2-dihexadecanoyl-sn-glycero-3-phosphoethanolamine, triethylammonium salt (Rho-DHPE) was obtained from Thermo Fisher Scientific(Waltham, US). 1,2-Dipalmitoyl-sn-glycero-3-phosphoethanolamine-N-(7-nitro-2-1,3-benzoxadiazol-4-yl) (ammonium salt) (NBD-PE) was obtained from Avanti Polar Lipids (Alabaster, AL). The molecular structures of lipids and fluorescent probes are showen in Fingure 3.1 and 3.2. The metal salts NaCl(+1), $CaCl_2$(+2) and $MgCl_2$(+2) were purchased from Nacalai Tesque, INC(Kyoto, Japan). Monovalent amine NH_4Cl(+1) was purchased from Nacalai Tesque(Kyoto, Japan). And the monovalent amine propylamine-hydrochloride(+1) was obtained from Tokyo Chemical Industry Co., Ltd(Tokyo, Japan). Diamines, 1,4-diaminobutane-dihydrochloride (Putrescine)(+2), 1,6-diaminohexane-dihydrochloride (Hexamethylenediamine)(+2), ethylenediamine-dihydrochloride(+2) were obtained from Tokyo Chemical Industry Co., Ltd(Tokyo, Japan). Polyamines, spermidine-trihydrochloride(+3), spermine-tetrahydrochloride(+4) were purchased from Nacalai Tesque, INC(Kyoto, Japan), N^4-bis(aminopropyl)spermidine, (3(3)(3)4)(+5) was provided by Professor Fujiwara of Kwansei Gakuin University. The molecular structures of added slats are showen in Fingure 3.3. Deionized water (specific resistance $\geq$ 18 MΩ) used in this chapter was obtained from a Millipore Milli-Q purification system(Burlington, MA).

- Unsaturated lipids

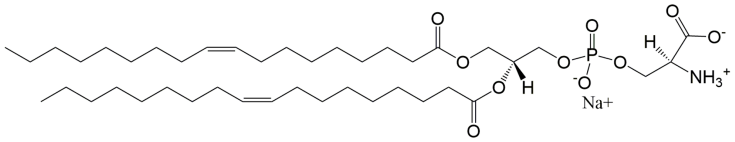

1,2-dioleoyl-*sn*-glycero-3-phospho-L-serine
DOPS (Negatively charged lipid)

- Saturated lipids

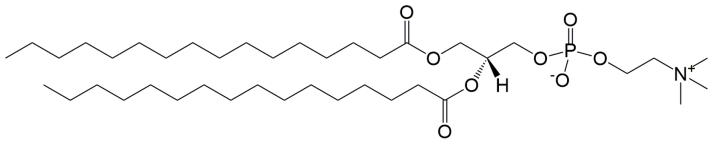

1,2-dipalmitoyl-*sn*-glycero-3-phosphocholine
DPPC (Zwitterionic lipid)

- Cholesterol

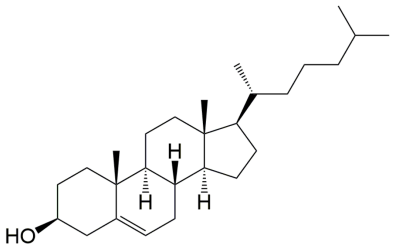

Figure 3.1: Molecular structures of lipids

- Fluorescent probes

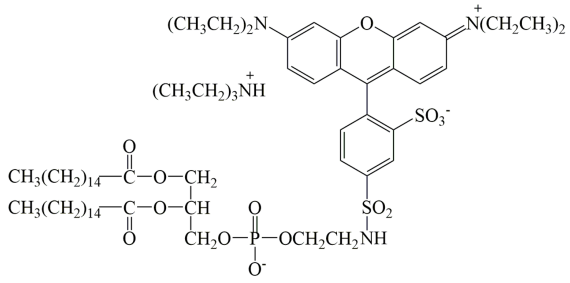

Rhodamine-DHPE

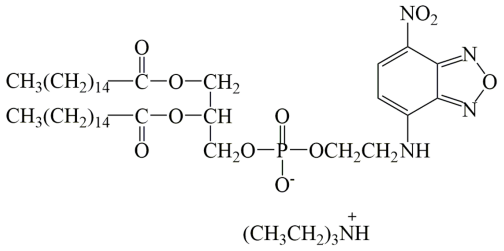

NBD-PE

Figure 3.2: Molecular structures of fluorescent probes

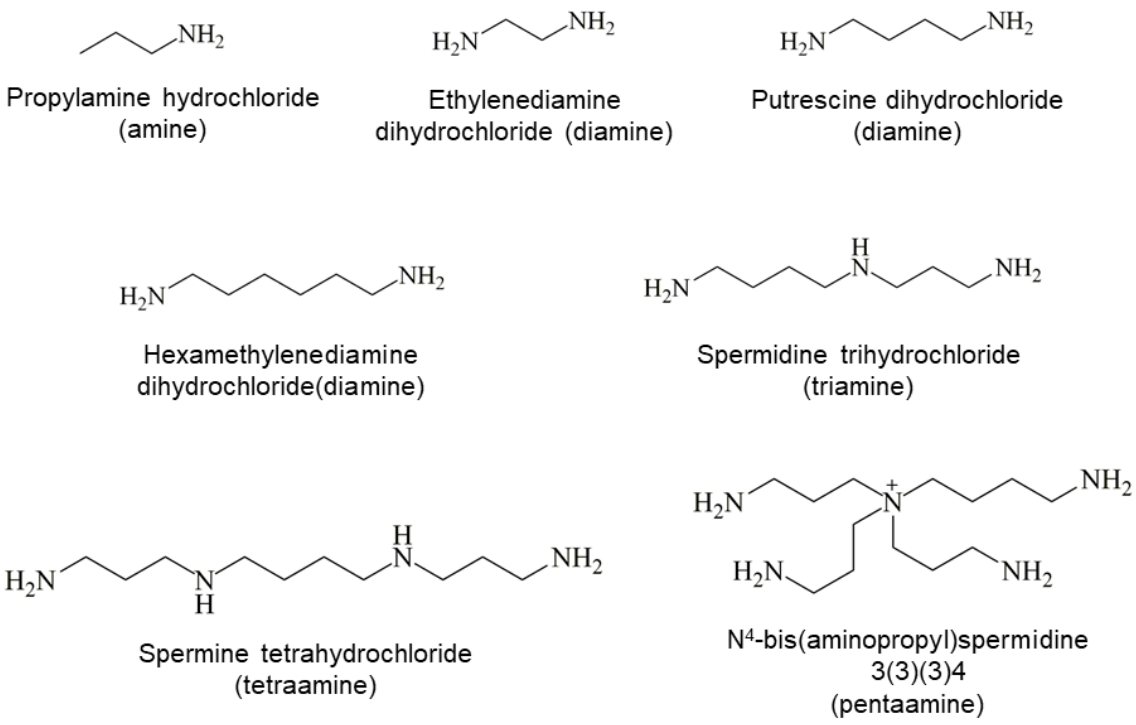

Figure 3.3: Molecular structures of slats

3.2.2 Preparation of GUVs

Liposomes were prepared by the natural swelling method. All lipids were dissolved in a 2:1 (v/v) chloroform/methanol solution and afforded concentrations of 2mM. All kinds of fluorescent probes were dissolved in chloroform, afford concentrations of 0.1mM. DOPS, DPPC, and Chol were mixed in the ratio of DOPS/DPPC/Chol=40/40/20, and the total volumes were kept with 20μL. Rho-DHPE 2μL was further added for fluorescence microscopy observation. After well mixed, the solution was dried with nitrogen gas, then the formed lipid films put into a vacuum desiccator for at least 3h. It was then prehydrated for 10min using 5μL Milli-Q water at 55°C and then was hydrated using 195μL salt solution at 55°C for at least 3h and under 24h. The salt was dissolved in a

required concentration by Milli-Q water to prepare the salt solution. The preparation process are shown in the Figure 3.4.

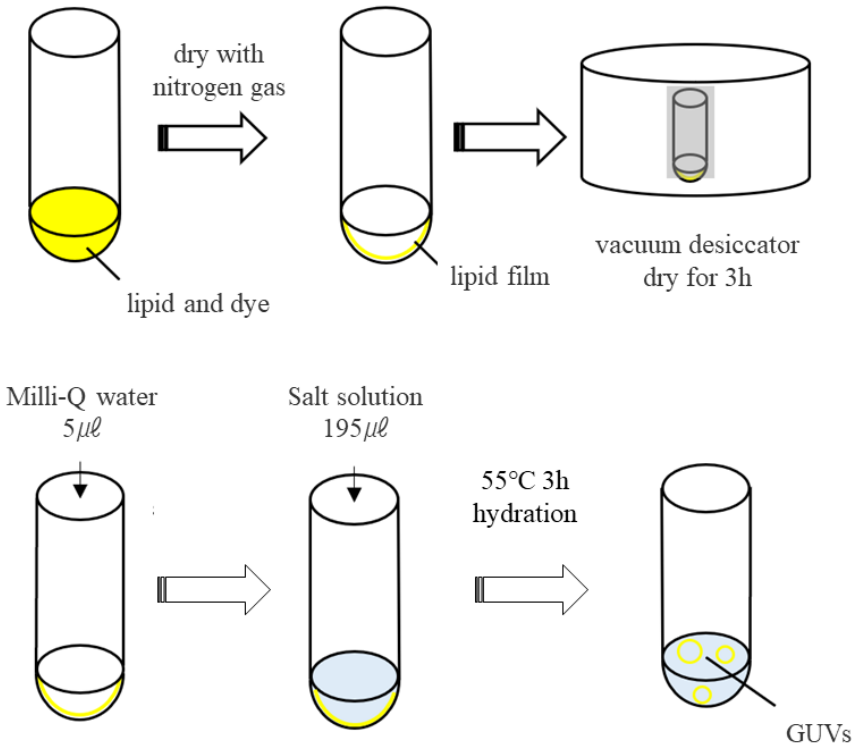

Figure 3.4: Preparation of GUVs

3.2.3 Microscopic Observations of GUVs under temperature changes

We used a small chamber, as shown in the Figure 3.5, for microscopic observation under temperature changes. A silicon sheet with a circular hole in the middle was placed on the slide glass, and the prepared GUV solution was dripped into the circular hole and added a cover glass on top. Then the observation was performed at a required temperature using a fluorescence microscope (IX71, Olympus).

To control the temperature of the sample, we used a controller that changes the temperature of the microscope stage (MATS-555, TOKAI HIT). The temperature controller

can adjust the stage temperature from 3°C to 100°C. However, since the stage temperature and the sample temperature are different, we used a thermocouple wire (manufactured by AZ-1 Corporation) on the sample surface to measure the exact temperature. The total temperature control schematic shown in Figure 3.6. We confirmed that the temperature was maintained within the target temperature range of ±0.5°C for 5 minutes before observation and then started observation. The observation was carried out at three temperatures, room temperature, 30°C, and 40°C. Also, we kept the observation time of each sample within 90sec to prevent photo-induced oxidation by the long observation time. For each salt concentration, we observed at least 90 GUVs with diameters $5\mu \sim 20\mu$m to obtain statistical data.

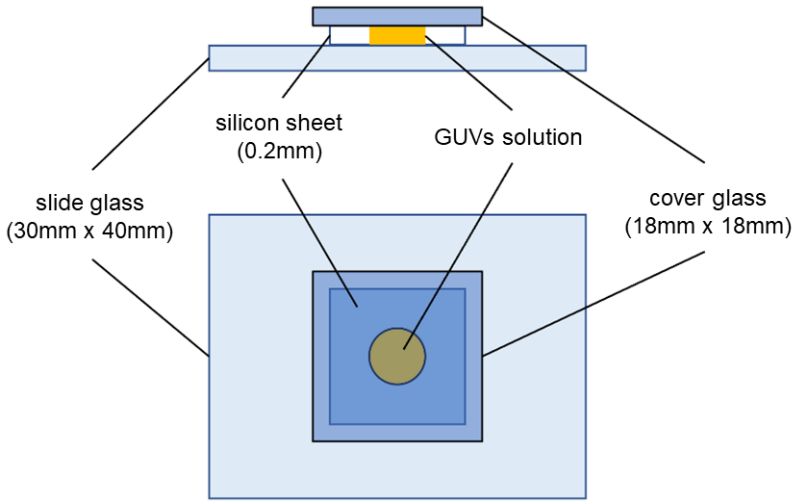

Figure 3.5: Schematic illustration of chamber for microscopic observation

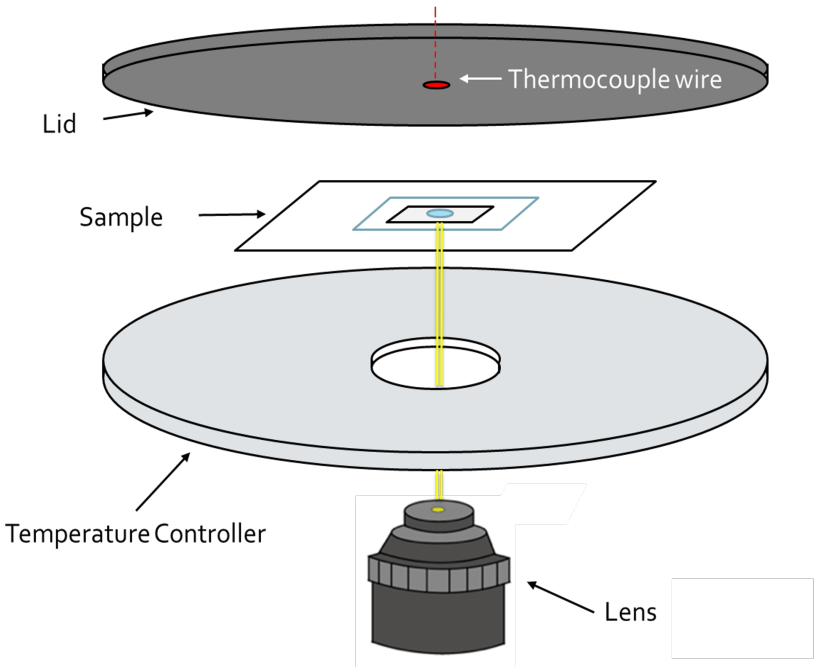

Figure 3.6: Schematic illustration of sample temperature

3.2.4 Calculation of the 50% phase separation salt concentration

To compare the difference between the required concentrations to reduce phase separation due to various salts, we calculated the 50% phase separation salt concentration. For the calculation, at least four data for each salt, concentration, and phase separation below 40% were selected for fitting. Since it is difficult to obtain the stable vesicles at higher salt concentrations and to measure the fraction of phase separation accurately, we use the fractions below 40% at lower salt concentrations to calculate the 50% phase separation salt concentration. The fitting was referenced Sigmoidal Boltzmann function, calculated by the following equation,

$$P = \frac{1}{1 + \exp\left[\left(C_{\mathrm{m}} - C\right)/d_{\mathrm{c}}\right]} \tag{3.1}$$

where P is the fraction of phase separation, C_m is the 50% phase separation salt concentration, C is the salt concentration, and d_c is the slope of curve. Results were plotted as chart.

3.2.5 Fluorescence recovery after photobleaching (FRAP) experiments

Fluorescence recovery after photobleaching (FRAP) is an experimental method widely used regarding the kinetic properties of membrane components [25]. The FRAP method takes advantage of the fact that fluorescent probes fade when exposed to continuous or intense light and uses intense light irradiation of specific areas to cause the fluorescent molecules to fade. Because of the Brownian motion of the molecules, there will be unbleached fluorescent probes and lipids molecules moving from other areas to the bleached area, so the fluorescence intensity of the faded areas will be recovered to some extent. Measuring the fluorescence intensity of the bleached area over a period of time, we can obtain the function of fluorescence intensity with time, and calculate the amount of fluorescent probes moving to the bleached area from the surrounding area and thus deduce the diffusion constant of the fluorescent probe in the membrane. In this chapter, we investigated the effect of added salt on lipid membrane fluidity by measuring the recovery of fluorescence intensity of NBD-PE. FRAP experiments were performed using confocal microscopy.

Preparation of supported lipid bilayer

GUV solutions were still prepared using the natural swelling method. The membrane used in the lipid membrane fluidity experiments was a DOPS single-component membrane. Therefore, only one lipid, DOPS, was used to prepare the GUVs. The preparation procedure was the same as described in 3.2.2.

DOPS were dissolved in a 2:1 (v/v) chloroform/methanol solution and afforded concentrations of 2mM. Fluorescent probes (NBD-PE) was dissolved in chloroform, afford concentrations of 0.1mM. DOPS 20μL and NBD-PE 4μL were under a well mixed, and the mixed solution dried with nitrogen gas, then the resulting lipid films are put into a vacuum desiccator for at least 3h. It was then prehydrated for 10min with 5μL Milli-Q water at 55°C and then further hydrated with 195μL Milli-Q water at 55°C for at least 3h and under 24h.

The prepared GUVs solution was filtered more than 20 times on a heated platform at 55°C with a Mini-Extruder which setting a pore size 400nm filter, to obtain vesicles with smaller and uniform sizes. Mini-Extruder was purchased from Avanti Polar Lipids, Inc(Alabaster, AL).

The poly-L-lysine-coating slides glass was covered with silicone film (thicknes 1mm) with a small hole in the middle to make a small chamber. 35 μL of the filtered GUV solution was dropped in the small chamber, covered with a coverslip, and left at room temperature for 30 min to wait for the SUVs to adsorb onto the glass substrate. After that, it was transferred to a heated platform (set as 55°C) above the DOPS main transition temperature T_m=-11°C and left for 60 min. The GUVs adsorbed on the glass substrate burst and fuse to form a flat film (supported lipid bilayer) on the glass substrate. After SLB formation, the solution in the chamber was replaced with Milli-Q water or salt solution whitout GUVs. The salt solution was dissolved in a required concentration by Milli-Q water. The SLB was observed within 3h after SLB formation. Figure 3.7 shows the process of SLB preparation.

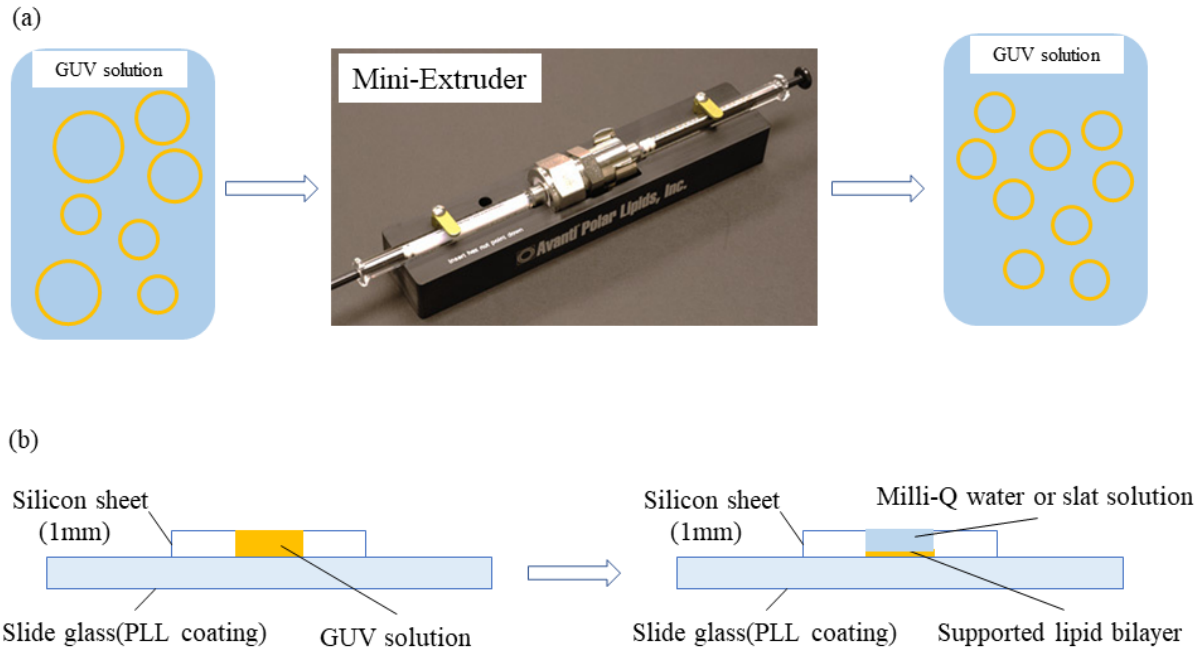

Figure 3.7: Schematic illustration of the device used to make the supported lipid bilayer.

FRAP experiments using confocal microscopy

Experiments were performed using a confocal laser scanning microscopy FV-1000D (Olympus) with the program already assembled. The laser wavelength was 473 nm. Bleach time was 100 msec, bleach radius was 6.35 μm, took 30 images acquired in 80 sec (3 images before prebleach and 27 images after bleach). Calculations were referenced from the reports of Soumpasis et al. [26] and Thomase et al. [27]. The average post-bleached fluorescence intensity in the circular bleached region was corrected and normalized to the average pre-bleached intensity. The experimentally obtained fluorescence recovery curve was fitted to the theoretical model to obtain the characteristic diffusion time τ_{d}. The fluorescent intensity after photobleach as a function of time can expressed as,

$$F(t) = [F(\infty) - F(0)][\exp(-2\tau_{\mathrm{d}}/t)(I_0(2\tau_{\mathrm{d}}/t) + I_1(2\tau_{\mathrm{d}}/t))] + F(0) \tag{3.2}$$

where $F(t)$ is the fluorescence intensity of the circular bleached region at time t, $F(\infty)$ is the recovered fluorescence intensity at time $t = \infty$, and $F(0)$ is the fluorescence intensity at time $t \longrightarrow 0$. Set t=0 as the point where the fluorescence intensity drops the most after bleach. I_0 and I_1 are the modified Bessel functions. Then, the diffusion coefficient D can be obtained from the following equation,

$$D = \omega^2/4\tau_{\mathrm{d}} \tag{3.3}$$

where ω is the radius of the circular bleached region. In our experiments we used several salt solutions whit several concentrations and calculated the respective diffusion coefficient D and then compared them to discuss.

3.3 Results

3.3.1 Phase separation with monovalent salts

To investigate whether the added salts can induce phase separation in charged lipids-containing membranes, fluorescent microscopic observations were performed with the observation chamber described in Figure 3.5. The lipid ratio of GUVs was DOPS/DPPC/-Chol=40/40/20, and we use the monovalent salts NaCl, NH_4Cl, propylamine with kinds of concentration.

The fraction of the phase separation structure at each concentration in summarized in the Figure 3.8. For each salt concentration, at least 90 GUVs were observed. We did a control group experiment without adding salt using Milli-Q water, Figure 3.9(a). The results showed that no phase separation structure was observed without the addition of salt. And the phase separation structure was observed in the case of added monovalent salts NaCl, NH_4Cl, propylamine in Figure 3.9(b-d), respectively. And the fraction of phase separation was promoted with the increase of salt concentration. This is consistent with the results of the prior study [9]. Also, we observed that NaCl, NH_4Cl caused phase separation at concentrations around 1.0×10^{-1} M, in contrast, whereas propylamine caused phase separation at concentrations around 1.0×10^{-4} M. Although they are the same monovalent salts, the salt concentrations that cause phase separation differ greatly.

We observed that in the experiments with the addition of NaCl, the formation of GUV was fugitive. Even a slight increase in NaCl concentration made the membrane rupture and prevented the formation of stable GUVs. Hence, we were not able to carry out the experiment to the concentration of NaCl that caused more than 40% phase separation. This phenomenon also occurred in NH_4Cl, where we were unable to increase the concentration of the experiment to a concentration that caused more than 20% phase separation.

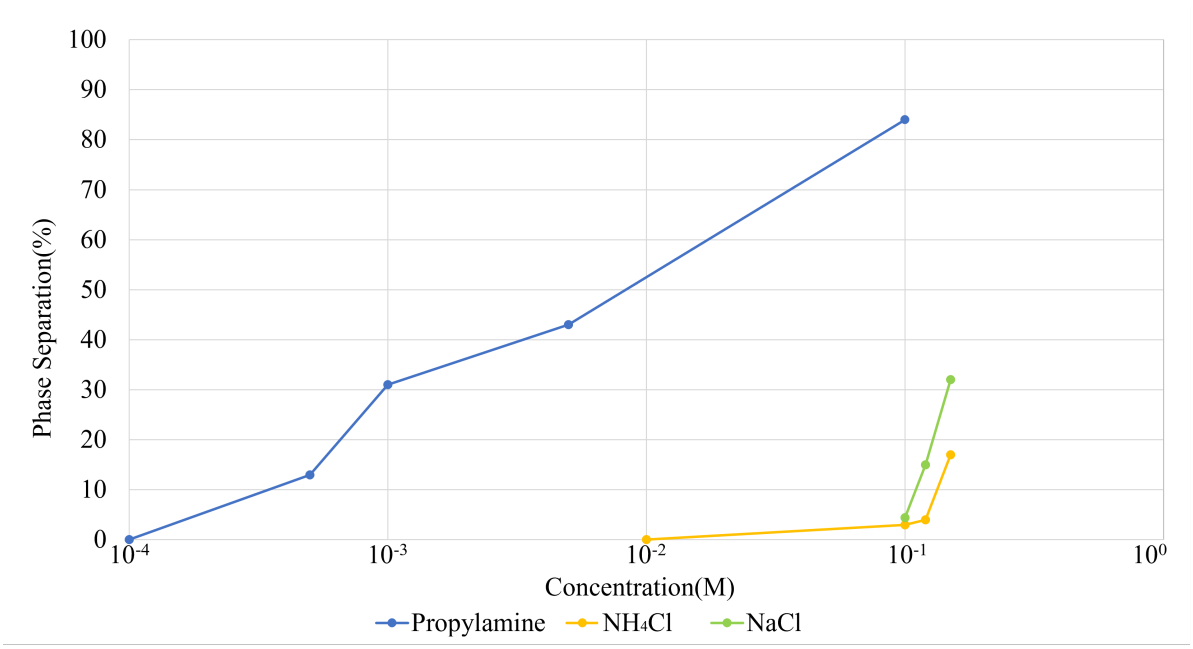

Figure 3.8: Fraction of the phase-separated structure as a function of the monovalent salt concentration in DOPS/DPPC/Chol=40/40/20 GUVs.

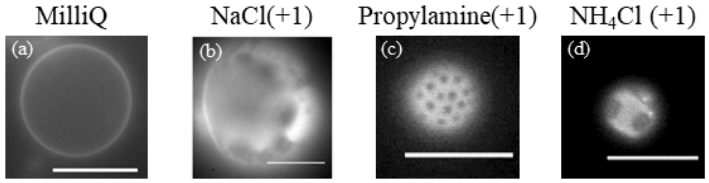

Figure 3.9: Microscopic images of the surfaces of GUVs. Hydration with (a)Milli-Q water (b)NaCl (c)propylamine (d)NH_4Cl. Scale bars are 10 μm.

3.3.2 Phase separation with divalent salts

Next, we observed the phase separation with the addition of the divalent salts $CaCl_2$, $MgCl_2$, ethylenediamine, putrescine, hexamethylenediamine at room temperature using fluorescence microscopy. The fractions of the phase separation structure at each concentration are shown in the Figure 3.10.

As observed with monovalent salts, the addition of divalent salts also led to the generation of phase separation structures in charged lipid membranes, Figure 3.11. Moreover, the phase separation formation was promoted as the salt concentration increased. In the divalent salts, we also observed that the added salts led to phase separation of charged lipid membranes at different concentrations, even though they had the same valence state. Among them, $CaCl_2$ led to the lowest required concentration for phase separation, followed by $MgCl_2$, hexamethylenediamine, ethylenediamine, and putrescine in that order. It can be seen that the concentration required for amines (hexamethylenediamine, ethylenediamine, putrescine) to induce phase separation in charged lipid membranes is much higher than that of metal salts ($CaCl_2$, $MgCl_2$).

We observed that in the experiments with the addition of $CaCl_2$, it was hard to form GUVs. And for $MgCl_2$ the same phenomenon with NaCl happened, even a slight increase in $MgCl_2$ concentration made the membrane rupture and prevented the formation of stable GUVs. Hence, we were not able to experiment with the concentration of $MgCl_2$ that caused more than 20% phase separation. On the other hand, this phenomenon did not observe in the experiments with diamines.

Comparing the results for the monovalent salts, it can be seen that, overall, the concentration of salt required to induce phase separation from the divalent salts is much lower than that of the monovalent salts. Although there is only a one-valent difference in charge, the typical monovalent salts (e.g. NaCl) require 1.0×10^{-1} M to induce phase separation, whereas the divalent salts require only 1.0×10^{-3} M to 1.0×10^{-5} M. We will discuss the possible reasons for this difference later.

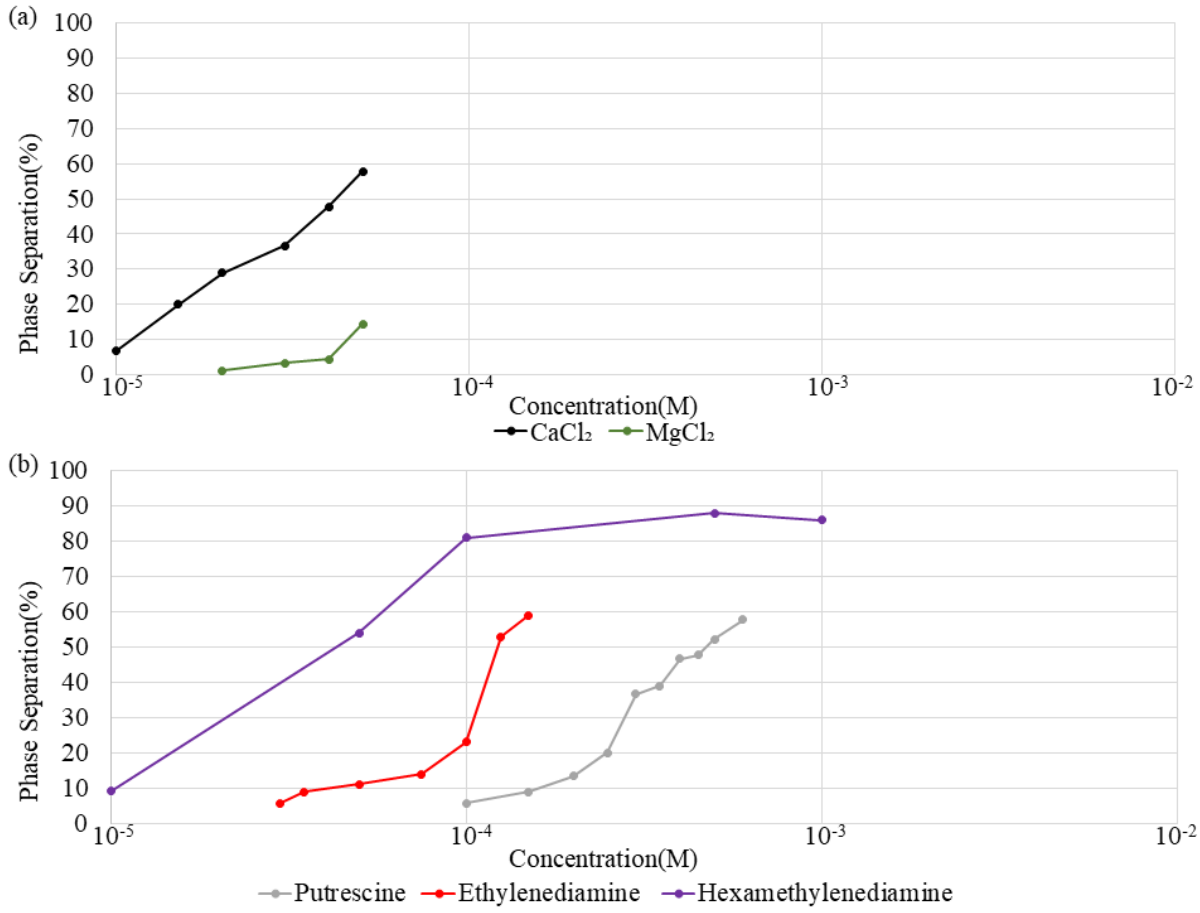

Figure 3.10: Fraction of the phase-separated structure as a function of the divalent salt concentration in DOPS/DPPC/Chol=40/40/20 GUVs. Hydration with (a)divalent metal salts and (b)diamines.

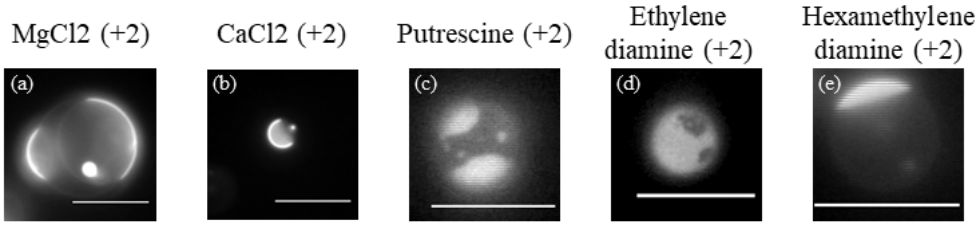

Figure 3.11: Microscopic images of the phase-separated GUVs. Hydration with (a)$MgCl_2$, (b)$CaCl_2$, (c)putrescine, (d)ethylenediamine, and (e)hexamethylenediamine. Scale bars are 10 μm.

3.3.3 Phase separation with polyvalent salts

Further, we used higher valence salts and did the same observations. The lipid composition of the GUVs was DOPS/DPPC/Chol=40/40/20, and three kinds of polyamines, trivalent polyamine spermidine, tetravalent polyamine spermine, and pentavalent polyamine 3(3)(3)4, were used to form the GUV solution and observed using fluorescence microscopy at room temperature. The fractions of the phase separation structure at each concentration are shown in the Figure 3.12.

The phase separation structure was also observed with the addition of polyvalent salts as shown in Figure 3.13. And also, the phase separation is promoted along with the increase in salt concentration. We found that even with different valence states, spermidine, spermine, and 3(3)(3)4 induced phase separation in the concentration region of 1.0×10^{-5} M to 1.0×10^{-6} M for charged lipid membranes.

Comparing the results for the monovalent and divalent salts, it can be found that the polyvalent salts require a lower concentration of approx 1.0×10^{-6} M to induce phase separation.

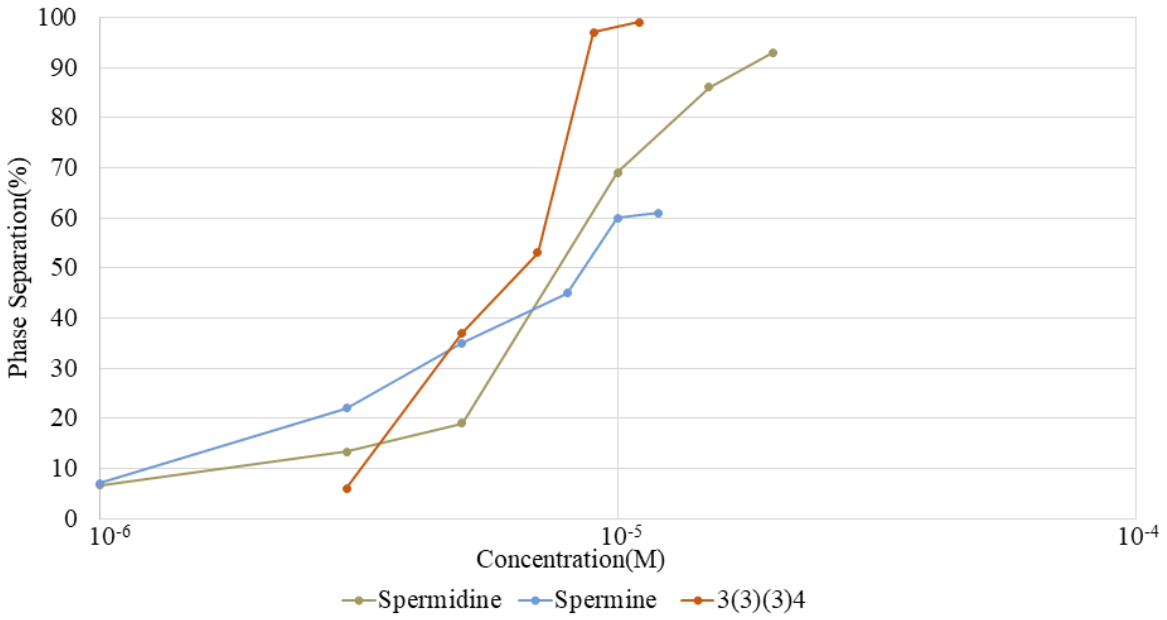

Figure 3.12: Fraction of the phase-separated structure as a function of the polyvalent salt concentration in DOPS/DPPC/Chol=40/40/20 GUVs.

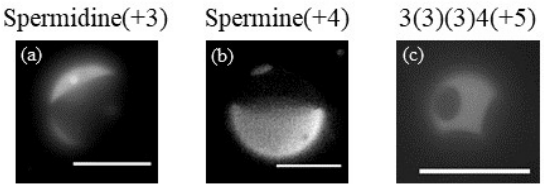

Figure 3.13: Microscopic images of the phase-separated GUVs. Hydration with (a)trivalent polyamine spermidine, (b)tetravalent polyamine spermine, and (c)pentavalent polyamine 3(3)(3)4. Scale bars are 10 μm.

3.3.4 Phase separation at higher temperatures

It was reported that when using charged lipids, the thermal stability of the phase separation was reduced, making it hard to form a phase separation structure, while when NaCl was added to the charged lipid membrane, the thermal stability of the phase separation structure increased. [9] It has also been reported that polyamines induce DNA to form a unique structures called nano-loop, at high temperatures [22]. Therefore, we made the same observation at different temperatures to investigate the effect of salt on the thermal stability of phase separation structures in the charged lipid membrane. The observation was at 30°C and 40°C using fluorescence microscopy. The fractions of the phase separation structure at each concentration are shown in the Figure 3.14, 3.15, and 3.16.

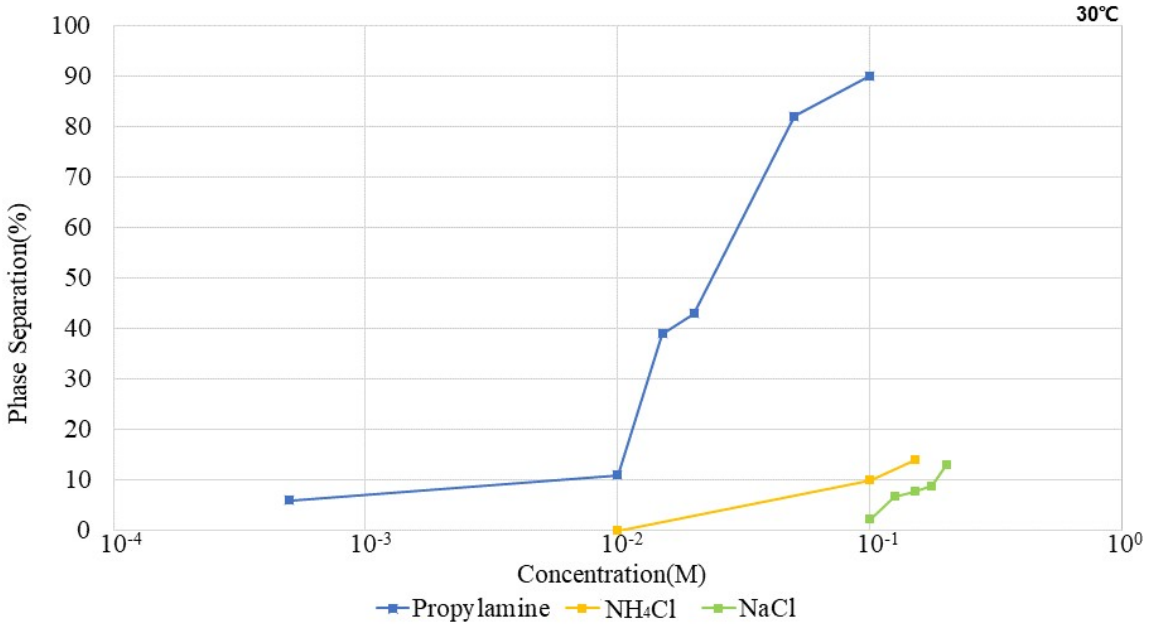

(a)

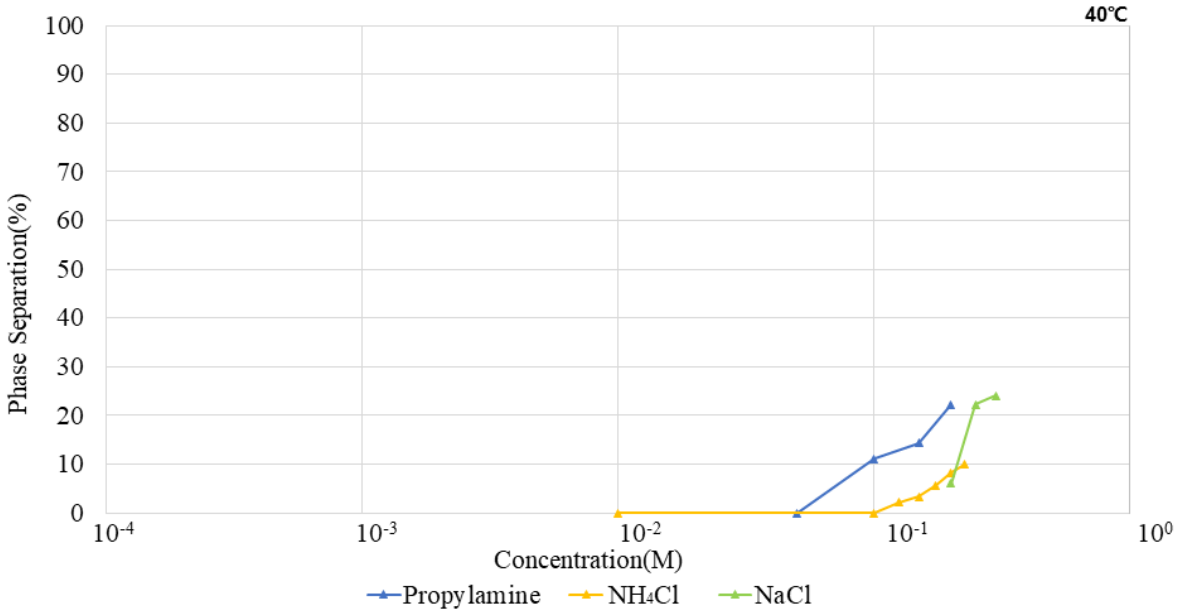

(b)

Figure 3.14: Fraction of the phase-separated structure as a function of the monovalent salt concentration in DOPS/DPPC/Chol=40/40/20 GUVs at (a)30°C and (b)40°C.

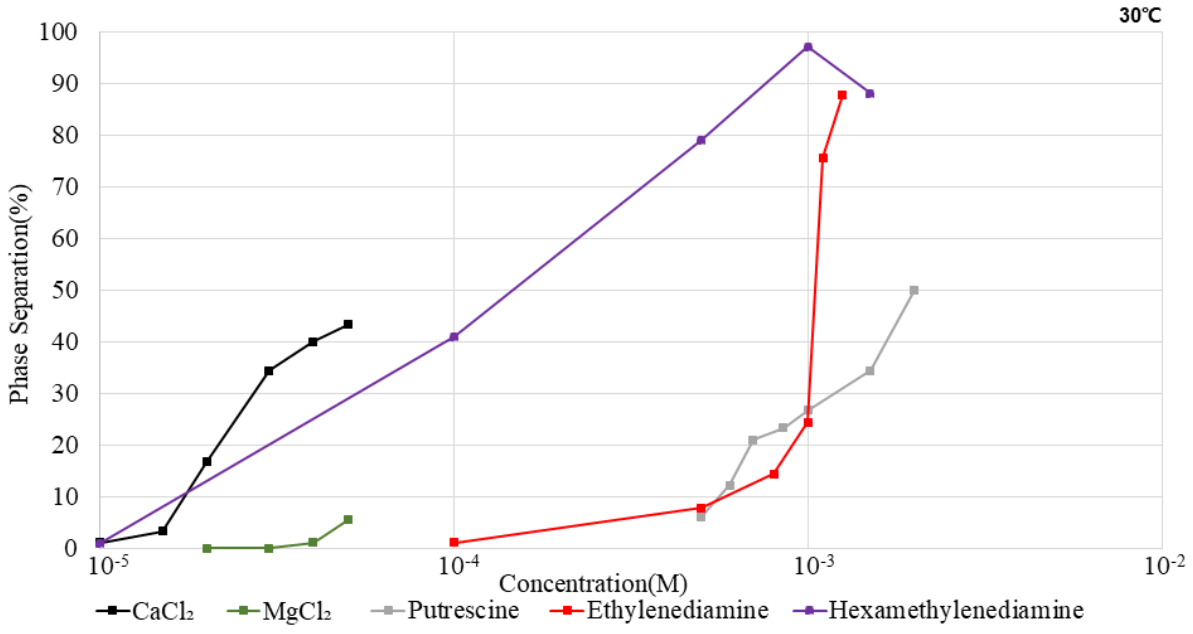

(a)

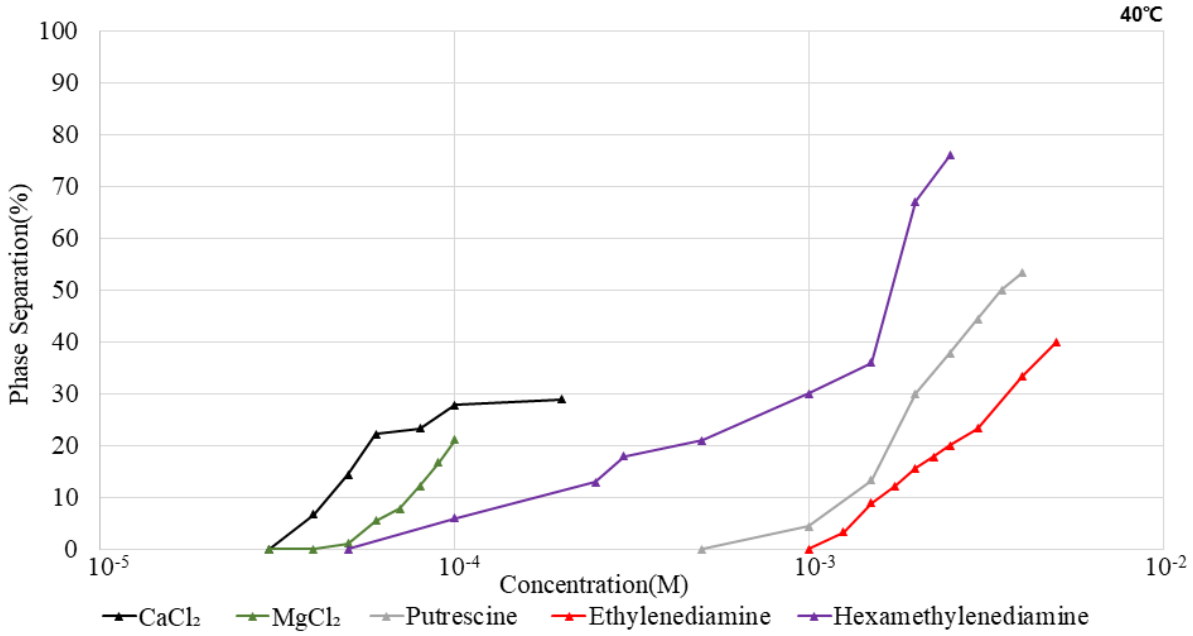

(b)

Figure 3.15: Fraction of the phase-separated structure as a function of the divalent salt concentration in DOPS/DPPC/Chol=40/40/20 GUVs at (a)30°C and (b)40°C.

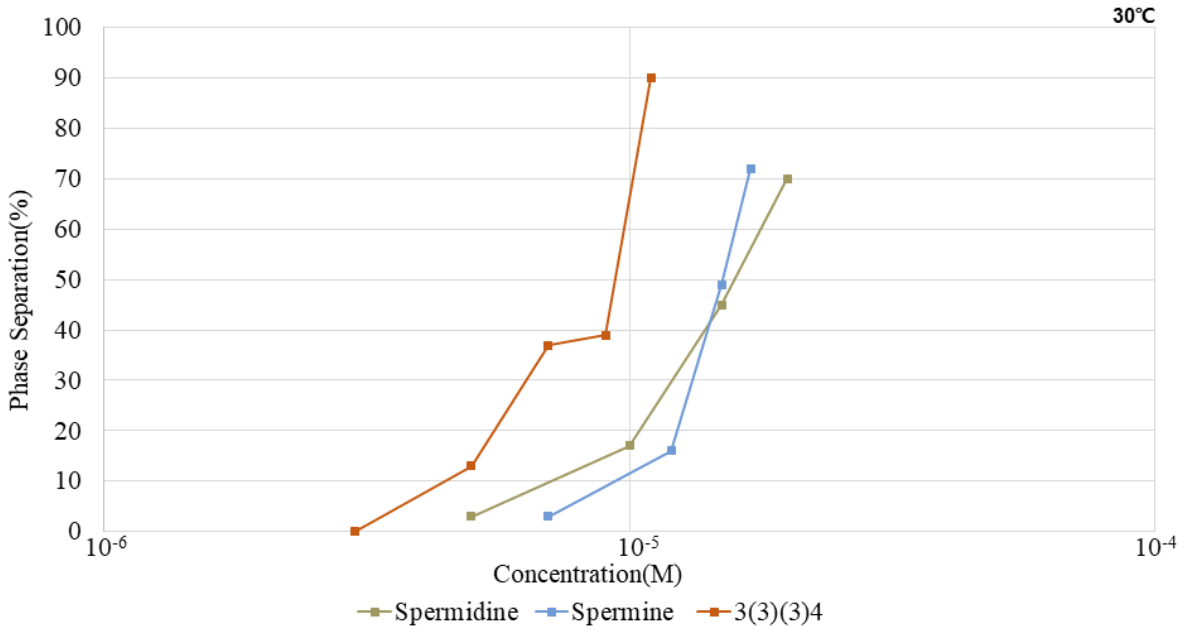

(a)

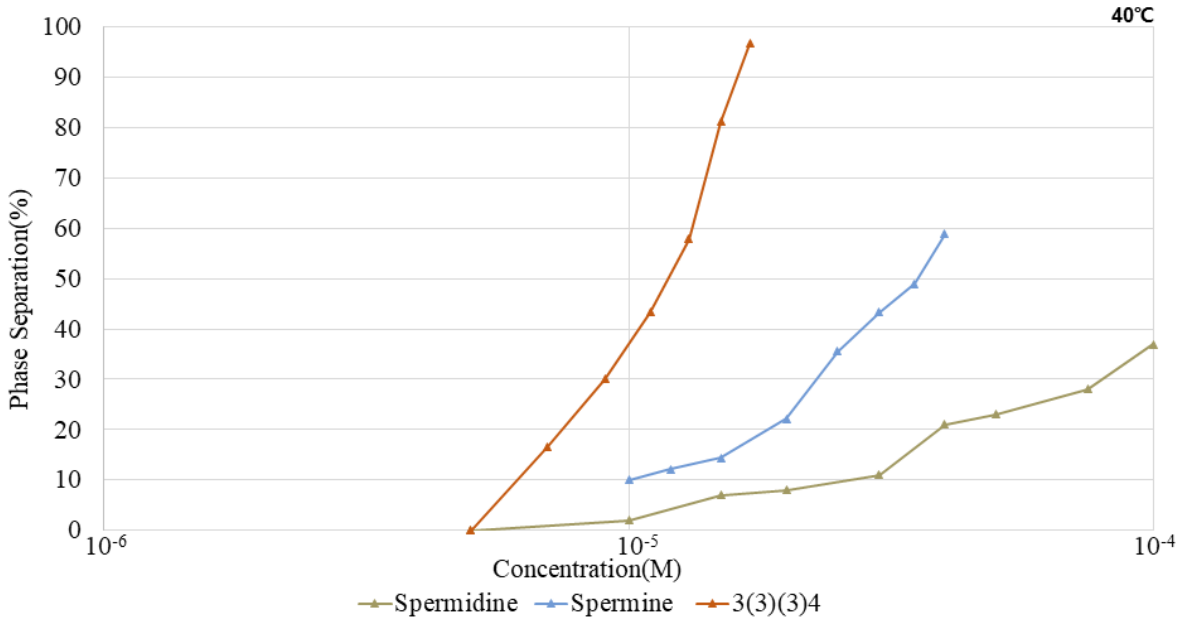

(b)

Figure 3.16: Fraction of the phase-separated structure as a function of the polyvalent salt concentration in DOPS/DPPC/Chol=40/40/20 GUVs at (a)30°C and (b)40°C.

While we calculated the salt concentration at a fraction of 50% phase separation and plotted it in Figure 3.17.

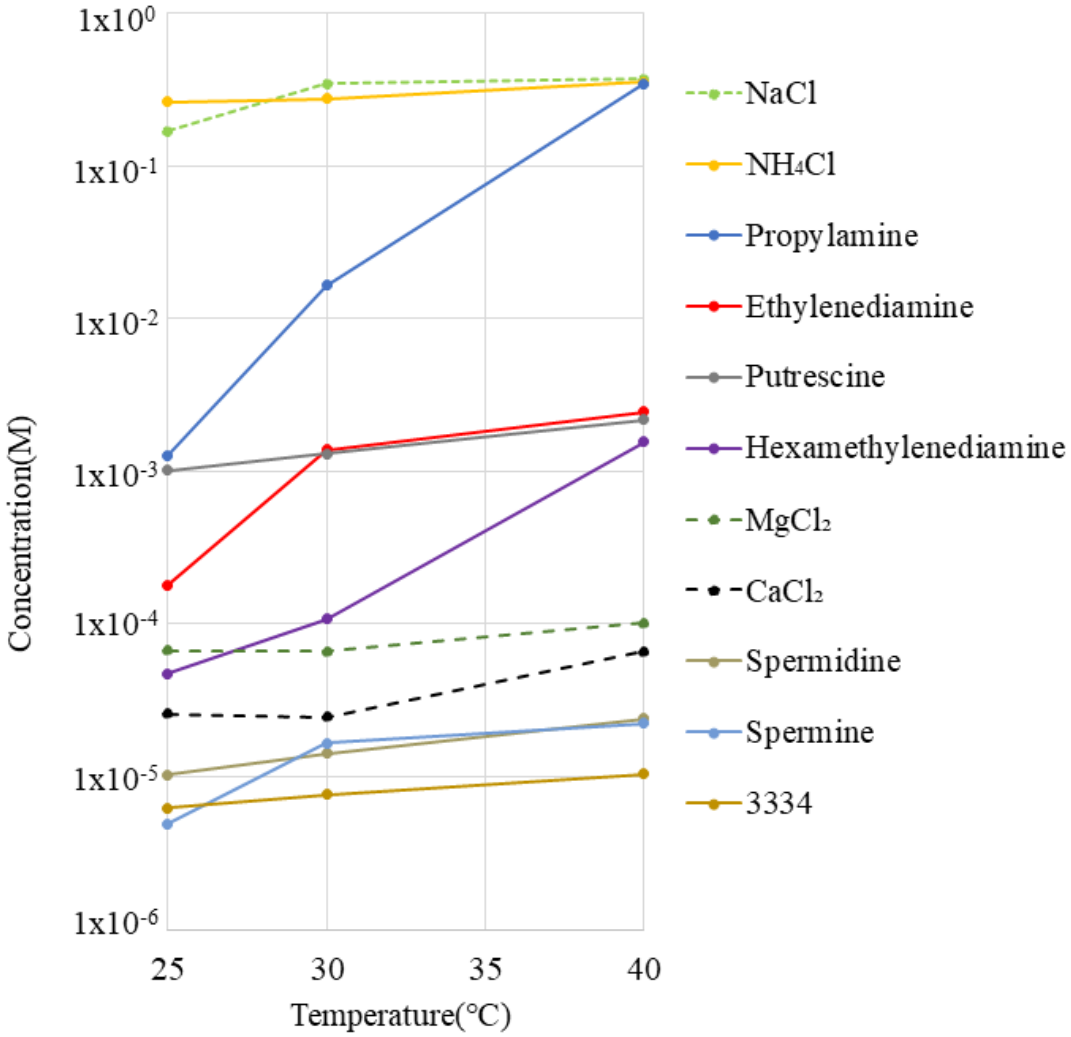

Figure 3.17: Fraction of the 50% phase separation salt concentration as a function of the temperature. The dashed and solid lines represent the results for metal salts and amine salts, respectively.

First, even though the temperature was changed, we still observed in all salt experiments that the generation of phase separation was promoted along with an increase in salt concentration, as in the results obtained earlier. We observed that as the temperature increased, the salt concentration required to cause phase separation became higher, and this phenomenon was observed for all added salts. Also, it is clear from the graph of the

salt concentration at 50% of phase separation that, basically, at any temperature, the lower the valency of the salt, the higher the salt concentration required to cause phase separation in the charge lipid membrane. A monovalent salt requires 1.0×10^{-1} M except for propylamine to induce phase separation, while a divalent salt requires just 1.0×10^{-3} M to 1.0×10^{-5} M. The salt concentration requires to induce phase separation for monovalent salt is two to four orders of magnitude larger than that for divalent salt.

Further, we found that for metal salts, an increase in temperature may increase the concentration required to cause phase separation, but this increase is not much significant. However, for amines, by the influence in temperature, the increase in the concentration required to cause phase separation changed a lot. This indicates that the behavior of amines on charged lipid membranes is more susceptible to temperature effects. The most significant change in concentration was for monovalent amines propylamine, and the most minor change in concentration was for pentavalent polyamine 3(3)(3)4. We discuss that this change in thermal stability may be related to the structure of the metal ions and amines later.

3.3.5 Measurement of membrane fluidity with added salt

As we discussed above, the addition of any salts induced the phase separation in charged lipid membranes. Therefore, we consider that the added cations contribute to suppress the repulsion between charged lipids or cause the attraction between charged lipids. If the interactions between charged lipids are changed by the added cations, the mobility of charged lipids in the membranes will be also changed. To discuss the effect of salt addition on the charged lipid mobility, we performed fluorescence recovery after photobleaching (FRAP) experiments to measure the diffusion coefficient in DOPS single-component supported lipid bilayers (SLBs). The results showed that the diffusion coefficient of the DOPS single-component membranes in Milli-Q water without any salts was 0.68 μm^2/sec. Typical DOPS SLB normalized fluorescence intensity plot in Figure 3.18, shows fluorescence intensity finally recovered about 60%.

After the addition of salt, all types of salt showed different degrees of diffusion coeffi-

cient, the minimum was decrease to arrouned 0.2 μm^2/sec. Typical DOPS SLB normalized fluorescence intensity with added slat plot in Figure 3.19, shows fluorescence intensity finally recovered less then 30%. And as the salt concentration decreased, the diffusion coefficients tended to be close to those without salt addition, Figure 3.20-3.22(diffusion coefficient without salt indicate as the red dotted line). Even though the results of the effect of salt addition on the diffusion coefficient of charged lipid membranes look somewhat different from the experiments in vesicles, we can still observe a significant decrease in the diffusion coefficient due to salt addition which demonstrates that the addition of cations alters the interaction between charged lipids.

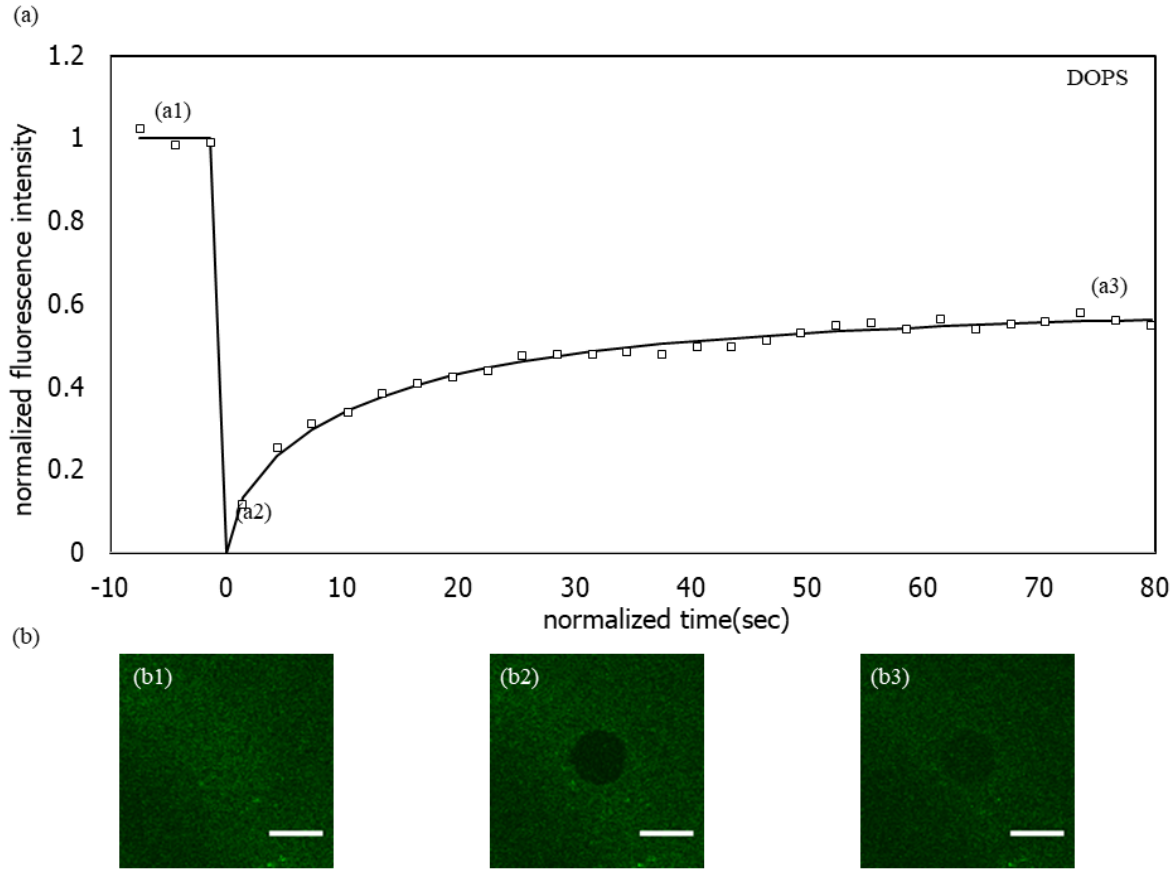

Figure 3.18: (a)Fraction of the Normalized fluorescence intensity as a function of normalized time in DOPS SLB without added salt and (b)confocal laser scanning microscopy images (b1-b3) correspond to the (a1-a3)in Fraction, respectively. Scale bars are 5 μm.

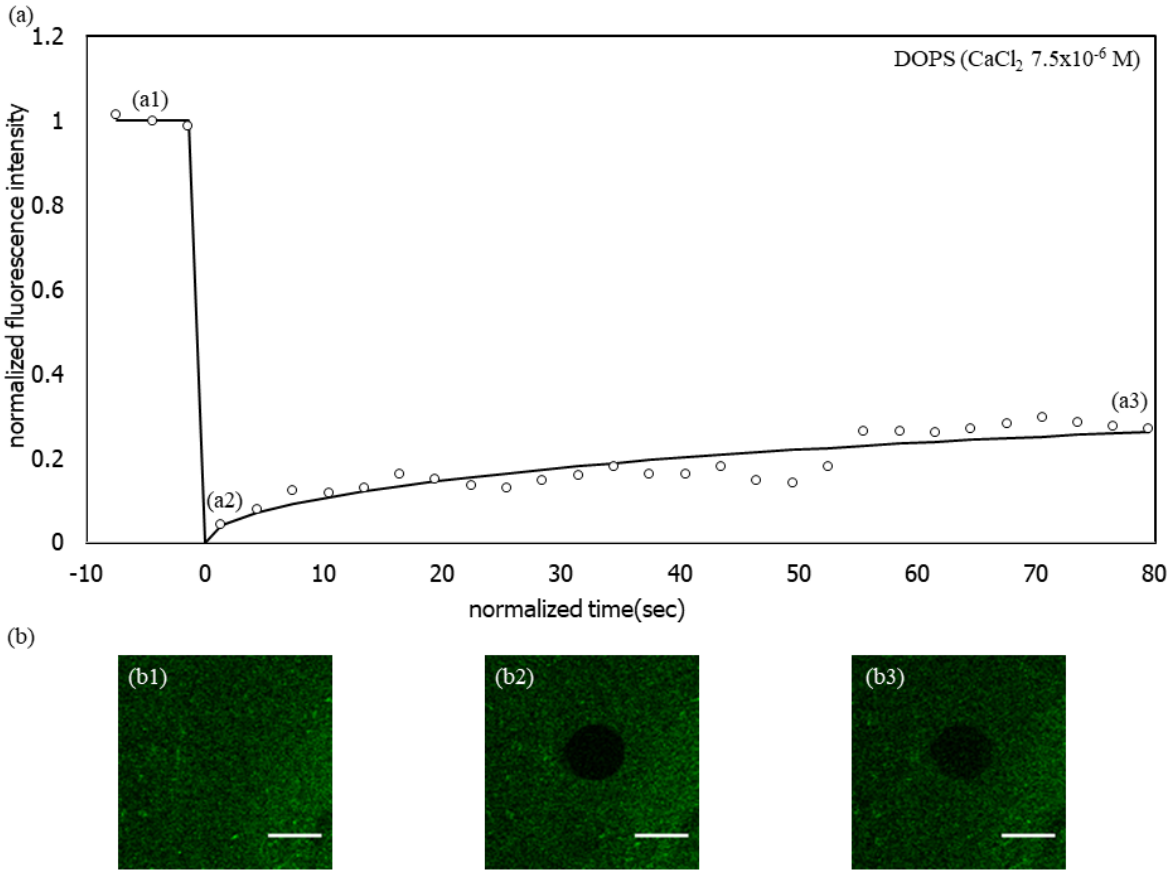

Figure 3.19: (a)Fraction of the Normalized fluorescence intensity as a function of normalized time in DOPS SLB with $CaCl_2$ 7.5μM and (b)confocal laser scanning microscopy images (b1-b3) correspond to the (a1-a3)in Fraction, respectively. Scale bars are 5 μm.

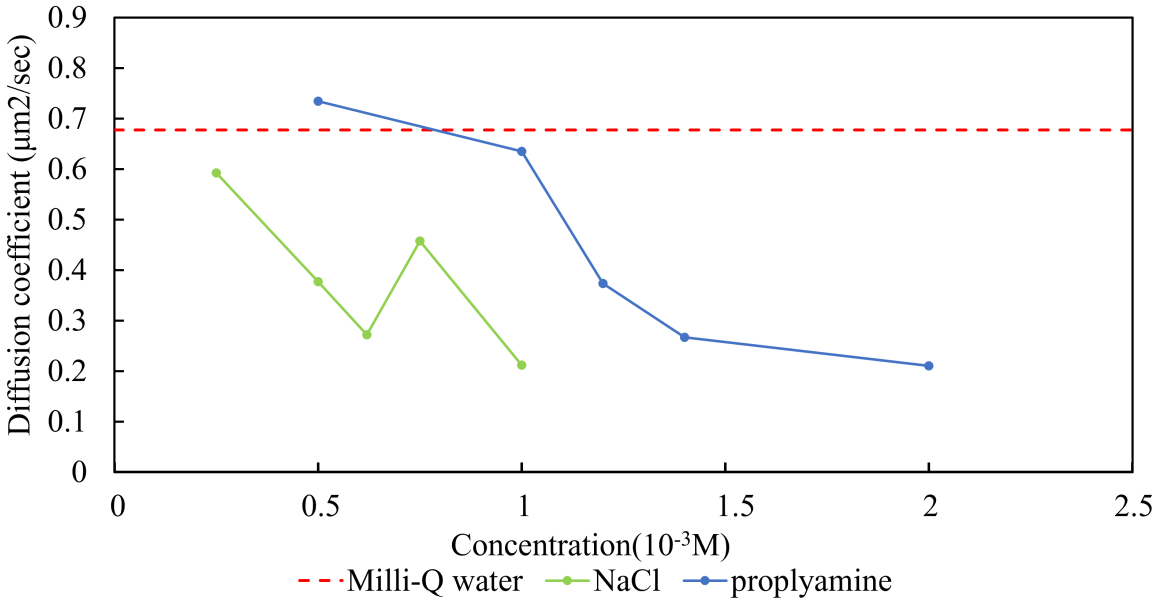

Figure 3.20: Fraction of the Diffusion coefficients as a function of the monovalent salt concentration in DOPS SLBs. Red dotted line repersent DOPS SLB diffusion coefficient without salt.

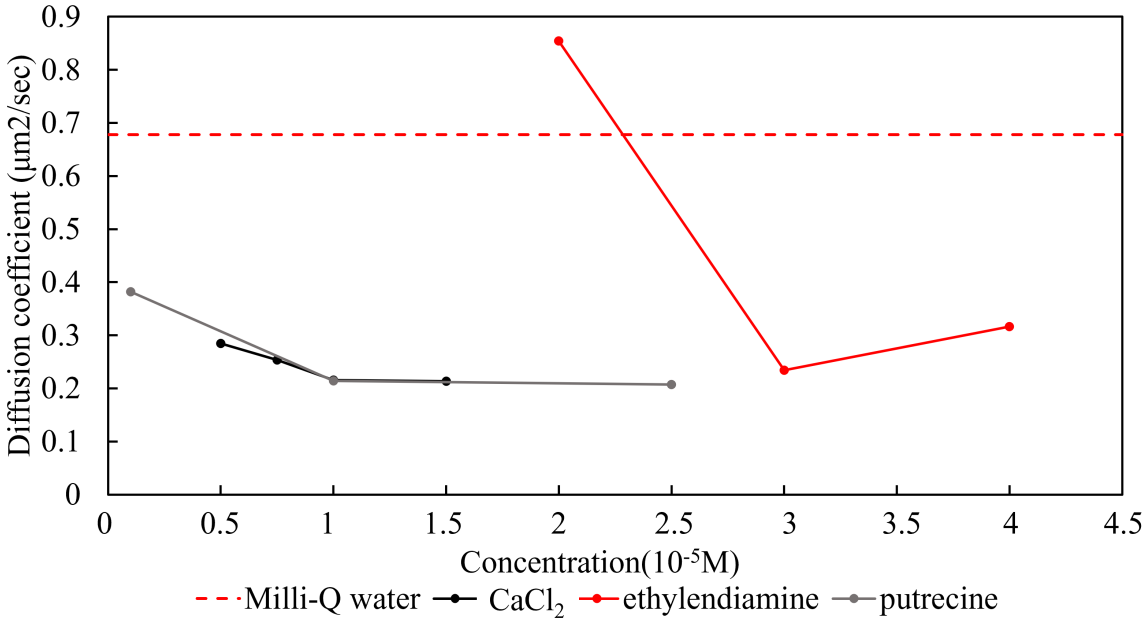

Figure 3.21: Fraction of the Diffusion coefficients as a function of the divalent salt concentration in DOPS SLBs. Red dotted line repersent DOPS SLB diffusion coefficient without salt.

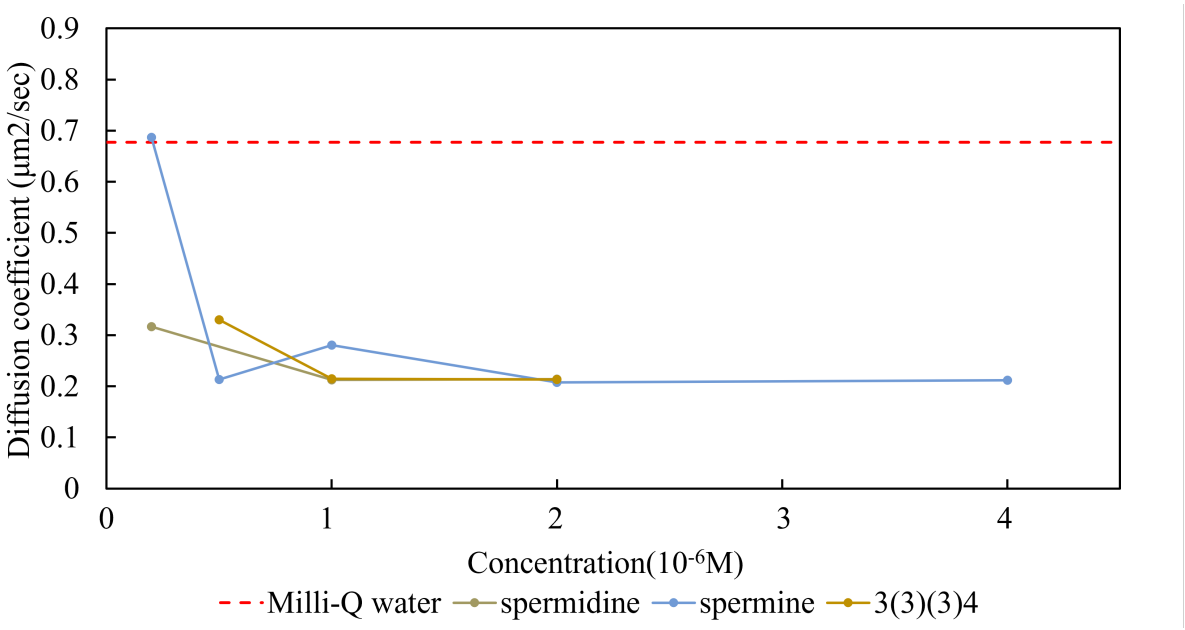

Figure 3.22: Fraction of the Diffusion coefficients as a function of the polyvalent salt concentration in DOPS SLBs. Red dotted line repersent DOPS SLB diffusion coefficient without salt.

3.4 Discussion

3.4.1 Influence of electrostatic screening by added salt on phase separation

In experiments with charged lipid membranes composed of the three components DOPS/DPPC/Chol, no phase separation structure was observed without any salts. This result is consistent with the prior studies [10] [28]. Since the DOPS headgroup is negatively charged, electrostatic repulsion between them prevent the formation of phase separation structures. And we observed the phase separation structure regardless of any added salt. This is because the addition of salt makes the electrostatic repulsion of the DOPS headgroups weaker. When the electrostatic interactions no longer dominate, the attractive interactions derived from the chain ordering induce the formation of the phase separation structure. When increasing the salt concentration, the screening of the electrostatic interactions becomes stronger. As a result, more GUVs formed phase separation structures. The screening effect can be expressed as the Debye screening length l_{D},

$$l_{\mathrm{D}} = \sqrt{\frac{\varepsilon_W k_{\mathrm{B}} T}{2 N_{\mathrm{A}} e^2 I}} \tag{3.4}$$

where ε_W is the dielectric constant of the solution, k_{B} is Boltzmann constant, T is absolute temperature, N_{A} is Avogadro's number, e is the elementary charge, and I is the ionic strength of the solution. Ionic strength I can expressed as,

$$I = \frac{1}{2} \sum_i c_i z_i^2 \tag{3.5}$$

where c is ion concentration, z is ion valence. The above equation simply shows that when the cation valence remain constant, the Debye length is shorter when the ion concentration c is larger. And the shorter the Debye length, the greater the screening effect. Which causes the orderliness of lipid tails dominate on lipid membrane behavior, instead of the electrostatic interaction of the head. Thus, DOPS and DPPC possessing different

saturation tails produce phase separation structure.

It is easy to see from equations (3.4) and (3.5) that if the variation of salt concentration required for phase separation follows only this rule, there should be a proportionality between the charge and the concentration required for phase separation. And by adjusting the concentration, it is possible that at some concentration, the monovalent salt can have the same ionic strength I as the divalent salt and can have the same phase separation behavior, which would not have that difference we observed. For example, the difference between monovalent salt NaCl and divalent $CaCl_2$. According to equation 3.4, we considered that the same ionic strength I of the salt can lead to the same Debye length and thus induce the same phase separation behavior. From equation 3.5, we can calculate that when the ionic strength I of NaCl and $CaCl_2$ are the same, the concentration of NaCl should be 4 times higher than that of $CaCl_2$. However, from Figure 3.17 we can see that the concentration required for the same induction of 50% phase separation for NaCl is nearly three orders of higher than for $CaCl_2$. This result is clearly inconsistent with the calculation. In this chapter, we will discuss these kind of exceptions in detail.

3.4.2 Influence of salt valence on phase separation

As dicsscued above, we revealed that salts with larger valence basically require lower concentrations to induce phase separation in charged lipid membranes. This behavior can be also interpreted by Debye length. In addition, in experiments using salts of different valence, we also observed a significant difference between the salt concentrations required to cause phase separation in charged lipid membranes.

Here we consider the possibility that a kind of banding occurs between metal ion with higher valence number and charged headgroup [29]. It has been reported that divalent metal ions Ca^{2+} strongly bind to lipids, and one Ca^{2+} ion binds two lipid molecules [30] [31]. Seelig et al. reported that the Ca^{2+} ions concentration on the phospholipid membrane surface was increased by at least two orders of magnitude compared to the solution ion concentration, indicating a strong binding of Ca^{2+}-phospholipids [31]. It also occurs in other divalent cations, such as Ba^{2+}, Sr^{2+}, and Mg^{2+}, but the binding

strength depends on the different cations [32]. But this kind of binding phenomenon is rarely happening in monovalent ions Na^+ [33] [34]. It has been indicated that the binding constant for monovalent Na^+ ions is more than an order of magnitude smaller than that of divalent Ca^{2+}. Divalent cations are more successful in binding to bilayer surfaces monovalent cations, despite their much lower concentration in the solution. [35] This is in agreement with our results that the concentration of divalent cations required to induce the phase separation is at least two orders of magnitude smaller than that of monovalent ions.

For charged lipis, Sinn et al. have reported that calcium ions tend to bind strongly to the negative charge of the DOPS headgroup and that this can occur at relatively low Ca^{2+} concentrations [36]. In this case, the negative charge of the PS head is offset by the bound divalent cations, directly reducing the surface charge of the membrane. This direct reduction of membrane surface charge may have a more significant impact on the screening of electrostatic interactions. And it has been reported that a divalent cation when combined with the negative charge on the head of DOPS, binds two DOPS molecules, which is equivalent to directly connecting two DOPS molecules to make them aggregate and form a kind of bridging structure [33]. Specific attraction by bridging causes lipids to aggregate and form a phase-separated structure. The reason for induced phase separation at very low concentrations compared to Na^+ can be thought that Ca^{2+} binds to PS and cancels the surface charge.

It has been indicated that because the negatively charged surface potential increased the concentration of Ca^{2+} ions near the surface, the result was an increase in Ca^{2+} binding to all lipids in the membrane [35]. This could potentially lead to an overall increase in membrane tension. Sinn et al. also reported similarly. They observed the rupture of vesicles in experiments with the addition of Ca^{2+} and indicated that the tight binding of Ca^{2+} to the membrane led to a tighter packing of lipid headgroups, thus causing the membrane tension increase. The tension approached the cleavage tension of the lipid membrane. [36] Since our experiment was not observed in real-time after adding salt, we did not directly observe rupture. However, we observed that it is challenging to form easily observable GUVs when higher concentrations of metal salts were added. It is likely that it has already led to partial GUV rupture during GUV preparation due to the addition

of salts and makes it difficult to observe the complete GUVs.

Plus, we found a significant difference between the concentrations required for the salt to induce phase separation in charged lipid membranes, even if the valence numbers were the same. This difference can not be explained by the screening effect.

3.4.3 Influence of cation size on phase separation

In experiments using divalent salts, it is evident to see that the concentration required for the metal ions to induce phase separation formation is lower then that for diamines. The difference between $CaCl_2$ and putrescine is most significant. The concentration required for $CaCl_2$ to induce phase separation is 1.0×10^{-4}, the concentration required for putrescine to induce phase separation is 1.0×10^{-3}, ten times the difference. Here, we considered that the difference might be due to the different sizes of the cations, which causes the different amount of cation adsorption onto the membrane surface.

The cation size shown in Figure 3.23 also takes into account the hydration of divalent cations [37] [38]. Schematic illustration of different size cations adsorb to charged lipid membranes showen in Figure 3.24.

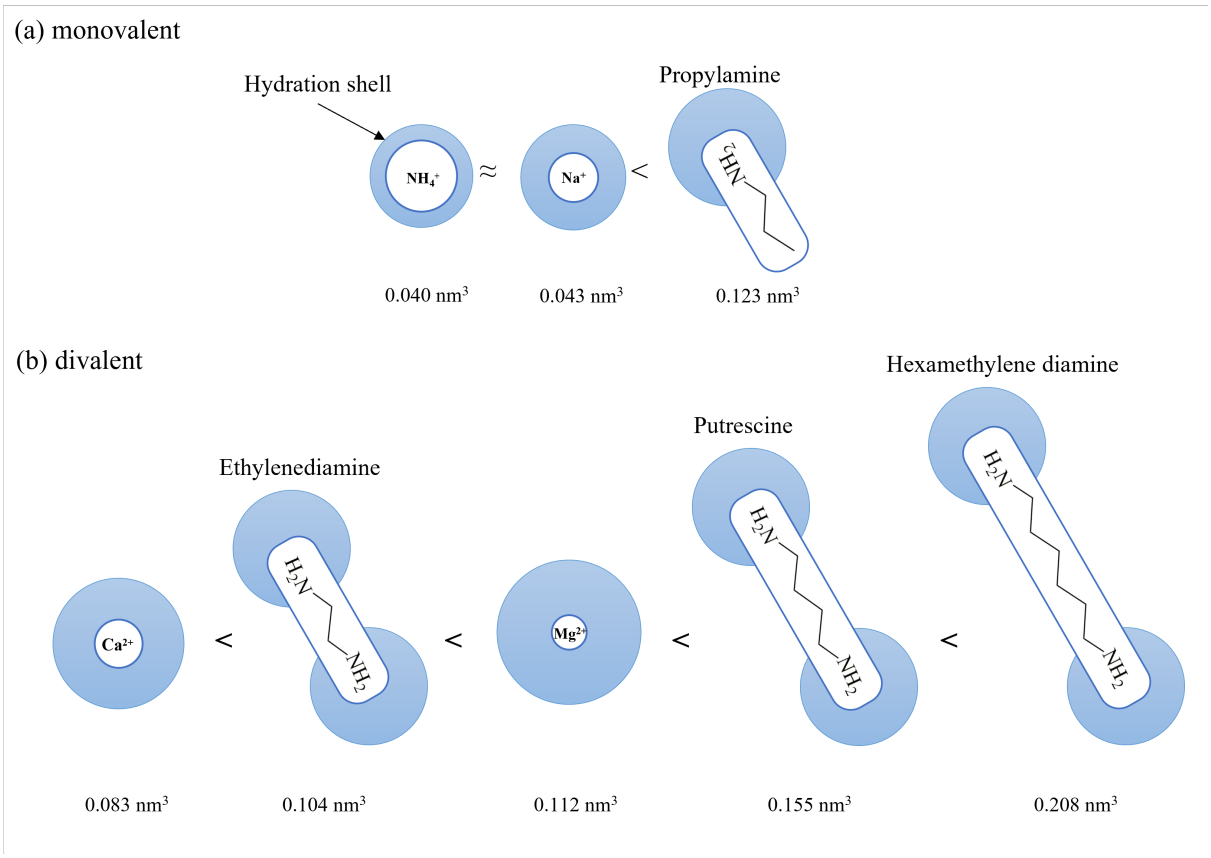

Figure 3.23: Schematic illustration of different cation size. (a)monovalent and (b)divalent cations.

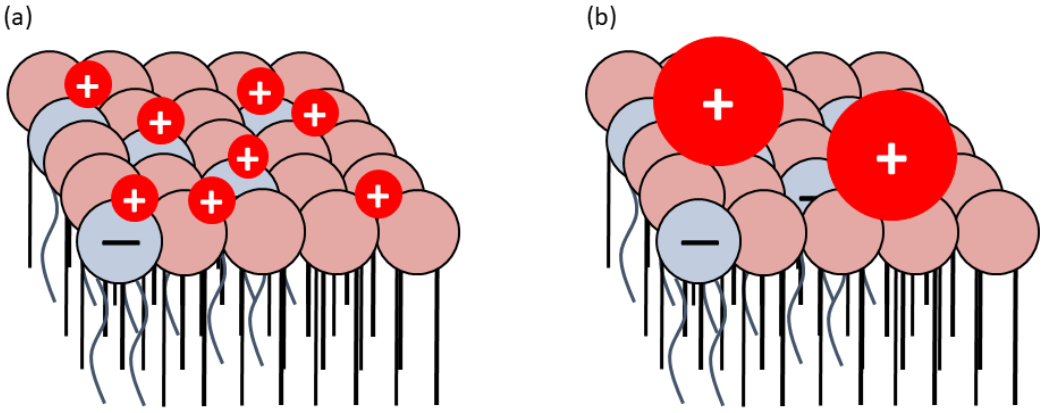

Figure 3.24: Schematic illustration of different size cations adsorb to charged lipid membranes. (a)smaller size and (b)larger size.

We have previously discussed that ions adsorbed onto membranes strongly influence phase separation formation. When ions are adsorbed onto lipid membranes, it becomes important to consider the steric repulsion between ions. In the case of a larger size cation, the steric repulsion between the cations adsorbed onto the membrane will also be larger, resulting in the inability to absorb more cations, making it difficult to form phase separation structures. On the contrary, the smaller size cation excluded volume is small and has smaller steric repulsion, which can adsorb more amount to the membrane, and the phase separation structure can be formed easily. Thus, for cations with larger sizes, the salt concentration required to induce phase separation structure also becomes higher. Also, we observed that in the same valence state, amines cause a higher concentration required for phase separation structure compared to metal ions, which may also be due to generally amines having a larger size.

ALthough propylamine and hexamethylenediamine are the largest cation in monovalent and divalent cations, respectively, the salt concentrations for phase separation are the lowest. Show in Figure 3.25. Here we consider that it is likely because both propylamine and hexamethylenediamine possess relatively long hydrophobic chains. In an aqueous solution environment, the hydrophobic parts tend to avoid water molecules. Thus, we believe that in solution, the longer hydrophobic parts of molecules may cross and overlap to form multimer, such as dimer.

The formation of the dimer leads to a change in the original valence state, with propylamine acting as a divalent and hexamethylenediamine as a tetravalent. (Figure 3.25) This elevated apparent valence leads to the formation of phase-separated structures at lower salt concentrations. Salts that possess shorter hydrophobic chains, on the other hand, fail to form dimers because the positive charges in a dimer come close each other and it causes the strong repulsion.

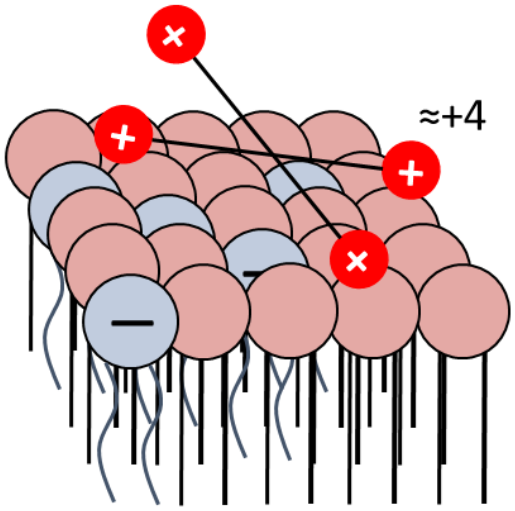

Figure 3.25: Schematic illustration of cations which form a dimer structure on charged lipid membranes.

3.4.4 Influence of temperature change on phase separation

We found that the salt concentration required for phase separation increased with increasing temperature. This phenomenon can also be explained by equations (3.4) and (3.5). For the same salt at a constant concentration, the higher the temperature make the longer the Debye length. This leads to a weaker electrostatic screening effect, making it more difficult to form phase separation structures. The mixing entropy of the membrane increases due to the increase in temperature, and maintaining an ordered structure such as phase separation leads to an overall loss of free energy of the system so that the lipids on the membrane surface tend to mix and it is difficult to form a phase separation structure. As a result, the ion concentration on the surface of charged lipid membranes is lower at higher temperatures.

As shown in Figure 3.17, as the temperature increases, the salt concentration for phase separation is dramatically increased for amine salts than for metal ions. Here we have considered the structures of cations and their behavior when adsorbed to lipid membranes. Most amines are linear and, therefore, generally adsorb to lipid membranes in a horizontal

orientation. As the entropy of cation orientation increases with increasing temperature, many cations cannot remain horizontally adsorbed, and form angles to the lipid membrane surface, resulting in a decrease in the apparent value. This weakens the effect of rod-like shape cations on the membrane surface. In contrast, metal ions are considered to be spherical, and the orientation entropy is less affected by temperature and, therefore, less sensitive to temperature as shown in Figure 3.26.

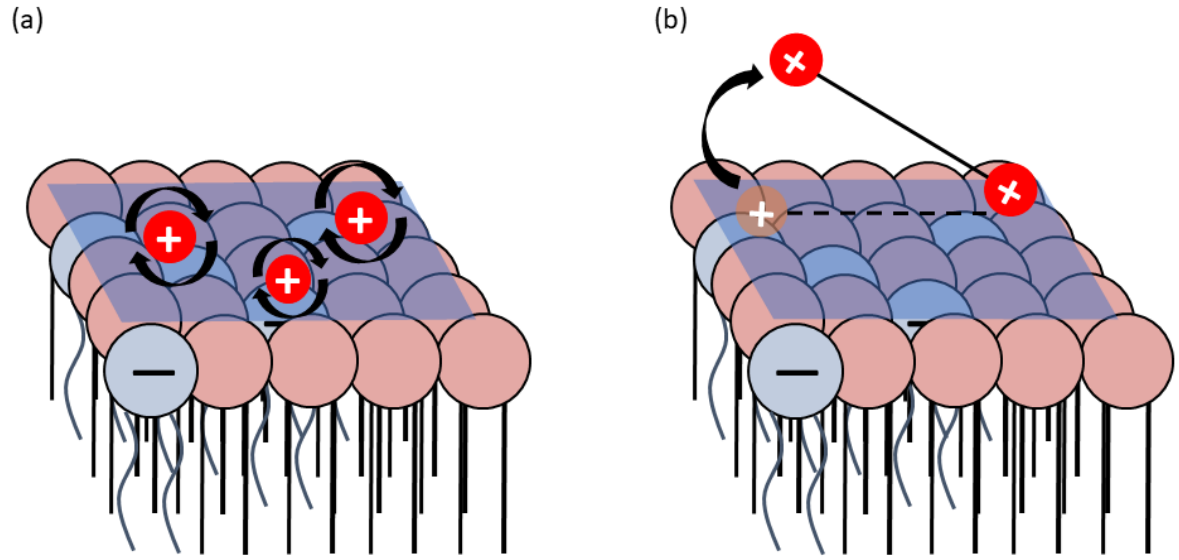

Figure 3.26: Schematic illustration of cations with different cation shape adsorbed onto charged lipid membranes. (a)Metal ion with spherical shape and (b)Amine with rod-like shape.

3.4.5 3(3)(3)4 on the membrane surface

Although the amine salts are sensitive to the change in the temperature, 3(3)(3)4 which was extracted from hyperthermophilis is less sensitive. We also observed that the concentration required to induce phase separation formation for the penta-valent 3(3)(3)4 was similar to that of the tetra-valent salt.

Here we considered the molecular structure of 3(3)(3)4. It can be assumed that 3(3)(3)4 has the potential to exhibit a tetrahedral structure closer to a sphere. This

makes it less affected by temperature and acts on the membrane more like a spherical metal ionas shown in Figure 3.27(a).

Also, it can be considered that 3(3)(3)4 can exhibit a tetrahedral configuration that possesses a larger molecular size. We discussed earlier that salts with larger size could lead to more significant steric repulsion between cations, inducing a need for higher salt concentration when phase separation occurs. And since this tetrahedral configuration is very close to a sphere, it speculated that the activity of 3(3)(3)4 on the lipid membrane surface is comparable to a sphere. This puts 3(3)(3)4 in a state where the face is adsorbed to the membrane, and the apex is far from the lipid membrane, and can roll on the lipid membrane, with an apparent valence state about 3-4 as shown in Figure 3.27(b). It is possible that the combination of these two causes the salt concentration required for 3(3)(3)4 to form phase separation structures may be close to a tetra-valent salt.

The hyperthermophiles possessing 3(3)(3)4 survive in a high-temperature environment of about 100°C. Considering the entropy point of view, higher valence cations are required to induce charged lipid membranes to form phase-separated structures at low concentrations. Higher valence metal ions are almost always toxic heavy metals, while higher valence polyamines are safer. Also, when considering the thermal stability of the phase separation structure, the contact of 3(3)(3)4 with the lipid membrane surface in a face rather than a straight line causes them to be less affected by the orientation entropy. Thus 3(3)(3)4 possesses higher thermal stability to the lipid membrane.

Comprehensive consideration, the high valence and steric configuration of the polyamines 3(3)(3)4 are more favorable for the survival of hyperthermophiles at high temperatures. It can also be speculated that some polyamines acquire some thermal stability due to their three-dimensional structure and become less sensitive to temperature effects. It is possible that in some cellular activities, polyamines can reduce their sensitivity to temperature by their three-dimensional structure and thus obtain some stability.

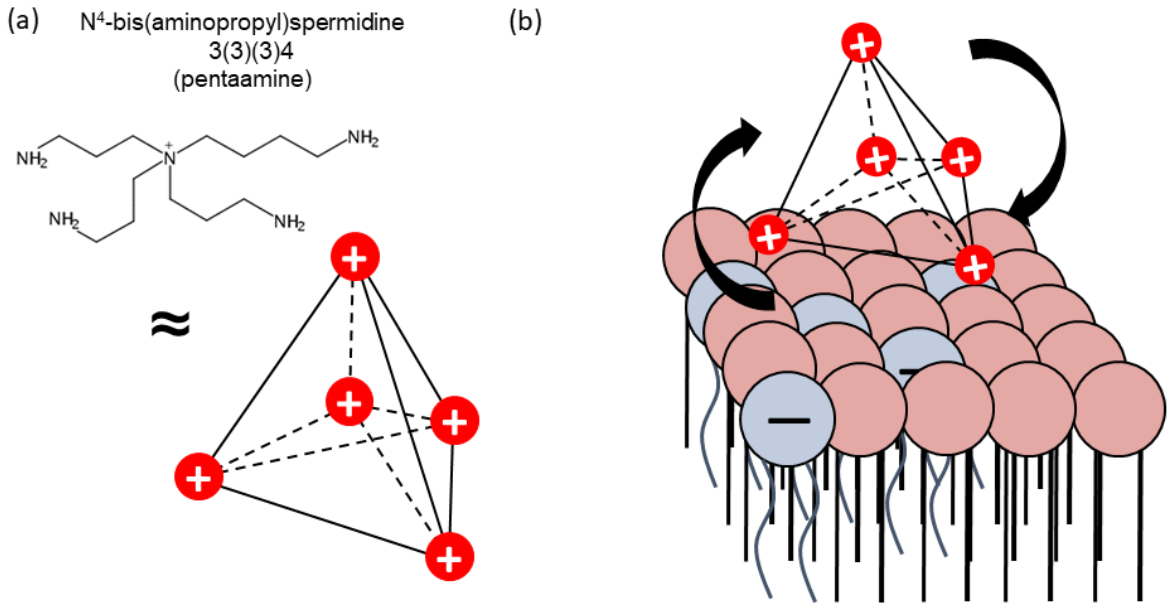

Figure 3.27: Schematic illustration of (a)3(3)(3)4 molecular structure and (b)3(3)(3)4 adsorbed onto charged lipid membranes.

3.4.6 Difference between metal ions and amines on biocellular functions

Two differences in the effects of metal ions and amines on the phase separation structure were found from our experimental results. One is that, in the case of minor additions, metal ions may also cause lipid membrane difficult to form GUVs. This phenomenon was not found in amines for the time being. The other is, the behavior of metal ion-induced phase separation formation is less influenced by temperature. In contrast, the amine-induced phase separation formation was more influenced by temperature.

In the previous discussion, we described the membrane rupture caused by the adsorption of high-valent metal ions and lipid membranes. The same phenomena did not find in diamines for the time being. Most likely, this is because polyamines are primarily linear, and the cationic groups are divided into both sides of the hydrophobic chains, which are far away and do not cause drastic changes in the local charge on the lipid membrane.

In contrast, divalent cations have a more concentrated charge and cause drastic local charge changes on charged lipid membranes, leading to rupture of the membrane or to bud due to changes in membrane curvature and eventually to the formation of new stable small vesicles. It has also been indicated in some studies that excessive intracellular Ca^{2+} concentrations can lead to cardiomyocyte hyperexcitability, thus triggering arrhythmias, and even in severe cases may lead to cell death [39] [40]. It can be speculated that since Ca^{2+} have a more significant impact on cellular functions such as cellular potential, some specific cellular processes require polyamines to provide cations.

The difference in thermal stability between metal salts and amines for the phase-separated structures comes more from the influence of entropy. The spherical metal ions are less affected by the orientation entropy, while the linear amines are more affected by the orientation entropy. This seems to indicate that to make cellular functions and life activities independent of the external environment or body temperature, the substances that regulate them need to be thermally stable. Metal ions are a good choice for this purpose. They have a small radius, are commonly found in nature, and as cations commonly found in cells and body fluids, are ions that tend to cause the formation of phase-separated structures in lipid membranes. And some experiments have reported that metal ions modulate a large number of cellular functions and life activities [41].

On the other hand, due to the prevalence of metal ions, they are relatively less suitable to modulate some specific reactions in vivo. Polyamines, on the other hand, fill this gap.

Male testicular tissue contains higher levels of polyamines than other tissues in the body, indicating that polyamines play a role in male spermatogenesis and fertilization [42]. Also, polyamines enhance sperm motility, energy metabolism, and sperm acrosome response [43]. Some studies have shown that exposure to high temperatures makes sperm motility decrease. The reason for this phenomenon has not been fully explained [44].

Kurhanewicz et al. [45] reported that brief exposure to hyperthermia triggers DNA damage in spermatocytes, which leads to reduced sperm viability. Although we are not sure of the role played by polyamines in this, we have previously described that polyamines have a role in stabilizing DNA structure. It is possible to speculate that temperature changes lead to changes in the physiological activities of temperature-sensitive polyamines. Further, it is also possible that the polyamine-induced lipid membrane phase separation

region is affected by the temperature change, thus affecting sperm viability. This needs further experimental proof.

In general, most of the differences in the formation of phase separation between polyamines and metal salts arise because polyamines have more valence and structural possibilities than metal salts. Also in some studies, suggested that polyamines bind to metal ions and protect DNA interactions [46]. Here we might speculate that perhaps polyamines bound to metal ions can reach higher valence states and thus drive some specific physiological functions. Although we have added metal salts or polyamines alone in this study, it will be necessary to mix metal salts and polyamines for further studies.

3.5 Chapter conclusion

In this chapter, salts with different valence(metal ions, amines) were added to DOPS/DPPC/Chol=40/40/20 three-component GUVs solution at arbitrary concentrations, and the phase-separated structures were observed by fluorescence microscopy at room temperature, 30°C, and 40°C.

No phase separation structure was observed in the liposomes prepared by DOPS/DPPC/Chol without salt addition. This may be due to the electrostatic repulsion between DOPS molecules, which inhibits the formation of phase separation domains. For adding salts, enhanced phase separation formation was observed as the salt concentration was increased, suggesting that the shielding of electrostatic repulsion promoted phase separation formation. The basic trend is that salts with smaller cation sizes and more significant valence induce phase separation at lower concentrations. And lower temperatures cause phase separation at lower salt concentrations.

This is because when the size of the cation is large, the steric repulsion between the cations adsorbed on the membrane surface is also significant, which reduces the amount of adsorption and increases the cation concentration required for phase separation formation. The increase in temperature also increases the entropy of the solution, which makes it harder for the cations to adsorb on the charged lipid membrane surface and decrease the cation concentration on the charged lipid membrane surface.

Among them, Propylamine and Hexamethylenediamine induced phase separation at low salt concentrations despite their large molecular sizes. Since Propylamine and Hexamethylenediamine have relatively large hydrophobic portions, it is thought that the hydrophobic interaction makes them form multimer such as a dimer and changed the apparent valence. The phase separation structure was affected by the electrostatic shielding effect by salts, the adsorption effect on the membrane surface, and the steric repulsion between the cations. It was found that the size, structure, and valence of the added salt were important in the formation of the phase separation structure on charged lipid membranes.

Also, due to the different states of contact with the lipid membrane, metal salts seem to be more thermally stable and less susceptible to temperature than amines for the

induced phase separation structure. The difference between metal salts and amines can be attributed to that amines have a richer valence and spatial structure. In turn, this rich valence and spatial structure are more favorable for the organism to utilize for various specific functions.

Up to this chapter, we have performed experiments with negative monovalent charged lipid-included membranes with applied osmotic pressure, metal salts, amines, and altered temperature as applied stimuli. We next altered the charge of the lipid membrane itself by adding a higher valence charged lipid and investigated the phase separation structure formation.

Reference

[1] C. E. Overton. *Über die osmotischen Eigenschaften der lebenden Pflanzen-und Tierzelle*. Fäsi & Beer, 1895.

[2] S. L. Veatch and S. L. Keller. Organization in lipid membranes containing cholesterol. *Physical Review Letters*, 89(26):268101, 2002.

[3] S. L. Veatch and S. L. Keller. Separation of liquid phases in giant vesicles of ternary mixtures of phospholipids and cholesterol. *Biophysical Journal*, 85(5):3074–3083, 2003.

[4] G. W. Feigenson. Phase diagrams and lipid domains in multicomponent lipid bilayer mixtures. *Biochimica et Biophysica Acta (BBA)-Biomembranes*, 1788(1):47–52, 2009.

[5] K. Simons and E. Ikonen. Functional rafts in cell membranes. *Nature*, 387(6633):569–572, 1997.

[6] K. Simons and J. L. Sampaio. Membrane organization and lipid rafts. *Cold Spring Harbor Perspectives in Biology*, 3(10):a004697, 2011.

[7] D. A. Brown and E. London. Structure and function of sphingolipid-and cholesterol-rich membrane rafts. *Journal of Biological Chemistry*, 275(23):17221–17224, 2000.

[8] M. A. Lemmon. Phosphoinositide recognition domains. *Traffic*, 4(4):201–213, 2003.

[9] H. Himeno, N. Shimokawa, S. Komura, D. Andelman, T. Hamada, and M. Takagi. Charge-induced phase separation in lipid membranes. *Soft Matter*, 10(40):7959–7967, 2014.

[10] N. Shimokawa, M. Hishida, H. Seto, and K. Yoshikawa. Phase separation of a mixture of charged and neutral lipids on a giant vesicle induced by small cations. *Chemical Physics Letters*, 496(1-3):59–63, 2010.

[11] B. Alberts, D. Bray, K. Hopkin, A. D. Johnson, J. Lewis, M. Raff, K. Roberts, and P. Walter. *Essential cell biology*. Garland Science, 2015.

[12] W. Maret and A. Wedd. *Binding, transport and storage of metal ions in biological cells*, volume 2. Royal Society of Chemistry, 2014.

[13] V. A. Bloomfield. Condensation of dna by multivalent cations: considerations on mechanism. *Biopolymers: Original Research on Biomolecules*, 31(13):1471–1481, 1991.

[14] R. Penner and E. Neher. The role of calcium in stimulus-secretion coupling in excitable and non-excitable cells. *Journal of Experimental Biology*, 139(1):329–345, 1988.

[15] L. Munaron. Calcium signalling and control of cell proliferation by tyrosine kinase receptors. *International Journal of Mmolecular Medicine*, 10(6):671–676, 2002.

[16] P. Kalac and P. Krausová. A review of dietary polyamines: Formation, implications for growth and health and occurrence in foods. *Food Chemistry*, 90(1-2):219–230, 2005.

[17] R. Kaur-Sawhney, A. F. Tiburcio, T. Altabella, and A. W. Galston. Polyamines in plants: an overview. *Journal of Cell and Molecular Biology*, 2:1–12, 2003.

[18] A. Muramatsu, Y. Shimizu, Y. Yoshikawa, W. Fukuda, N. Umezawa, Y. Horai, T. Higuchi, S. Fujiwara, T. Imanaka, and K. Yoshikawa. Naturally occurring branched-chain polyamines induce a crosslinked meshwork structure in a giant dna. *The Journal of Chemical Physics*, 145(23):235103, 2016.

[19] H. M. Wallace, A. V. Fraser, and A. Hughes. A perspective of polyamine metabolism. *Biochemical Journal*, 376(1):1–14, 2003.

[20] A. Kanemura, Y. Yoshikawa, W. Fukuda, K. Tsumoto, T. Kenmotsu, and K. Yoshikawa. Opposite effect of polyamines on in vitro gene expression: Enhancement at low concentrations but inhibition at high concentrations. *PLoS One*, 13(3):e0193595, 2018.

[21] T. Nishio, Y. Yoshikawa, C. Shew, N. Umezawa, T. Higuchi, and K. Yoshikawa. Specific effects of antitumor active norspermidine on the structure and function of dna. *Scientific Reports*, 9(1):1–12, 2019.

[22] T. Nishio, Y. Yoshikawa, Wakao F., N. Umezawa, T. Higuchi, S. Fujiwara, T. Imanaka, and K. Yoshikawa. Branched-chain polyamine found in hyperthermophiles induces unique temperature-dependent structural changes in genome-size dna. *ChemPhysChem*, 19(18):2299, 2018.

[23] L. Miller-Fleming, V. Olin-Sandoval, K. Campbell, and M. Ralser. Remaining mysteries of molecular biology: the role of polyamines in the cell. *Journal of Molecular Biology*, 427(21):3389–3406, 2015.

[24] T. J. Thomas, H. A. Tajmir-Riahi, and T. Thomas. Polyamine–dna interactions and development of gene delivery vehicles. *Amino Acids*, 48(10):2423–2431, 2016.

[25] B. C. Lagerholm, G. E. Weinreb, K. Jacobson, and N. L. Thompson. Detecting microdomains in intact cell membranes. *Annu. Rev. Phys. Chem.*, 56:309–336, 2005.

[26] D. M. Soumpasis. Theoretical analysis of fluorescence photobleaching recovery experiments. *Biophysical Journal*, 41(1):95–97, 1983.

[27] T. J. Pucadyil, S. Mukherjee, and A. Chattopadhyay. Organization and dynamics of nbd-labeled lipids in membranes analyzed by fluorescence recovery after photobleaching. *The Journal of Physical Chemistry B*, 111(8):1975–1983, 2007.

[28] G. Denisov, S. Wanaski, P. Luan, M. Glaser, and S. McLaughlin. Binding of basic peptides to membranes produces lateral domains enriched in the acidic lipids phosphatidylserine and phosphatidylinositol 4, 5-bisphosphate: an electrostatic model and experimental results. *Biophysical Journal*, 74(2):731–744, 1998.

[29] R. Ekerdt and D. Papahadjopoulos. Intermembrane contact affects calcium binding to phospholipid vesicles. *Proceedings of the National Academy of Sciences*, 79(7):2273–2277, 1982.

[30] C. Altenbach and J. Seelig. Calcium binding to phosphatidylcholine bilayers as studied by deuterium magnetic resonance. evidence for the formation of a calcium complex with two phospholipid molecules. *Biochemistry*, 23(17):3913–3920, 1984.

[31] J. Seelig. Interaction of phospholipids with ca2+ ions. on the role of the phospholipid head groups. *Cell Biology International Reports*, 14(4):353–360, 1990.

[32] S. McLAUGHLIN, N. Mulrine, T. Gresalfi, G. Vaio, and A. McLAUGHLIN. Adsorption of divalent cations to bilayer membranes containing phosphatidylserine. *The Journal of General Physiology*, 77(4):445–473, 1981.

[33] D. E Leckband, C. A. Helm, and J. Israelachvili. Role of calcium in the adhesion and fusion of bilayers. *Biochemistry*, 32(4):1127–1140, 1993.

[34] S. Ohki, N. Duzgunes, and K. Leonards. Phospholipid vesicle aggregation: effect of monovalent and divalent ions. *Biochemistry*, 21(9):2127–2133, 1982.

[35] D. Huster, K. Arnold, and K. Gawrisch. Strength of ca2+ binding to retinal lipid membranes: consequences for lipid organization. *Biophysical Journal*, 78(6):3011–3018, 2000.

[36] C. G. Sinn, M. Antonietti, and R. Dimova. Binding of calcium to phosphatidylcholine–phosphatidylserine membranes. *Colloids and Surfaces A: Physicochemical and Engineering Aspects*, 282:410–419, 2006.

[37] Y Marcus. Thermodynamics of solvation of ions. part 5.—gibbs free energy of hydration at 298.15 k. *Journal of the Chemical Society, Faraday Transactions*, 87(18):2995–2999, 1991.

[38] S. Okouchi, T. Moto, Y. Ishihara, H. Numajiri, and H. Uedaira. Hydration of amines, diamines, polyamines and amides studied by nmr. *Journal of the Chemical Society, Faraday Transactions*, 92(11):1853–1857, 1996.

[39] M. Hiraoka, Y. Okamoto, and T. Sano. Effects of ca+ and k+ on oscillatory afterpotentials in dog ventricular muscle fibers. *Journal of Molecular and Cellular Cardiology*, 11(10):999–1015, 1979.

[40] S. Kurihara, O. Okazaki, M. Konishi, and k. Kawamura. Study on the underlying mechanism of the exercise induced arrhythmia. *Bulletin of the Physical Fitness Research Institule*, 65:72–79, 1987.

[41] K. Walker-Bone, E. Dennison, and C. Cooper. Epidemiology of osteoporosis. *Rheumatic Disease Clinics of North America*, 27(1):1–18, 2001.

[42] B. P. Singh, I. Saha, I. Nandi, and M. J. Swamy. Spermine and spermidine act as chemical chaperones and enhance chaperone-like and membranolytic activities of major bovine seminal plasma protein, pdc-109. *Biochemical and Biophysical Research Communications*, 493(4):1418–1424, 2017.

[43] Y. Tao, D. Liu, G. Mo, H. Wang, and X. J. Liu. Peri-ovulatory putrescine supplementation reduces embryo resorption in older mice. *Human Reproduction*, 30(8):1867–1875, 2015.

[44] D. Durairajanayagam, A. Agarwal, and C. Ong. Causes, effects and molecular mechanisms of testicular heat stress. *Reproductive Biomedicine Online*, 30(1):14–27, 2015.

[45] N. A. Kurhanewicz, D. Dinwiddie, Z. D. Bush, and D. E. Libuda. Elevated temperatures cause transposon-associated dna damage in c. elegans spermatocytes. *Current Biology*, 30(24):5007–5017, 2020.

[46] L. Zhou, N. Wang, and X. Yu. The interaction of macrocyclic polyamine derivatives and their complexes with dna. *Progress in Chemistry*, 19(012):1909, 2007.

Chapter 4

Reduction of line tension at phase-separated lipid domain boundary by multivalent negatively charged lipids

4.1 Chapter Introduction

The phase-separated structures in lipid membranes can be a model for raft domain. The ternary lipid mixtures consisting of saturated lipids, unsaturated lipids, and cholesterol exhibit the phase separation between saturated lipids and cholesterol-rich liquid-ordered (L_o) phase and unsaturated lipids-rich liquid-disordered (L_d) phase. [1] In this liquid-liquid phase separation, domain area appears as circular region. There is an excess energy at the domain boundary and the energy is called the line energy [2]. The line energy can be obtained by the product of the domain boundary length and the interfacial tension called line tension. The line tension is an important parameter to discuss the stability of the phase separation. It is believed that the origin of the line tension is the height mismatch between the two coexisting phases [3] [4] [5]. In addition, the physical property difference between the two phases such as spontaneous curvature, degree of chain ordering, and dipole density, plays an important role in the line tension. [6] [7] [8].

When some molecules are added to this system, the line tension will be influenced. The hybrid lipid with one saturated hydrocarbon tail and one unsaturated hydrocarbon tail, is expected to decrease the line tension significantly. This is because the saturated tail of the hybrid lipid faces the L_o phase, whereas the unsaturated tail faces the L_d phase and the hybrid lipid behaves like a surfactant at the interface between water and oil. [9] However, some experiments reported that hybrid lipids do not localize at the domain boundary, since the hybrid lipid localization at the domain boundary reduces the entropy of the hybrid lipids. Instead, some hybrid lipid molecules are partitioned into the both L_o and L_d phases and the physical property difference between these two phases comes close each other. [10] As a result, the line tension is decreased by the hybrid lipids.

Similar behavior is observed in the lipid membranes with unsaturated fatty acids and the branched fatty acids. Since the fatty acids are much smaller than phospholipids, it is easier to be partitioned into the L_o phase. In addition, the unsaturated fatty acid (e.g. oleic acid) and the branched fatty acid (e.g. phytanic acid) have bulky hydrophobic part. When they are included in the L_o phase, the chain ordering of the L_o phase is efficiently disturbed and the line tension is decreased. In fact, the clear domain boundary fluctuation which indicates the small line tension is observed and the modulated phases, for example,

stripe and hexagonal phases appear. [8]

Based on these previous studies, we consider two important factors to achieve the reduction of line tension by addition of molecules. First factor is that the molecule should disturb the chain ordering of the lipids in the ordered phase. This is necessary to disturb the chain ordering in the L_o phase and reduce the chain ordering difference between the L_o and L_d phases. Second factor is that the small amount of the molecule should be partitioned into the ordered phase. If the large amount of the molecule is included in the L_o phase, the phase-separated structure disappears. To maintain the phase separation, the molecule is mainly partitioned in to the L_d phase and the small amount of the molecule should be included in the L_o phase. And, if the molecule fulfills the two factors, it may decrease the line tension.

We suggest an negatively charged unsaturated lipid as such a molecule in this chapter. Here, we consider that we add negatively charged unsaturated lipids to the L_o/L_d phase-separated lipid membranes. Since negatively charged unsaturated lipids, such as DOPS, have the unsaturated hydrocarbon tails, they are mainly partitioned into the L_d phase. As the charged lipid composition increases, the electrostatic repulsion between the charged lipids in the L_d phase increases. As a result, some charged lipids migrate from the L_d phase to the L_o phase to decrease the repulsion. Therefore, the small amount of charged lipids may be included in the L_o phase. Moreover, the charged lipids with unsaturated hydrocarbon tails disturb the chain ordering in the L_o phase. Therefore, an negatively charged unsaturated lipid can be a good candidate to reduce the line tension.

Phosphatidylinositol (PI) is a monovalent negatively charged headgroup and many organisms, including mammals, have PI in cell membranes and some biomembranes [11]. PI acts as a substrate for the production of second messenger in intracellular signaling pathway and plays an important role in protein adsorption onto biomembranes. [12] [13] In these functions, the phosphorylation process of the inositol ring of PI is important. The phosphorylated PIs become multivalent negatively charged lipids and seven types of phosphorylated PIs are found. [14] [15] [16] Since PI has a negative charge on the phosphate group, PIP which is phosphorylated at one position in the inositol ring becomes divalent negatively charged lipid, PIP_2 at two positions becomes trivalent, and PIP_3 at three positions becomes tetravalent. [11] [17] In particular, PIP, PIP_2, and PIP_3 which

are multivalent negatively charged lipids are called phosphoinositide and they are also interesting from the physical point of view.

In this chapter, we observed the phase behavior of lipid membranes with PI and PIP_2 as the representative of multivalent charged lipids by fluorescence and confocal laser scanning microscopies. Based on the above argument, we used PI and PIP_2 with unsaturated hydrocarbon tails. Also, we used DOPS as a control group for monovalent lipids. We focus on whether the added charged lipids can reduce the line tension at the phase-separated domain boundary or not. We observed the phase behavior of DOPC/DPPC/Chol with DOPI or $DOPIP_2$. From the domain boundary fluctuation, we calculated the line tension values with the addition of DOPS, DOPI, and PIP_2, respectively. In addition, we also measured the line tension with the addition of $CaCl_2$ to cancel out the electrostatic repulsions. We comprehensively discussed the behavior of negatively charged unsaturated lipids in the phase-separated membranes, the charged lipid localization in the heterogeneous membranes, and the influence of valency on the headgroups.

4.2 Materials and Methods

4.2.1 Materials

The zwitterionic saturated lipid, 1,2-dipalmitoyl-sn-glycero-3-phosphocholine (DPPC), the zwitterionic unsaturated lipid, 1,2-Dioleoyl-sn-glycero-3-phosphocholine (DOPC), the negatively charged unsaturated lipid, 1,2-dioleoyl-sn-glycero-3-phospho-l-serine (sod-ium salt) (DOPS), the negatively charged unsaturated lipid, 1,2-dioleoyl-sn-glycero-3-phospho-(1'-myo-inositol) (DOPI), 1,2-dioleoyl-sn-glycero-3-phospho-(1'-myo-inositol-4',5'-bispho-sphate) (DOPI(4, 5)P_2, (PIP_2)) and cholesterol (Chol) were purchased from Avanti Polar Lipids, Inc(Alabas-ter, AL). Rhodamine B 1,2-dihexadecanoyl-sn-glycero-3-phosphoethan-olamine, triethylammonium salt (Rho-DHPE) was obtained from Thermo Fisher Scien-tific(Waltham, US). 1,2-Dipalmitoyl-sn-glycero-3-phosphoethanolamine-N-(7-nitro-2-1,3-benzoxadiazol-4-yl) (ammonium salt) (NBD-PE) was obtained from Avanti Polar Lipids (Alabaster, AL). Deionized water (specific resistance $\geq$ 18 MΩ) used in this study was obtained from a Millipore Milli-Q purification system(Burlington, MA). The metal salts, $CaCl_2$(+2) was purchased from Nacalai Tesque(Kyoto, Japan). The molecular structures of fluorescent probes and lipids are showen in Fingure 4.1 and 4.2.

- Fluorescent probes

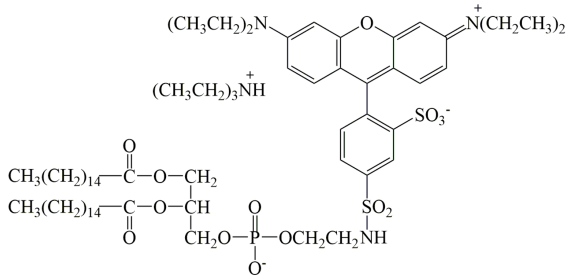

Rhodamine-DHPE

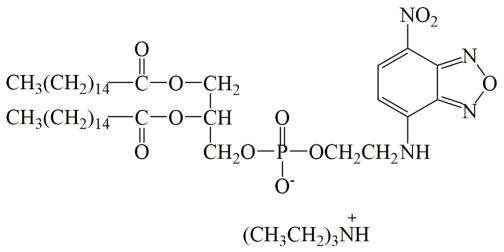

NBD-PE

Figure 4.1: Molecular structures of fluorescent probes

- Unsaturated lipids

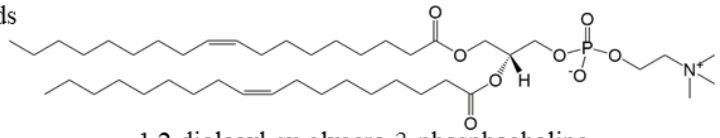

1,2-dioleoyl-*sn*-glycero-3-phosphocholine
DOPC (Zwitterionic lipid)

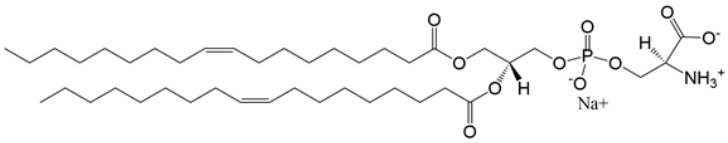

1,2-dioleoyl-*sn*-glycero-3-phospho-L-serine
DOPS (Negatively charged lipid)

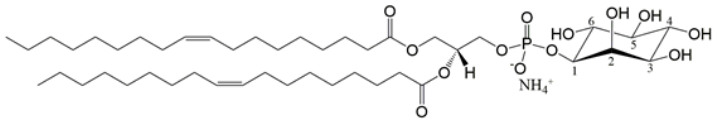

1,2-dioleoyl-*sn*-glycero-3-phospho-(1'-myo-inositol)
DOPI (Negatively charged lipid)

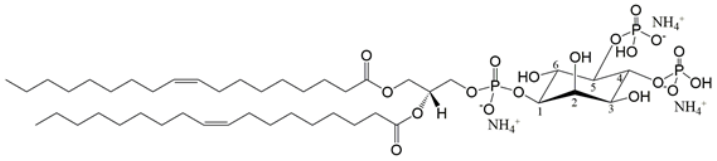

1,2-dioleoyl-*sn*-glycero-3-phospho-(1'-myo-inositol-4',5'-bisphosphate)
DOPI(4, 5)P_2 (Negatively charged lipid)

(a)

- Saturated lipids

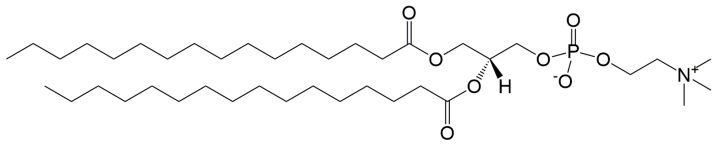

1,2-dipalmitoyl-*sn*-glycero-3-phosphocholine
DPPC (Zwitterionic lipid)

(b)

- Cholesterol

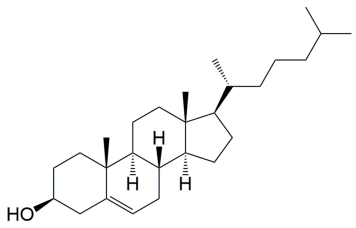

(c)

Figure 4.2: Molecular structures of lipids. (a)Unsaturated lipids, (b)saturated lipid, and (c)cholesterol.

4.2.2 Preparation of GUVs

Liposomes were prepared by the natural swelling method. All lipids were dissolved in a 2:1 (v/v) chloroform/methanol solution and afforded concentrations of 1mM. All kinds of fluorescent probes were dissolved in chloroform, afford concentrations of 0.1mM. For the control groups, DOPC, DPPC adn Chol were mixed as DOPC/DPPC/Chol=40/40/20, and the total volumes were kept with 10μL. In experiments with the addition of charged lipids, DOPS, DOPI or DOPI(4,5)P_2 was added on top of DOPC/DPPC/Chol = 40/40/20. Rho-DHPE 2μL was used for fluorescence microscopy observation. NBD-PE 4μL was used for confocal laser microscopy observation. After well mixed, the mixed solution was dried with nitrogen gas, then the resulting lipid films are put into a vacuum desiccator for at least 3h. It was then prehydrated for 10min using 3μL Milli-Q water at 55°C and then was hydrated using 97μL Milli-Q water or $CaCl_2$ solution at 37°C for at least 3h and under 24h. The $CaCl_2$ solution was dissolved in Milli-Q water, afford concentrations of 0.05mM and 0.1mM. The preparation procedure is shown in the Figure 4.3.

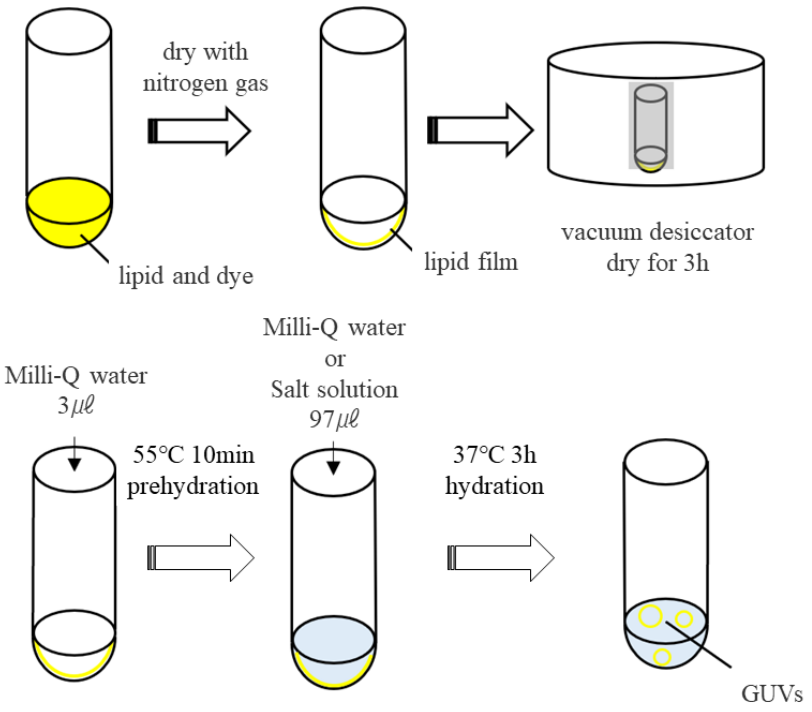

Figure 4.3: Preparation of GUVs

4.2.3 Microscopic Observations of GUVs

We used a small chamber, as shown in Figure 4.4, for microscopic observation. A silicon sheet with a circular hole in the middle was placed on the slide glass, and the prepared GUVs solution was dripped into the circular hole and added a cover glass on top. Then the observation was performed at room temperature using a fluorescence microscope (IX71, Olympus, Tokyo, Japan). For each sample, a GUV with diameters 5μ $\sim 20\mu$m was selected to take video.

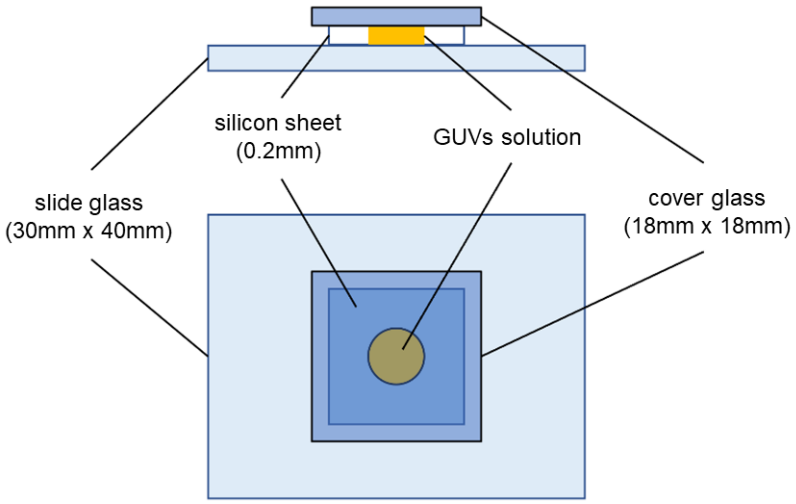

Figure 4.4: Schematic illustration of chamber for microscopic observation

4.2.4 Flicker spectroscopy

The method for the line tension calculation was referred to the studies by Stottrup et al. [18] and Shimokawa et al. [8]. We imaged the domain boundary fluctuation for 3 sec at least by 30 frame/sec. The obtained images were processed using ImageJ software to obtain zoomed-in images with only one domain. Processed all images into binary images

and traced the domain shape. We plotted the domain radius r as a function of the polar angle ψ and used Fourier series expansion to represent the boundary of the fluctuating phase separation domain,

$$r(\psi) = r_{\mathrm{av}} \left[1 + a_0 + \sum_{k=1}^{\infty} a_k \cos(k\psi) + \sum_{k=1}^{\infty} b_k \sin(k\psi) \right], \tag{4.1}$$

where r_{rmav} is the average domain radius, ψ is the polar angle, k is the mode number, a_k and b_k are Fourier coefficients. The excess energy ΔF generated by the fluctuations can be expressed as,

$$\Delta F \simeq \frac{\pi r_{\mathrm{av}}}{2} \gamma \sum_{k=2}^{\infty} (k^2 - 1)(a_k^2 + b_k^2), \tag{4.2}$$

where γ is the line tension. According to the generalized equipartition theorem, free energy for each independent mode is $k_{\mathrm{B}}T$. Thus, the following expression is obtained as,

$$\left\langle a_k^2 \right\rangle + \left\langle b_k^2 \right\rangle = \frac{2k_{\mathrm{B}}T}{\pi r_{\mathrm{av}} \gamma} \left(\frac{1}{k^2 - 1} \right), \tag{4.3}$$

where $\langle a_k^2 \rangle$ and $\langle b_k^2 \rangle$ are the averaged Fourier coefficients of all images. According to Equation (4.3), the value of line tension can be derived by the linear regression equation between k and the Fourier coefficients (a_k and b_k).

4.3 Results

4.3.1 Phase behavior of DOPI and PIP_2-containing lipid membranes

First, we observed the phase behavior of lipid membranes with DOPI. As a control composition, we chose DOPC/DPPC/Chol=40/40/20 which forms the L_o/L_d phase separation stably. Next, we basically added DOPI to this system in three ways. First is that DOPC was replaced with DOPI. Second is that DPPC was replaced with DOPI. Third is that DOPC and DPPC was replaced with DOPI with fixing DOPC:DPPC=1:1. The obtained results are summarized in Figure 4.5.

In the replacement with DOPC, between DOPC/DPPC/DOPI/Chol=40:40:0:20 to 0:40:40:40, the phase-separated structures were found. Next, in the replacement with DPPC, the phase separation can be observed up to DOPI=10%, that is DOPC/DPPC/-DOPI/Chol=40:30:10:20. When more DOPI was added to the membranes, the phase separation disappeared. Finally, when DOPC and DPPC were replaced with DOPI, the phase separation was found up to DOPI=20%, that is DOPC/DPPC/DOPI/Chol=30:30:20:20. Overall, regardless of the type of lipid replaced with DOPI, the increase in the amount of DOPI led to suppressing the phase separation. This is due to the electrostatic interactions that exist between DOPI headgroups.

Next, we performed the same observation in PIP_2 containing lipid membranes. The obtained results are summarized in Figure 4.6, and the phase-separated region in the phase diagram is almost the same as that for DOPI-containing membranes. But when all DOPC was replaced with PIP_2, that is DOPC/DPPC/PIP_2/Chol=0:40:40:20, the phase separation was no longer observed and the homogeneous phase appeared.

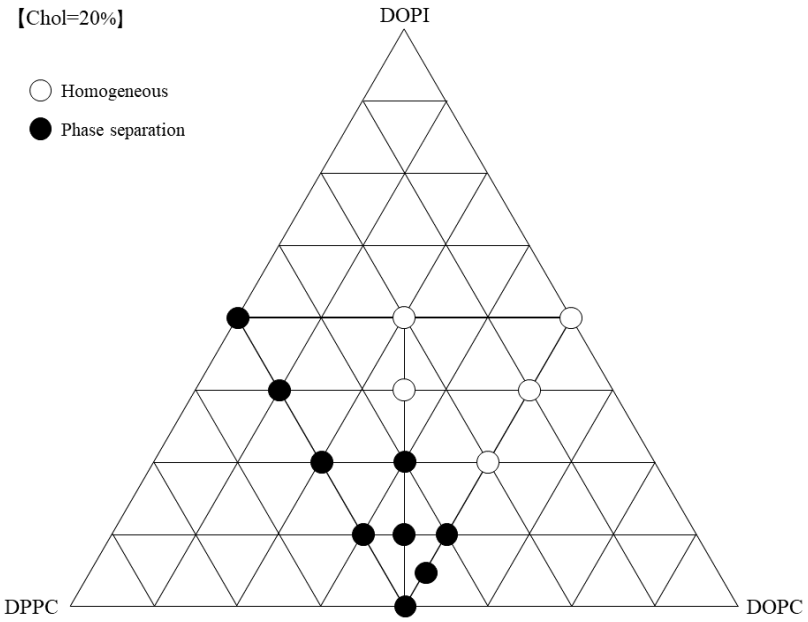

Figure 4.5: Phase diagram of DOPC/DPPC/DOPI/Chol membranes with Chol = 20%. Open and filled circles denote homogeneous and phase-separated region, respectively.

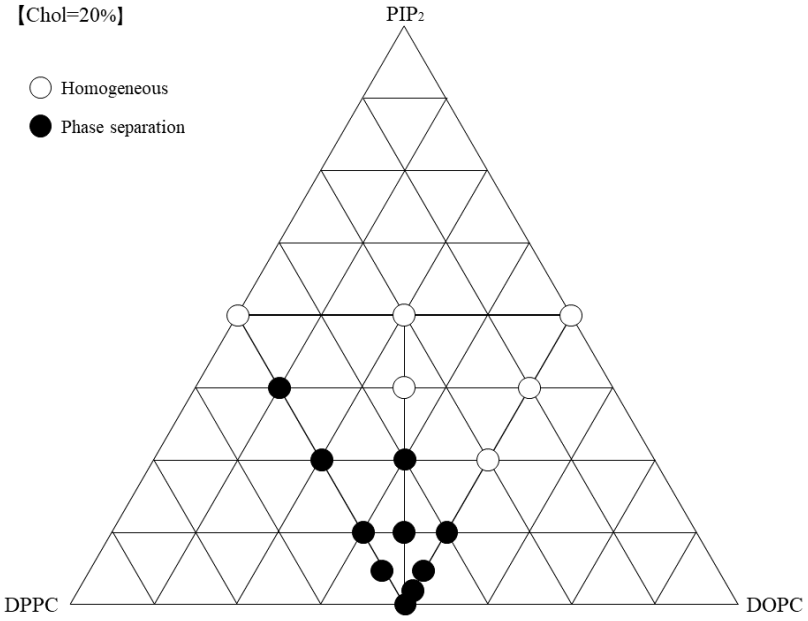

Figure 4.6: Phase diagram of DOPC/DPPC/PIP_2/Chol membranes with Chol = 20%. Open and filled circles denote homogeneous and phase-separated region, respectively.

4.3.2 Line tension measurements of DOPS, DOPI and PIP_2-containing lipid membranes

Although we cannot observe the domain boundary fluctuation at DOPC/DPPC/-Chol=40/40/20 without any charged lipids, it was clearly observed in the membranes with charged lipids. Since the fluctuation becomes clearer at the boundary between the homogeneous phase and phase-separated state in the phase diagram, we measured the line tension values in the replacement with DPPC.

For DOPI, the representative domain fluctuation was shown in Figure 4.7 and the measured line tension values were summarized in Figure 4.8. The line tension was 2.33±0.84 pN for DOPC/DPPC/Chol=40/40/20 without DOPI. By increasing the DOPI composition, the line tension decreased to 1.69±0.62 pN at DOPI=5 % and 0.97±0.53 pN at DOPI=10 %. Therefore, DOPI contribute to decrease the line tension at domain boundary.

As a control group we next measured the line tension of DOPS. The domain boundary fluctuation and the measured line tension values were shown in Figure 4.9 and 4.10, respectively. By increasing the DOPS composition, the line tension decreased to 1.39±0.59 pN at DOPS=5 % and 0.83±0.54 pN at DOPS=10 %. Shows that DOPS also contribute to decrease the line tension at domain boundary. The decrease in line tension is due to the addition of charged lipids and not to the specificity of the PI headgroup.

Also, we measured the line tension for PIP_2 to further explore the effects of charged headgroup. The domain boundary fluctuation and the measured line tension values were shown in Figure 4.11 and 4.12, respectively. The obtained values were 2.76±0.84 pN at PIP_2=1 %, 2.42±1.26 pN at PIP_2=3 %, 1.14±0.45 pN at PIP_2=5 %, and 0.81±0.41 pN at PIP_2=10 %. The line tension did not change up to PIP_2=3 %. However, it dramatically decreased beyond PIP_2=5 %. In this range, from Figure 4.8 and 4.12, PIP_2 reduced the line tension strongly than DOPI.

Interestingly, although we observed circular domains in DOPI-containing lipid membranes, we often observed some modulated phases in PIP_2 containing lipid membranes as shown in Figure 4.13. The modulated phase is some pattern formation, such as stripe and hexagonal domain array. The conditions for the formation of modulated phase are (i)

sufficient reduction of line tension and (ii) long-range repulsion between domains. Long-range repulsion between domains is called interdomain interaction. In previous studies, the modulated phase formation was reported by the reduction of line tension. In our system, line tension was sufficiently decreased by the charged lipids. In addition, the electrostatic repulsion between charged domains may work as the interdomain interaction. Therefore, the modulated phases stably appear.

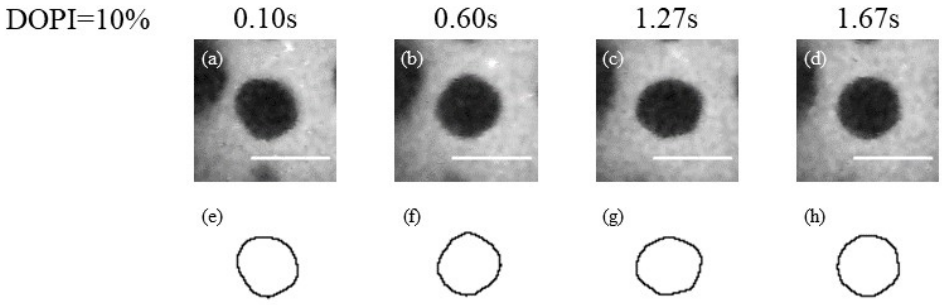

Figure 4.7: Domain boundary fluctuation at DOPC/DPPC/DOPI/Chol = 30/40/10/20. (a-d)Fluorescence microscopic images, and (e-h)Corresponding domain outline images obtained from binarization of microscopic images. Scale bar: 5 μm.

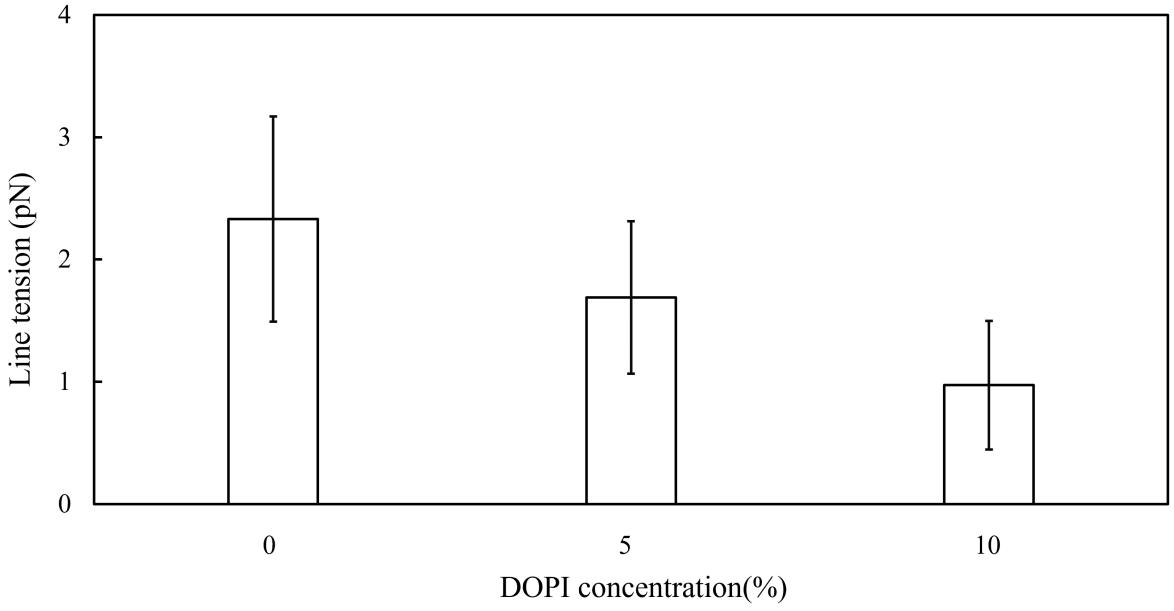

Figure 4.8: Line tension at the phase-separated domain in DOPC/DPPC/DOPI/Chol as a function of DOPI fraction.

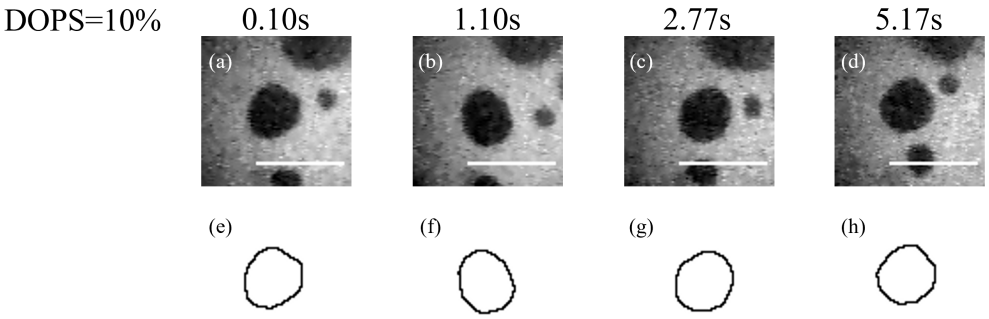

Figure 4.9: Domain boundary fluctuation at DOPC/DPPC/DOPS/Chol = 30/40/10/20. (a-d)Fluorescence microscopic images, and (e-h)Corresponding domain outline images obtained from binarization of microscopic images. Scale bar: 5 μm.

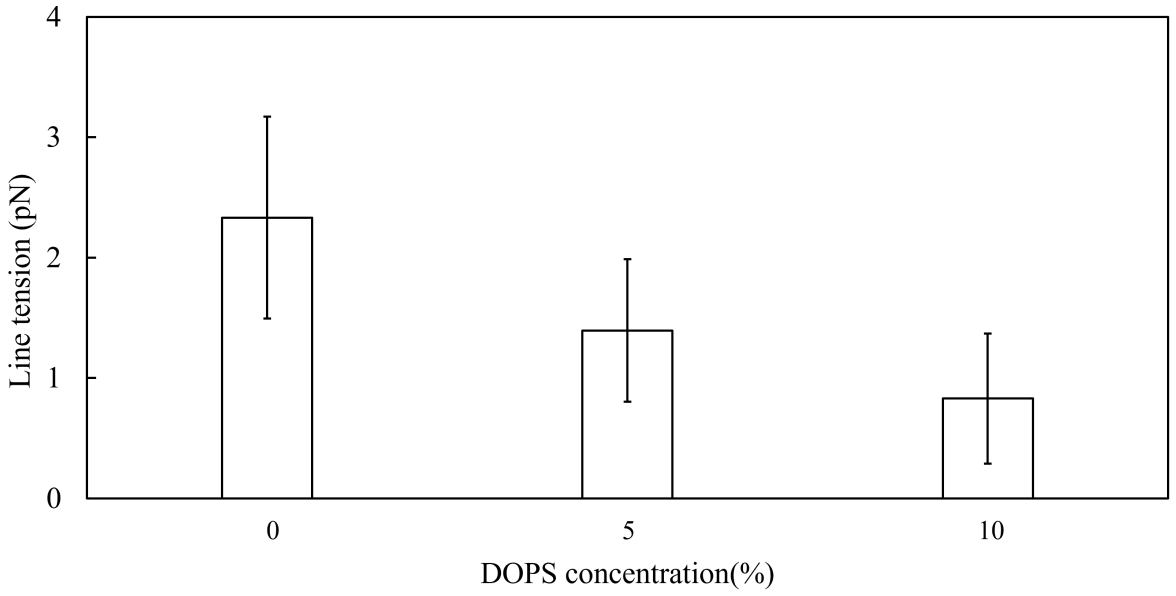

Figure 4.10: Line tension at the phase-separated domain in DOPC/DPPC/DOPS/Chol as a function of DOPS fraction.

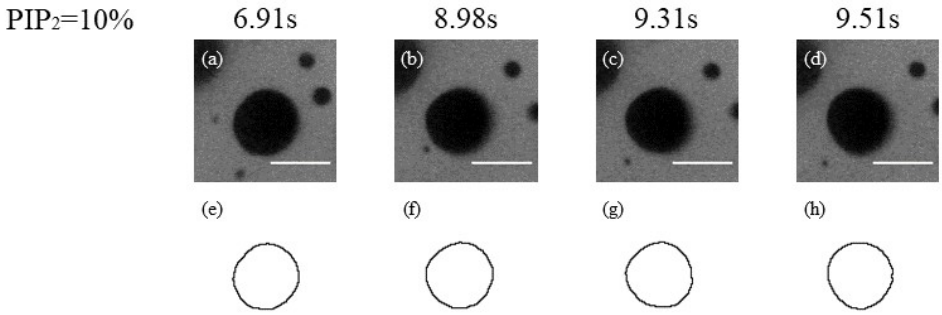

Figure 4.11: Domain boundary fluctuation at DOPC/DPPC/PIP_2/Chol = 30/40/10/20. (a-d)Fluorescence microscopic images, and (e-h)Corresponding domain outline images obtained from binarization of microscopic images. Scale bar: 5 μm.

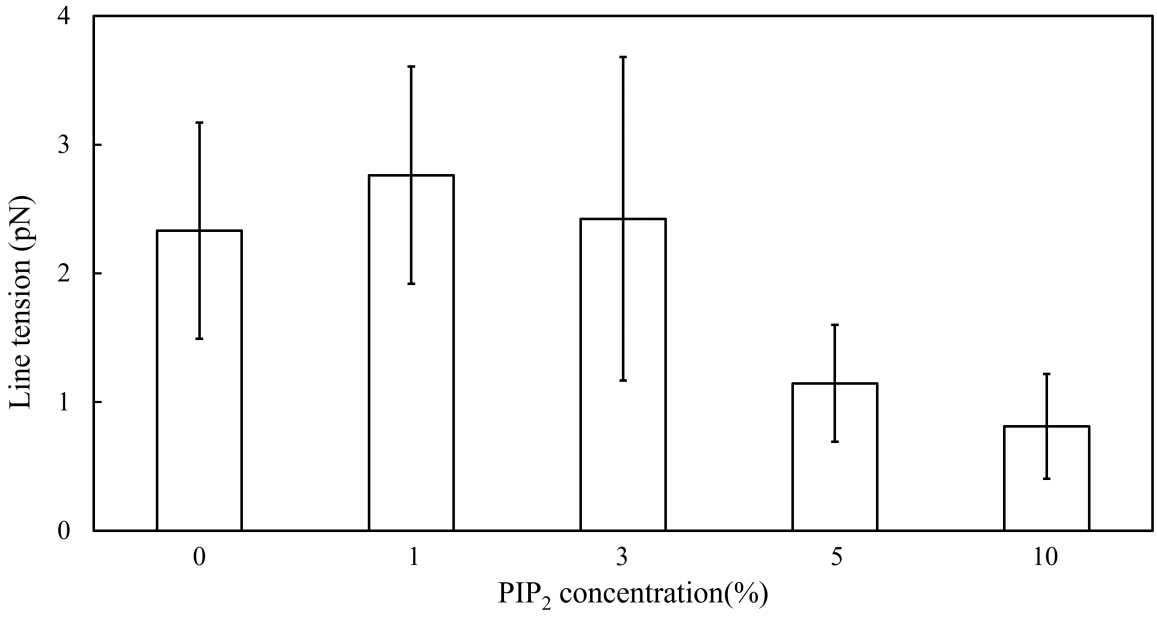

Figure 4.12: Line tension at the phase-separated domain in DOPC/DPPC/PIP_2/Chol as a function of PIP_2 fraction.

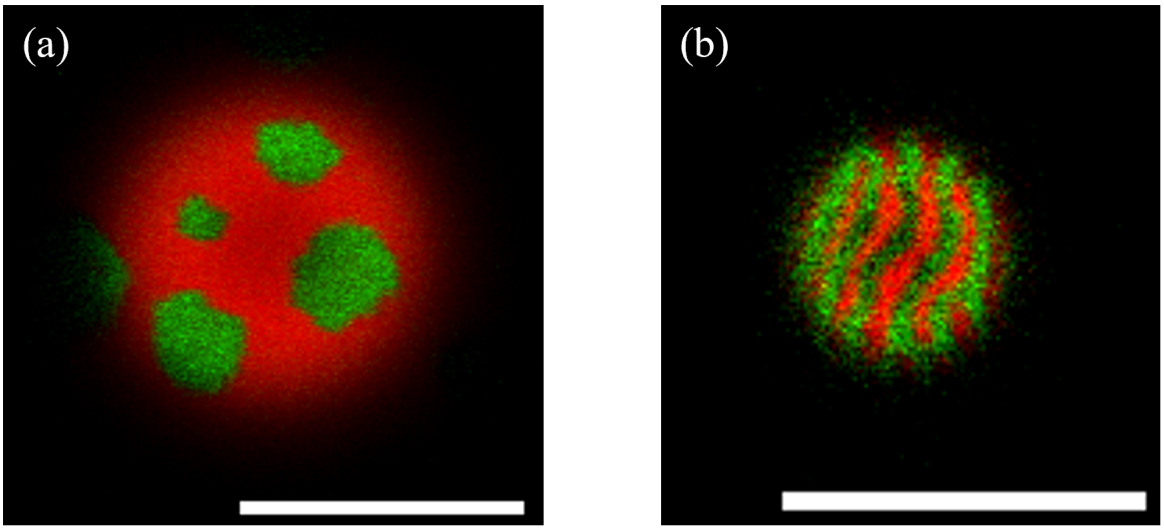

Figure 4.13: Confocal laser scanning microscopic images for DOPC/DPPC/DOPI/-Chol=40/35/5/20 in (a) and DOPC/DPPC/PIP_2/Chol=40/35/5/20 in (b). Red and green regions correspond to Rho-DHPE-rich L_d phase and NBD-PE-rich L_o phase, respectively. Scale bar: 10 μm.

4.3.3 Line tension measurement with $CaCl_2$ addition

In order to evaluate the effects of electrostatic interaction on the line tension, we added $CaCl_2$ to the membranes and measured the line tension by the same procedure. The measured line tension values for DOPI and PIP_2 were summarized in Figure 4.14 and 4.15, respectively. At charged lipid fractions are 5 and 10 %, the line tension values were increased by adding $CaCl_2$. However, we cannot see the clear difference between $CaCl_2$ 0.05 mM and 0.1 mM. In addition, at lower fractions of PIP_2 (PIP_2= 1 and 3 %), we also cannot clear effects of $CaCl_2$ on the line tension since the PIP_2 fractions are too low.

On the other hand, we cannot find any modulated phases such as stripe phase in $CaCl_2$ solution. This is because $CaCl_2$ increased the line tension and may cancel out the interdomain interaction.

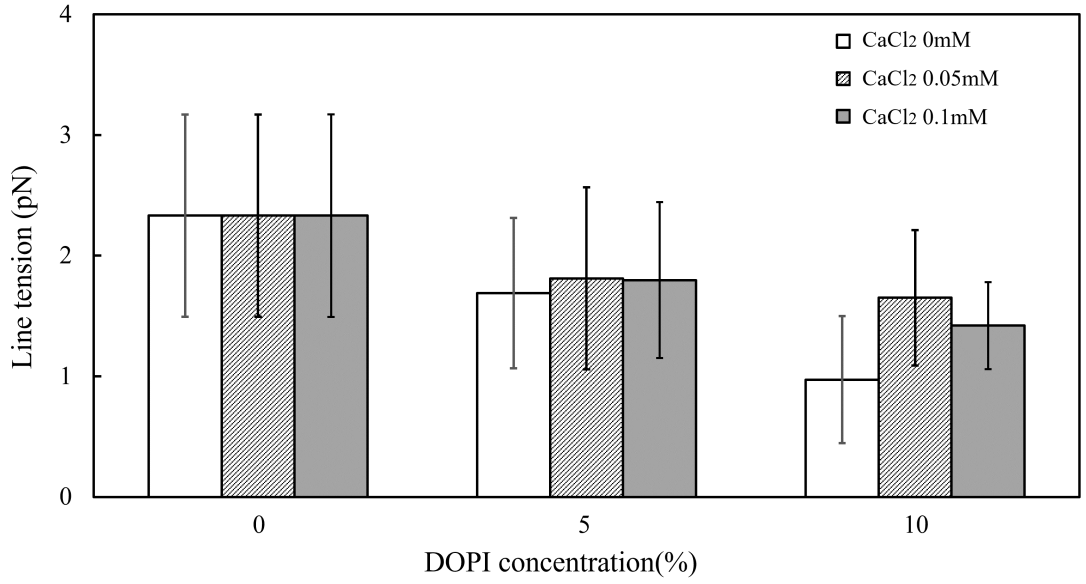

Figure 4.14: Line tension at the phase-separated domain in DOPC/DPPC/DOPI/Chol as a function of DOPI fraction. The white, dotted, and gray bars correspond to the measurements in Milli-Q water, $CaCl_2$ 0.05 mM, and $CaCl_2$ 0.1 mM, respectively.

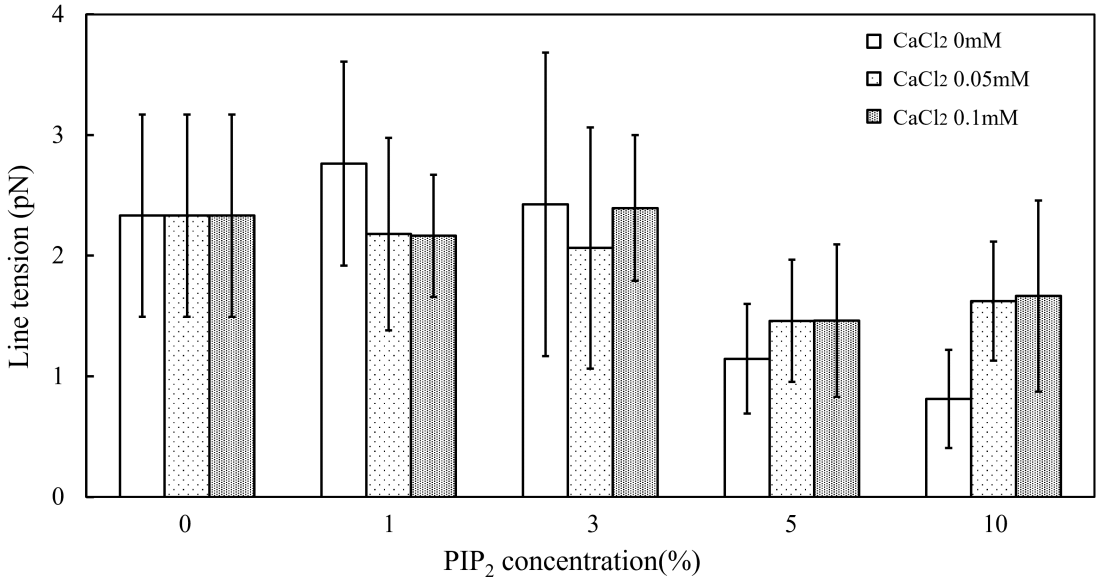

Figure 4.15: Line tension at the phase-separated domain in DOPC/DPPC/PIP_2/Chol as a function of PIP_2 fraction. The white, dotted, and gray bars correspond to the measurements in Milli-Q water, $CaCl_2$ 0.05 mM, and $CaCl_2$ 0.1 mM, respectively.

4.4 Discussion

In our experiments, we indicated that the negatively charged unsaturated lipids, DOPI and $DOPIP_2$, significantly decreased the line tension at the domain boundary in the phase-separated lipid membranes. Here, we discuss how the charged lipids reduce the line tension. Since DOPI and PIP_2 have unsaturated hydrocarbon tails, they are partitioned into the DOPC-rich L_d phase. When the charged lipid fraction is low, most of charged lipid can be partitioned into the L_d phase and they did not give some effects on the L_o phase. In fact, at PIP_2=1 and 3 %, the line tension values are not changed from PIP_2=0 %. On the other hand, when the charged lipids are crowded in the L_d phase at higher charged lipid fraction, the electrostatic repulsion in the L_d phase increases. Therefore, some charged lipids escape from the L_d phase to decrease the electrostatic repulsion and migrate to the L_o phase. Since the charged lipids have unsaturated hydrocarbon tails, the charged lipids included in the L_o phase disturb the chain ordering of the L_o phase. As a result, the chain ordering difference between the L_o and L_d phases becomes smaller, and the line tension is decreased.

Since PIP_2 has three negative charges and DOPI has a negative charge, the electrostatic repulsion between PIP_2 molecules is much stronger than that between DOPI molecules at the same charged lipid fraction. Therefore, charged lipid migration from the L_d phase to the L_o phase becomes notable for PIP_2 as compared to DOPI. Therefore, PIP_2 decreases the line tension significantly than DOPI. In addition, the modulated phases are often found in PIP_2 containing membranes, whereas they are not formed in DOPI-containing membranes. As we mentioned above, the modulated phases are stabilized by the interdomain interaction. Since DOPI is a monovalent negatively charged lipid, the electrostatic repulsion between charged domains is weaker as compared with the case of PIP_2. Therefore, the modulated phases are hardly observed in DOPI-containing membranes.

The addition of $CaCl_2$ contributes to weakening the electrostatic interactions. The electrostatic repulsion in the L_d phase becomes weaker and the charged lipid migration to the L_o phase is suppressed. Thus, the line tension reduction is suppressed by the addition of $CaCl_2$. In addition, we considered that the interdomain interaction which

stabilizes the modulated phase is the electrostatic repulsion between charged domains. This interdomain interaction also becomes weaker by the addition of $CaCl_2$. Therefore, we cannot find the modulated phase in $CaCl_2$ solutions.

On the other hand, the phase behaviors of DOPI- and PIP_2-containing membranes are almost the same, although the valences of headgroups are different. This is most likely because the electrostatic repulsion between PIP_2 is too strong, thus part of PIP_2 is repelled outside the lipid membrane. The apparent concentration of PIP_2 present on the membrane was not as much as added. Therefore, it shows the same behavior out of the monovalent DOPI. Some studies have shown that the higher electrostatic charge on PIP_2 leads to a larger hydrodynamic radius of the PIP_2 head group so that PIP_2 is more likely to free in solution to form micelles than to form bilayer structures [19] [20] [21]. Moreover, when using PIP_2 to prepare vesicles, PIP_2 also tends to have a shorter residence time on the lipid membrane than other membrane composition phospholipids [22] [23]. Our experimental results verified these phenomena from the side.

4.5 Chapter conclusion

In this chapter, we added monovalent negatively charged unsaturated lipid DOPS, DOPI and trivalent negatively charged unsaturated lipids DOPI(4,5)P_2 (PIP_2) to the DOPC/DPPC/Chol three-component GUVs stepwise for comparison to discuss the effect of higher valent charged lipids on membrane behavior. The line tension at the phase-separated domain boundary was measured by Flicker spectroscopy, and we evaluated the effect of $CaCl_2$ on the line tension based on the screening of the electrostatic interactions. As a result, the charged lipids decreased the line tension significantly, and the line tension reduction was suppressed by the addition of $CaCl_2$. In addition, the modulated phases such as the stripe phase appear for PIP_2. The modulated phase is stabilized by the line tension reduction and the interdomain interaction, and both are mediated by the electrostatic repulsion between the charged lipids.

Endocytosis and exocytosis are being related to lipid rafts which can simulate by phase separation [24] [25]. It is not confirmed that there is a relationship between the inhibition of phase separation formation by PIP_2 and endocytosis and exocytosis. However, some studies have reported that PIP_2 has the function of inhibiting Ca-mediated exocytosis [26], while a reduction in lipid membrane tension leads to a spontaneous reorganization of PIP_2 to the invaginated membrane domains (similar to endocytosis) [27]. The enrichment of PI lipids, especially PIP_2, in the raft domain has been reported [28] [29]. It is most likely because it requires lipid with highly charged and a high degree of unsaturation tails to regulate its formation. PI lipids may also indirectly regulate membrane proteins through their effect on line tension, as there may have some line tension-mediated enrichment of membrane proteins at the boundaries of the raft domain [30] [31].

Reference

[1] C. Dietrich, L. A. Bagatolli, Z. N. Volovyk, N. L. Thompson, M. Levi, K. Jacobson, and E. Gratton. Lipid rafts reconstituted in model membranes. *Biophysical Journal*, 80(3):1417–1428, 2001.

[2] P. I. Kuzmin, S. A. Akimov, Y. A. Chizmadzhev, J. Zimmerberg, and F. S. Cohen. Line tension and interaction energies of membrane rafts calculated from lipid splay and tilt. *Biophysical journal*, 88(2):1120–1133, 2005.

[3] C. Yuan, J. Furlong, P. Burgos, and L. J. Johnston. The size of lipid rafts: an atomic force microscopy study of ganglioside gm1 domains in sphingomyelin/dopc/cholesterol membranes. *Biophysical journal*, 82(5):2526–2535, 2002.

[4] J. C. Lawrence, D. E. Saslowsky, J. M. Edwardson, and R. M. Henderson. Real-time analysis of the effects of cholesterol on lipid raft behavior using atomic force microscopy. *Biophysical journal*, 84(3):1827–1832, 2003.

[5] M. Gandhavadi, D. Allende, A. Vidal, S. A. Simon, and T. J. McIntosh. Structure, composition, and peptide binding properties of detergent soluble bilayers and detergent resistant rafts. *Biophysical journal*, 82(3):1469–1482, 2002.

[6] W. Tsai and G. W. Feigenson. Lowering line tension with high cholesterol content induces a transition from macroscopic to nanoscopic phase domains in model biomembranes. *Biochimica et Biophysica Acta (BBA)-Biomembranes*, 1861(2):478–485, 2019.

[7] D. Lee, Y. Min, P. Dhar, A. Ramachandran, J. N. Israelachvili, and J. A. Zasadzinski. Relating domain size distribution to line tension and molecular dipole density in model cytoplasmic myelin lipid monolayers. *Proceedings of the National Academy of Sciences*, 108(23):9425–9430, 2011.

[8] N. Shimokawa, R. Mukai, M. Nagata, and M. Takagi. Formation of modulated phases and domain rigidification in fatty acid-containing lipid membranes. *Physical Chemistry Chemical Physics*, 19(20):13252–13263, 2017.

[9] T. M. Konyakhina, S. L. Goh, J. Amazon, F. A. Heberle, J. Wu, and G. W. Feigenson. Control of a nanoscopic-to-macroscopic transition: modulated phases in four-component dspc/dopc/popc/chol giant unilamellar vesicles. *Biophysical journal*, 101(2):L8–L10, 2011.

[10] N. Shimokawa, M. Nagata, and M. Takagi. Physical properties of the hybrid lipid popc on micrometer-sized domains in mixed lipid membranes. *Physical Chemistry Chemical Physics*, 17(32):20882–20888, 2015.

[11] B. Payrastre, K. Missy, S. Giuriato, S. Bodin, M. Plantavid, and M. Gratacap. Phosphoinositides: key players in cell signalling, in time and space. *Cellular signalling*, 13(6):377–387, 2001.

[12] H. Kim, B. M. McGrath, and P. H. Silverstone. A review of the possible relevance of inositol and the phosphatidylinositol second messenger system (pi-cycle) to psychiatric disorders—focus on magnetic resonance spectroscopy (mrs) studies. *Human Psychopharmacology: Clinical and Experimental*, 20(5):309–326, 2005.

[13] E. M. Haugsten, A. Oppelt, and J. Wesche. Phosphatidylinositol 5-phosphate is a second messenger important for cell migration. *Communicative & Integrative Biology*, 6(5):e25446, 2013.

[14] K. Ma, S. M. Cheung, A. J. Marshall, and V. Duronio. Pi(3,4,5)p_3 and pi(3,4)p_2 levels correlate with pkb/akt phosphorylation at thr308 and ser473, respectively; pi(3,4)p_2 levels determine pkb activity. *Cellular Signalling*, 20(4):684–694, 2008.

[15] F. M. Foster, C. J. Traer, S. M. Abraham, and M. J. Fry. The phosphoinositide (pi) 3-kinase family. *Journal of Cell Science*, 116(15):3037–3040, 2003.

[16] C. D. Ellson, S. Andrews, L. R. Stephens, and P. T. Hawkins. The px domain: a new phosphoinositide-binding module. *Journal of cell science*, 115(6):1099–1105, 2002.

[17] L. Stephens, F. T. Cooke, R. Walters, T. Jackson, S. Volinia, I. Gout, M. D. Waterfield, and P. T. Hawkins. Characterization of a phosphatidylinositol-specific phosphoinositide 3-kinase from mammalian cells. *Current biology*, 4(3):203–214, 1994.

[18] B. L. Stottrup, J. TigreLazo, V. B. Bagonza, J. C. Kunz, and J. A. Zasadzinski. Comparison of line tension measurement methods for lipid monolayers at liquid–liquid coexistence. *Langmuir*, 35(48):16053–16061, 2019.

[19] P. D. J. Moens and L. A. Bagatolli. Profilin binding to sub-micellar concentrations of phosphatidylinositol (4, 5) bisphosphate and phosphatidylinositol (3, 4, 5) trisphosphate. *Biochimica et Biophysica Acta (BBA)-Biomembranes*, 1768(3):439–449, 2007.

[20] Y. Sugiura. Structure of molecular aggregates of 1-(3-sn-phosphatidyl)-l-myo-inositol 3, 4-bis (phosphate) in water. *Biochimica et Biophysica Acta (BBA)-Biomembranes*, 641(1):148–159, 1981.

[21] M. Hirai, T. Takizawa, S. Yabuki, Y. Nakata, T. Hirai, and K. Hayashi. Salt-dependent phase behaviour of the phosphatidylinositol 4, 5-diphosphate–water system. *Journal of the Chemical Society, Faraday Transactions*, 92(9):1493–1498, 1996.

[22] J. N. Israelachvili. *Intermolecular and surface forces*. Academic press, 2015.

[23] A. Beber, M. Alqabandi, C. Prévost, F. Viars, D. Lévy, P. Bassereau, A. Bertin, and S. Mangenot. Septin-based readout of pi(4,5)p_2 incorporation into membranes of giant unilamellar vesicles. *Cytoskeleton*, 76(1):92–103, 2019.

[24] C. Salaün, D. J. James, and L. H. Chamberlain. Lipid rafts and the regulation of exocytosis. *Traffic*, 5(4):255–264, 2004.

[25] R. G. Parton and A. A. Richards. Lipid rafts and caveolae as portals for endocytosis: new insights and common mechanisms. *Traffic*, 4(11):724–738, 2003.

[26] Y. Aikawa and T. F. J. Martin. Arf6 regulates a plasma membrane pool of phosphatidylinositol(4,5)bisphosphate required for regulated exocytosis. *The Journal of Cell Biology*, 162(4):647–659, 2003.

[27] M. Riggi, K. Niewola-Staszkowska, N. Chiaruttini, A. Colom, B. Kusmider, V. Mercier, S. Soleimanpour, M. Stahl, S. Matile, A. Roux, and R. Loewith. Decrease in plasma membrane tension triggers ptdins(4,5)p_2 phase separation to inactivate torc2. *Nature Cell Biology*, 20(9):1043–1051, 2018.

[28] Y. Liu, L. Casey, and L. J. Pike. Compartmentalization of phosphatidylinositol 4, 5-bisphosphate in low-density membrane domains in the absence of caveolin. *Biochemical and Biophysical Research Communications*, 245(3):684–690, 1998.

[29] M. G. Waugh, D. Lawson, S. K. Tan, and J. J. Hsuan. Phosphatidylinositol 4-phosphate synthesis in immunoisolated caveolae-like vesicles and low buoyant density non-caveolar membranes. *Journal of Biological Chemistry*, 273(27):17115–17121, 1998.

[30] S. Yang, V. Kiessling, J. A. Simmons, J. M. White, and L. K. Tamm. Hiv gp41-mediated membrane fusion occurs at edges of cholesterol-rich lipid domains. *Nature Chemical Biology*, 11(6):424, 2015.

[31] S. Yang, V. Kiessling, and L. K. Tamm. Line tension at lipid phase boundaries as driving force for hiv fusion peptide-mediated fusion. *Nature Communications*, 7(1):1–9, 2016.

Chapter 5

General conclusion

5.1 General conclusion

In this thesis, we clarify the changes of phase separation on the DOPS/DPPC binary GUVs in a hypotonic solution under isothermal conditions. We investigated the formation of the phase separation of DOPS/DPPC/Chol trinary GUVs adding monovalent to pentavalent metal salts and amines at room temperature, 30°C, 40°C. We discussed the effect of multivalent charges on the membrane behavior based on line tension calculations.

In chapter 2, we investigated the phase separation behavior of lipid membranes containing unsaturated charged lipids (DOPS) induced by osmotic stress. Phase separation was induced by subjecting GUVs composed of DOPS/DPPC to a hypotonic solution. A three-phase coexistence was observed, especially at the ratio of DOPS/DPPC = 30/70. Due to the specificity of the DOPS head group, we consider these three phases as rich in DPPC, charged DOPS [DOPS(-)], and neutral DOPS [DOPS(N)], respectively. The composition of the three phases was identified using adsorption experiments of positively charged particles. Coarse-Grained Molecular Dynamics Simulations successfully reproduced the arrangement of the three-phase coexistence on the membrane. The DPPC-rich phase is shown to surround the DOPS(-)-rich phase and to wrap a circular region of DOPS(N) in the center. In this part, it was demonstrated that the osmotic stress caused by the hypotonic solution can induce phase separation in charged lipid membranes at a constant temperature and that the charged lipid head group is extremely important for phase separation.

In chapter 3, we investigated the phase separation behavior of charged lipid membranes with added salts and temperature changes. GUVs of DOPS/DPPC/Chol were prepared by salts solution, which induced phase separation. As increased the salts concentration (metal salts and amines), observed that phase separation formation was promoted. And it was easier to form phase separation structures at low temperatures. It was also observed that there was a significant difference in the concentrations required to induce phase separation formation by metal salts or by amines. The results showed that the concentration required to induce phase separation was related to the cation configuration and valence. Moreover, the concentration required to induce phase separation is more sensitive to temperature changes for linear-chain amines.

In chapter 4, we investigated the phase separation behavior of charged lipid membranes that contain multivalent charged lipids. By adding monovalent and trivalent charged lipids, observed the phase separation disappeared. The domain boundary line tension was measured. We found that the addition of charged lipids decreased the domain boundary line tension. Trivalent charged lipids DOPI(4,5)P_2 tended to decrease the boundary tension of domains significantly. On the other hand, the addition of $CaCl_2$ inhibited the decrease of domain boundary line tension. These results suggest that electrostatic interactions between charged lipids are related to decreasing domains boundary line tension. This effect is more pronounced for multivalent lipids.

5.2 Summary

In summary, our experimental results in this thesis suggest that the ionization state of negatively charged lipids headgroup is a crucial element to be considered when studying lipid raft models. On the other hand, osmotic pressure, temperature change, type and concentration of added salts (especially the differences between metal salts and amines), and the valence state of lipids, all have a strong influence on raft formation. In future studies, we expect to use some molecules with more complex structures (such as polymers, DNA, proteins) to explore their relationship with lipid membranes and investigate if they affect the phase separation structure formation. It is also expected that the results in this thesis may help better to understand the construction of ordered regions in living organisms and to realize industrial applications, such as functional carriers that can be used for drug delivery and consumer product manufacturing.

Acknowledgments

To the Universe

The title of my acknowledgment is big, but every person and everything I want to thank, from my country to a small lipid molecule, are all part of this universe. They accompanied me through my schooldays, without which I would not be here. The acknowledgment will be a little longer cause I would like to seize this rare opportunity to thank those who have helped me.

(1)

At the very beginning, I would like to thank my supervisor, Professor Takagi Masahiro. I have always believed that a good teacher will lead students to a brighter future. And Professor Takagi is just such a good teacher. "One word from Professor Takagi can change a person's life." This is the greatest feeling I have had in the past five years. Professor Takagi has given me the inspiration and courage to face myself finally and re-examine what I thought was "right" all along, in both my research and daily life. I have been able to grow spiritually while moving forward academically. I was surprised that Professor Takagi is not only an excellent researcher but also possesses the temperament of a philosopher. It is also because I was fortunate to meet Professor Takagi that I can confidently tell myself that it is worthwhile when I occasionally examine whether it is worthwhile for me to study abroad.

Also, I would like to thank Dr. Shimokawa Naofumi. He always guided me carefully and patiently, pointed out my shortcomings, listened to the difficulties I encountered in my research, and provided me with very insightful ideas for my research. Without Dr. Shimokawa, I would not have achieved what I have today. I admire Dr. Shimokawa's unique vision as a physics researcher and his rigorous logical thinking, which constantly reminds me to improve my research in detail, sort out the research from time to time, and lay the foundation for subsequent research. Discussions with Dr. Shimokawa are usually accompanied by a sense of pleasure when a problem is solved or advanced. Every time, I feel that I have gained a new motivation to move forward and enjoy my research more.

I would like to thank my Ph.D. defense committee members: Professor Fujimoto Kenzo, Professor Kamiya Noriho, Professor Takamura Yuzuru, Associate Professor Miyako Eijiro, and Associate Professor Yamaguchi Takumi. They helped me improve the deficiencies in my dissertation and provided detailed and careful revisions suggestions. Sincere thanks to Assistant Professor Higuchi Yuji, Assistant Professor Ito Hiroaki, and Assistant Professor Klemen Bohinc, for their cordial support, invaluable information and supervision, which helped me in completing this work. Also, my special thankfulness extends to the members of Takagi laboratory who were

and are still here. Although I will not mention the names of all of them, they have all helped me a lot in my research and life, whether they are researchers, secretaries, seniors, peers, or juniors. Thank you all.

At the end of this part, thanks to all the lipids molecules I used, thanks to they spontaneously formed closed bilayer structures in water. Every single data of my experiment stems from that they strictly follow physics laws. The tens of thousands of liposomes that I have observed over the past five years are essential treasures in my life.

(2)

I am a person who treats family and friends very strictly. Even then, they did not leave me away. Thanks so much to them for never giving up on me and listening to my complaints when I couldn't hold on in a foreign country. This acknowledgment is probably not just about the people who helped me during my doctoral studies but also about the people who helped me during my 22 years of school days. I won't mention every name, but still thankful to all of them.

I have always believed that learning is the easiest thing to do, and knowledge will never betray you as long as you study hard. It is true that I have not encountered so many difficulties in studying. But learning is also the most challenging thing. I have never thought about when I pay no attention to what is going on beyond my study and bury myself in the classics, who gives me a clean and comfortable classroom, who let me enjoy a perfect education, who allows me not to worry about my next meal, and who was taking care of my life. Five years of studying abroad finally gave me the answer. They are my great country, China, and my loving parents, Ms. Xu Hong and Mr. Guo Min. I would like to put my motherland and my parents in the same place in my heart, thanking them for letting me come into this world, thanking them for providing me with education, and thanking them for supporting me to study abroad. Because of such wonderful parents, I have seen a wider and more gorgeous world. They could have lived a better life, but they chose to support me all the way and never gave up. Even when I was disappointed in myself, my parents still thought I am the best in the world. But just as I was lifted to see the high places when I was a child, now I am still lifted by parents to see the world. And the rest of the way, I will walk independently, turning my gratitude into action to repay my parents.

Also, I have a big, warm family. In addition to my parents, my grandmother, aunts and uncles, godparents, my younger brothers and sisters are all pillars of my soul. I am always proud to have such loving family members who are genuinely happy for my achievements and bless me with everything that makes me feel warm and wonderful. Thanks for their love.

For almost 30 years of my life, my husband, Mr. Yuan Xida, has been with me for nearly 10 years, and we have been learning together during these 10 years. Many people say I have married too young, but I never think so. I have never written love letters to my husband, feeling pretentious and squirming, not in line with my big woman persona. But I'd like to take this opportunity to say thanks. Thank him for going to the library in the morning to help me take a seat, thank him for helping me to solve various electronic products problems, thank him for

cooking, thank him for brushing the dishes, thank him for doing the laundry, thank him for also drying the clothes, and thank him for loving me.

For my friends who are not in Japan, we could only meet once a year on rare occasions. Even someone living in Australia at the time came back across the seasons to attend my wedding. Thanks to modern technology, we can always be in touch, text, and make video calls. They listen to my joy, happiness, uncertainty, and disappointment, never perfunctorily help me, and always treat my affairs sincerely and carefully. Thanks to them, allowed me to take up their precious time.

I also want to thank the friends I met in Japan. It seems normal for people from the same country to get together in a foreign country. But I was really lucky to meet them. I don't know where to start, the tennis we played together, the same Chinese characters in our names, the nicknames we remember better than the real names, the same house, the same birthday, the sudden addition of a brother, a kangaroo, a rabbit, a lamb, or Arashi we loved together. All these little things supported me through the five years in JAIST and made my life happy and beautiful.

I would also like to thank one of the most important people in my life, Ms. Xu Tingting. I would like to thank her for her efforts to walk through a long academic path of more than twenty years that was not difficult but somewhat bumpy. Thank her for her thirst for knowledge and her curiosity about the world. Thank her for every choice she made at every turn in her life. Thank her for making it all the way through on her own. Thank her for never giving up.

Finally, to borrow a line from my favorite movie, The Lion King, "The great kings of the past look down on us from those stars". Thank my grandfather, Mr. Xu Wenjun, for watching over me in the stars of the universe. Grandpa, I miss you, and I will always miss you. Although I know that you will never hear me say these words again, I still want to tell you that I love you. Past, present, and future.

(3)

So much for rambling, just to express that I can't do it without you all.

Thank you.

To you.

To the universe.

Publications

Journal Papers

- J. Guo, H. Ito, Y. Higuchi, K. Bohinc, N. Shimokawa, M. Takagi. (2021). Three-Phase Coexistence in Binary Charged Lipid Membranes in a Hypotonic Solution. *Langmuir*, 37(32), 9683-9693.

Presentations at academic conferences (Oral)

1. J. Guo, N. Shimokawa, M. Takagi. (2019, Mar). Phase separation in binary charged lipid membranes dependent on lipid ionization, presented at 74th annual meeting (2019), *The Physical Society of Japan*, Kyushu, Japan.

2. J. Guo, Y. Nagata, N. Shimokawa, M. Takagi. (2020, Sep). Structure of added salts and temperature dependence in phase separation of charged lipid membranes, presented at Autumn meeting (2020), *The Physical Society of Japan*, Online, Japan.

3. J. Guo, H. Ito, Y. Higuchi, R. Hidese, S. Fujiwara, N. Shimokawa, M. Takagi. (2021, Sep). Domain formation affected by temperature and added polyamines in charged lipids-containing biomimetic membranes, presented at 15t Symposium on Biorelevant Chemistry (2021), *Division of Biofunctional Chemistry and Division of Biotechnology, The Chemical Society of Japan*, Online, Japan.

4. J. Guo, Y. Nagata, H. Ito, Y. Higuchi. N. Shimokawa, M. Takagi. (2021, Sep). Formation of phase-separated structures by temperature changes and added salts in negatively charged lipid membranes, presented at Autumn meeting (2021), *The Physical Society of Japan*, Online, Japan.